Chapter 4
Special Engineering Aspects

P. Czermak, R. Pörtner, and A. Brix

Abstract The specific characteristics of mammalian cells discussed in Chap. 2 require adapted solutions for bioreactor design and operation. Especially, cell damage by shear stress and aeration has to be considered. Therefore this chapter starts with a detailed discussion of shear stress effects on mammalian cells (anchorage-dependent and suspendable cells) in model systems and bioreactors, respectively, and consequences for reactor design. Appropriate oxygen supply is another critical issue, as adapted oxygen supply systems are required. Techniques for immobilization of cells, either grown on microcarriers in suspension culture or within macroporous carriers in fixed bed or fluidized bed reactors, are discussed as well. With respect to the operation of bioreactors, the characteristics of different culture modes (batch, fed-batch, chemostat, perfusion) are introduced and practical examples are given. Finally, concepts for monitoring of bioreactors, including offline and online methods as well as control loops (e.g. O_2, pH), are considered.

4.1 Cell Damage by Shear and Aeration

4.1.1 General Aspects

Unlike other microorganisms (e.g. bacteria), mammalian cells are not surrounded by a cell wall adapted to support survival as an individual within the natural environment, but only by plasmatic membrane, which can only withstand weak mechanical

P. Czermak
Institute of Biopharmaceutical Technology, University of Applied Sciences Giessen-Friedberg, Giessen, Germany and Department of Chemical Engineering, Kansas State University, Durland Hall 105, KS 66506-5102, Manhattan, USA

A. Brix
Department of Chemical Engineering, Kansas State University, Durland Hall 105, KS 66506-5102, Manhattan, USA

R. Pörtner
Hamburg University of Technology (TUHH), Institute of Bioprocess and Biosystems Engineering, Denickestr. 15, D-21073 Hamburg, Germany
poertner@tuhh.de

R. Eibl et al., *Cell and Tissue Reaction Engineering: Principles and Practice,*

forces. The cell membrane is basically composed of phospholipids that build a double layer. In conventional bioreactor systems, aerated stirred tanks and bubble columns, adherent cells grown on microcarriers or suspended cells are exposed to variously intense hydrodynamic forces. A sufficiently intense force will destroy the cell wall. Forces of lesser magnitude may induce various physical responses, including reduced growth, cell death (apoptosis) or other metabolic reactions. A number of reviews have summarized the main fluid-mechanical and biological aspects of cell damage (Cherry 1993; Papoutsakis 1991; Chisti 2000, 2001). According to Papoutsakis (1991) fluid mechanical questions include the following:

- What forces affect cells in a flow environment, and how?
- Are the flow effects due to the intensity and/or the frequency of the forces?
- What types of interactions are most damaging to the cells in various reactors and/or processing devices?

Biological questions include the following:

- Does fluid-mechanical stress cause cell death, or simply reduce cell growth?
- Do fluid mechanical forces affect the physiology (e.g. the cell cycle), product expression, molecular processes, receptor-mediated processes and the cytoskeleton of the cells? How?
- Do cells react to and adapt in response to fluid-mechanical forces?

In addition it is relevant to ask:

- Do fluid-mechanical forces affect adherent and suspendable cells differently?
- Is it possible to protect the cells against this kind of damage?
- Does the sensitivity of cells to fluid-mechanical stress depend on the scale?

Finally, the objective should be to formulate the extent and the mechanism of the damages as well as allow calculation and lay-out of bioreactors with respect to parameters such as reactor size, stirrer rotation speed or aeration rate for bubble aeration (Tramper et al. 1993).

Generally, the effects caused by mechanical forces in a mixed culture and damaging effects caused by gas bubbles are discussed separately. The many kinds of mechanical forces (e.g. the motion of microcarriers or free suspended cells relative to the surrounding fluid, to each other and to moving or stationary solid surfaces) are collectively referred to as “shear forces”, as the underlying damaging phenomena cannot be ascribed to gas bubbles (Chisti 2001).

By definition, shear in a fluid system has two components, shear stress τ and shear rate γ. A shear stress is a force per unit area acting on and parallel to a surface. Shear rate is a measure of a velocity gradient (velocity/length). The two quantities are related; thus, in laminar Newtonian fluid

$$\tau = \eta_{\mathrm{fl}} \gamma, \tag{4.1}$$

where η_{fl} is the viscosity of the fluid. In model systems such as laminar flow between two parallel plates, in a cone-and-plate viscometer or a coaxial cylinder Searle viscometer the shear rate and the corresponding shear stress can be calculated

by simple mathematical equations (see below) and the damaging effects can be related to exact values. In a complex, mostly turbulent environment within a bioreactor, the local shear rate varies within the vessel and it is more difficult to associate cell damage with the magnitude of the prevailing shear rate or the associated shear stress. Even more complex are the mechanisms of cell damage caused by gas bubbles in sparged bioreactors.

In general, cell damage typically follows first-order kinetics. Thus, the rate of cell loss (dX_v/dt) depends on the concentration of viable cells X_v and can be described by

$$\frac{dX_v}{dt} = -k_d X_v, \tag{4.2}$$

where k_d is the cell specific death rate. The k_d value is influenced by the rate of shear stress and the operating conditions within the cultivation system (stirring, bubble aeration, and medium composition) as well as the properties of the cells. In the following sections, available data for the different culture conditions will be discussed.

In the next sections, discussions about model systems will be presented in order to describe the main effects. Later, the effect of shear stress and bubble aeration in real bioreactors will be shown. Finally some recommendations will be given for the design and operation of bioreactors. Note that a distinction between adherent and suspendable cells will be made.

4.1.2 Model Analysis

The intention of these most studies was mainly to understand the basic mechanism of cell death due to flow shear forces or bubbles. In most cases the cells were exposed to defined levels of shear stress in defined flow geometries in order to correlate the effects with known values for the level of shear stress. From these findings, conclusions for design and operation of bioreactors were drawn. Furthermore it was to ask whether critical shear stress levels found in model systems can be used for the estimation of design criteria for large scale bioreactors (e.g. power input, stirrer speed or aeration rate).

4.1.2.1 Shear Stress on Anchorage-Dependent Cells

The damaging effect of shear on anchorage-dependent cells adhered to a solid surface is frequently studied in a flow chamber (Fig. 4.1) (Diamond et al. 1990; Frangos et al. 1985; 1988; Ludwig et al. 1992; Shiragami and Unno 1994; Spraque et al. 1987; Stathopoulos and Hellums 1985). In this apparatus, a laminar flow causes a defined shear stress at the wall τ_w on the bottom plate where the cells are adherently growing. The flow velocity $U(y)$ can be calculated for given values of the flow rate F, the viscosity η_{fl}, the height h and the width b of the flow chamber (Fig. 4.2):

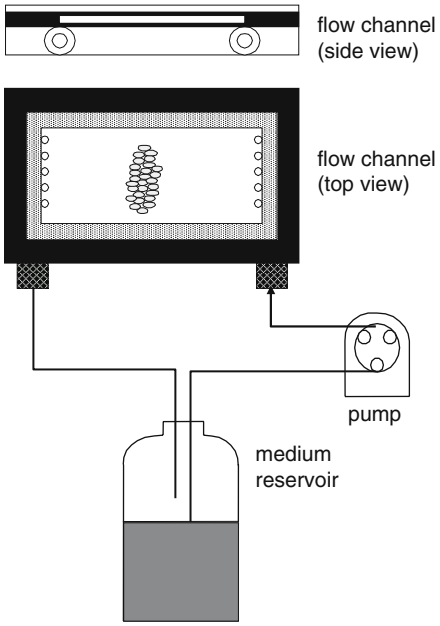

Fig. 4.1 Flow chamber for investigation of shear effects on adherent cells (reproduced from Shiragami and Unno 1994, modified, with kind permission of Springer)

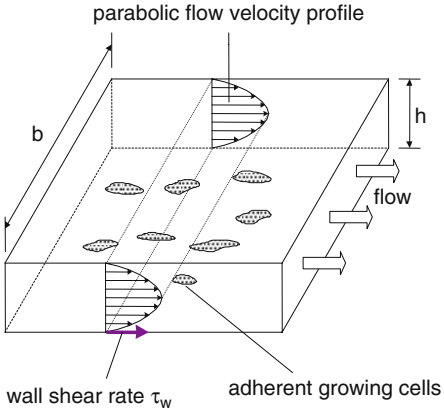

Fig. 4.2 Determination of wall shear rate in a flow chamber for investigation of shear effects on adherent cells

$$U(\mathrm{y}) = \frac{6F}{bh^3}(hy - y^2). \tag{4.3}$$

The wall shear stress τ_w acting on the cells is given by:

$$\tau_w = \eta_{fl}\left(\frac{dU}{dy}\right)_{y=0} = \frac{6\eta_{fl}\dot{F}}{bh^2}. \tag{4.4}$$

In experiments performed with the aim to determine a critical shear stress, the cells are allowed to grow on the bottom plate of a flow chamber until they have reached confluence (Fig. 4.3). Afterwards, the medium flows with a defined velocity through the chamber for a certain time and the cell morphology, the number of viable cells and the concentration of substances that are released by the damaged cells [i.e. lactate dehydrogenase (LDH)] are evaluated (Chisti 2001). The following conclusions can be drawn from the available data:

- Cell attachment to a surface is affected by shear stress levels between 0.25 and 0.6 Nm^{-2} (Olivier and Truskey 1993)
- Under stress the cells orientate themselves within the liquid flow lines (as shown in Fig. 4.3)
- Laminar shear stress in the order of 0.5–10 Nm^{-2} may remove adherent cells from the surface (Aunins and Henzler 1993). Kretzmer (1994) as well as Shiragami and Uno (1994) gave some numbers for CHO and BHK cells for the influence of shear stress on the living cells ratio (50% viability): 3 h > τ_w = 6 Nm^{-2}; 24 h > τ_w = 0,75–1 Nm^{-2}
- Laminar shear stress in the order of 0.1–1.0 Nm^{-2} may affect cellular morphology, permeability, and gene expression (Aunins and Henzler 1993).
- The combined effect of shear stress and the stress duration can be expressed by the energy ε dissipated during a certain time (Shiragami and Unno 1994)

$$\varepsilon = t\int \eta_{fl}\left(\frac{dU}{dy}\right)^2 dy = \frac{h\tau_w^2 t}{3\eta_{fl}} \tag{4.5}$$

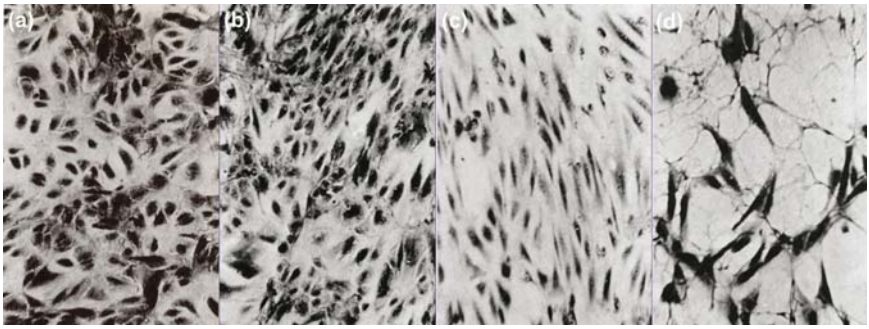

Fig. 4.3 Effect of shear stress on adherent growing primary epithelial cells in a flow chamber after (**a**) 1 week of culture without shear stress (controls), (**b**) 4 h with a shear stress of 1.3 Nm^{-2} (**c**) 24 h with a shear stress of 1.3 Nm^{-2}, (**d**) 24 h with a shear stress of 5.4 Nm^{-2} (adapted from Stathopoulos and Hellums 1985, with kind permission of John Wiley & Sons)

4.1.2.2 Shear Stress on Suspended Cells

The reaction of freely suspended cells on shear forces in a bubble-free environment can be regarded as similar to the behaviour of drops or suspended particles in a shear field. They experience extensional or elongational forces depending on the flow pattern, e.g. whenever the cross-sectional area of a flow channel reduces, as at the entrance of capillaries or within bioreactors in the direction of flow. The cells subjected to extension or extensional flow can rupture similar to drops. From this point of view the mechanical strength of the cell, expressed by the bursting membrane tension, could be an appropriate parameter to describe the allowed level of stress. But as the cells can rotate or tumble in an extensional flow field to relax the imposed stress, in addition to hydrodynamic stress, the possibility of rotation-associated stress relaxation also needs to be considered. The effect of shear forces on suspendable cells was investigated as follows:

- Determination of the surface tension of the cell membrane
- Correlation of the cell damage with the shear stress in a surrounding fluid.

The basic theory for the behaviour of emulsified, viscous liquid drops was developed by Taylor (1934). According to this model, the resistance and stability of a cell exposed to shear forces are basically influenced by the surface tension and the size of the cell. Cell deformation is the result of the action of external hydrodynamic forces and the cell would burst if the following condition is fulfilled:

$$\tau_{crit} r_Z^2 = 2 r_Z \sigma_Z \tag{4.6}$$

with the the critical shear stress τ_{crit}, the cell radius r_Z and the membrane tension at cell burst σ_Z. In order to determine the membrane tension at cell burst, Zhang et al. (1992b) applied an experimental set-up as shown in Fig. 4.4. Initially, the single cells were fixed between two glass fibres (diameter approx. 50 µm) that can slide against each other. After the immobilization, the cells were compressed in the gap between the fibres until they burst. The burst strength and cell diameter were recorded to calculate the membrane tension. By this, values of σ_Z = 1.7–2.5×10^{-3} Nm^{-1} for the membrane tension were determined leading to critical shear rates of 500–700 Nm^{-2}.

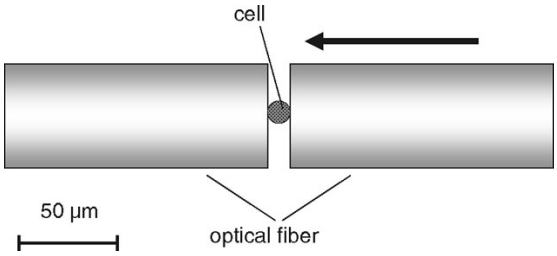

Fig. 4.4 Experiment for determination of the force required to burst the cell. Cell entrapped between two optical fibers (adapted from Zhang et al. 1992b)

Based on the hypothesis that a cell should burst whenever its bursting membrane tension is exceeded in a laminar flow, Born et al. (1992) developed a model predicting cell damage in laminar flow. For a critical discussion see Chisti (2001). Even if the model seems to be supported by experimental data from cells sheared in a cone-and-plate viscometer, the practical utility of this approach is regarded as limited.

Cell damage due to shear stress was investigated in certain devices, where the cells could be exposed to defined high-shear levels in laminar or turbulent flow (e.g. cone-and-plate-viscometer, coaxial cylinder Searle viscometer, capillary flow (Abu-Reesh and Kargi 1989; Born et al. 1992; Kramer 1988; Smith et al. 1987; Tramper et al. 1986) (reviewed extensively by Chisti 2001). In most cases the cells were cultivated under unharmful conditions e.g. in a small spinner reactor and then transferred to one of the devices mentioned above. Here the cells were exposed to a certain shear level for a certain time.

For a coaxial cylinder Searle viscometer (couette viscometer), within a narrow gap between the two cylinders, the shear rate and shear stress are constant within the gap and proportional to the rotation speed. From the measured torque M_d, height h and inner radius $r_{i,cou}$ the shear stress τ can be calculated.

$$\tau = \frac{M_d}{2\prod hr_{i,cou}^2}. \tag{4.7}$$

The laminar-turbulent flow transition is defined by the Taylor number Ta

$$Ta = \left(\frac{\rho_{fl} U_T w}{\eta_{fl}}\right)\left(\frac{2w}{d_{i,cou}}\right)^{0.5}. \tag{4.8}$$

with gap width w, diameter of inner cylinder $d_{i,cou}$ rotating at peripheral speed U_T and fluid density ρ_{fl}. The flow is laminar when Ta < 41.3. Laminar flow with Taylor vortices occurs for 41.3 < Ta < 400. When Taylor number exceeds 400, the turbulent flow is fully developed. An example is shown in Fig. 4.5.

As can be seen from Table 4.1, critical values between 1 and 2×10^3 Nm^{-2} have been reported. Reasons for this large range of values can be seen in (i) different criteria for the threshold shear stress (e.g. total cell disruption, certain level of cell death, appearance of cell lyses, and induction of cell inactivation among others), (ii) different cell lines, (iii) different devices, and (iv) different culture conditions (medium with or without serum, etc.). Nevertheless some general conclusions can be drawn from these data:

- Turbulent flow is more damaging than laminar
- Duration of shear stress is relevant
- The mechanism of cell damage is very complex and depends on the device used for the studies
- The shear rate seems not to be the appropriate parameter to describe the effect.

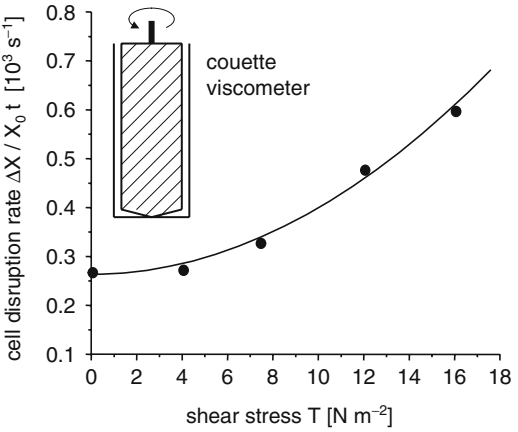

Fig. 4.5 Influence of shear stress on the cell disruption rate of hybriodm cells in a couette viscosimeter (adapted from Kramer 1988)

Table 4.1 Impact of shear stress on suspendable cells

Reference	Cell type	System	Type of flow	Threshold shear stress [N m^{-2}]	Exposure time
Kramer (1988)	Hybridom	Coaxial cylinder	n.d.	4	
Tramper et al. (1986)	Insect cells	Coaxial cylinder	n.d.	1–4	1–3 h
Born et al. (1992)	Hybridom	Cone-and-plate	Laminar	208	20 min
				350	180 s
Abu-Reesh and Kargi (1989)	Hybridom	Couette	Turbulent	5	
McQueen et al. (1987)	Myeloma	Capillary	Turbulent	180	
Cited by McQueen et al. (1987)	Hybridom	Capillary	n.d.	0.87	
Cited by McQueen et al. (1987)	Insect	Capillary	n.d.	1.5	
Augenstein et al. (1971)	HeLa/L293	Stainless steal capillaries	n.d.	0.1–2×10^3	

According to data from Abu-Reesh and Kargi (1989), cell damage followed first-order kinetics both under laminar and turbulent conditions. For turbulent shear stress levels of 5–30 Nm^2, the death rate constant k_d varied between 0.1 and 1 h^{-1} and increased exponentially with increasing stress level.

4.1.2.3 Cell Damage Caused by Bubbles

The specific events responsible for the bubble-associated cell damage include

- Bubble formation at the sparger
- Bubble detachment
- Rise through the fluid
- Break-up of bubbles at the surface and foam formation (Chisti 2000).

Among others, Jordan (1993) studied the damaging effect of bubbles to understand the main mechanisms. The interaction between cells and bubbles was strongly influenced by the concentration of protecting agents (e.g. Pluronic F68, see below) and the retention time of the bubbles in the medium. Based on his phenomenological observations he suggested subdividing the way of a bubble from the sparger to the surface into four zones (Fig. 4.6). Cells getting in contact with a bubble directly after bubble formation are damaged instantly, mainly due to a difference in surface tension (zone 1). After longer retention of the bubble in the medium, several medium compounds, especially high molecular weight compounds or proteins, are adsorbed at the surface of the bubble, and the surface tension is reduced. Thus the cells are not damaged any more, but are still attached at the surface and therefore float with the rising bubble (zone 2). In zone 3, attachments of cells at the surface is further reduced. In zone 4 the gas bubbles burst at the surface of the fluid and form a foam layer. Cells can be damaged either during bubble collapse or when trapped in the foam (Fig. 4.7). When a bubble collapses at the surface, cells adsorbed to the bubble surface or trapped in the wake of the bubble are exposed to relatively high

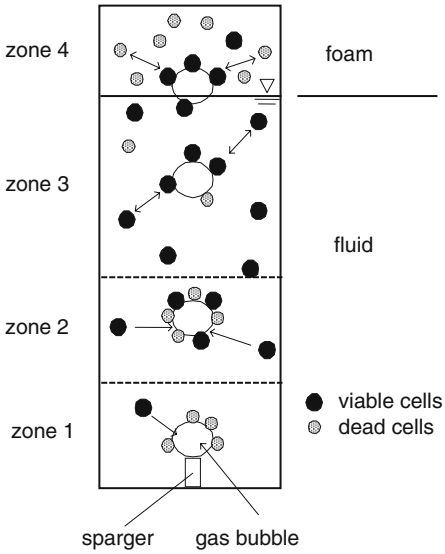

Fig. 4.6 Mechanisms of cell damage in a bubble column (adapted from Jordan 1993)

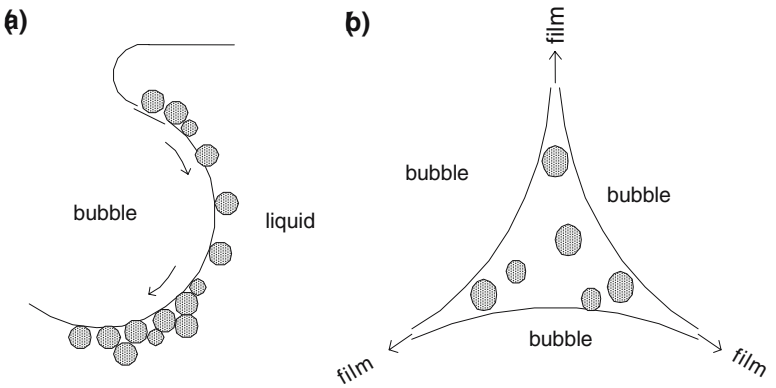

Fig. 4.7 Cell damage in a foam layer (adapted from Papoutsakis 1991, with kind permission of Elsevier). (a) cells near the bubble interface, large shear stress due to bubble break up, (b) cells are sheared in the thinning films either between bubbles or around bubbles

shear forces. These forces are strong enough to rupture the cell's membrane. The shear forces can originate from the velocity gradient arising from the upward movement of the bubbles and the downward jet resulting from the bursting bubbles. Cells entrapped in the foam layer are exposed to shear by the movement of the bubbles surrounding a cell in different directions and nutritional effects (e.g. oxygen limitation). Meanwhile it is generally accepted that these effects are mainly responsible for cell damage in aerated systems.

Some general statements can be made regarding bubble-associated damage (Chisti 2000):

- Cell lines differ tremendously in their sensitivity to aeration (e.g. in sparged bioreactors, mouse hybridom are generally more robust than insect cells)
- Small bubbles (e.g. <2 mm diameter) are more damaging than large bubbles (e.g. ~10 mm diameter). Large bubbles have mobile interfaces (wobbling) and, because they rise faster, they carry fewer attached cells to the surface. Furthermore, larger bubbles (unlike smaller ones) do not remain on the surface as stable foam.
- Furthermore cell damage is directly affected by the aeration rate.
- Sparging-associated damage may be enhanced by impeller agitation.
- Cells can be protected by certain media additives.

Implications on design and operation of sparged bioreactors will be discussed in Sect.. 4.1.3.3.

4.1.3 Cell Damage in Bioreactors

The above sections described the main mechanisms responsible for cell damage due to defined shear forces or bubbles. In a complex, mostly turbulent environment within a bioreactor, the local shear rate varies within the vessel and it is more difficult

to associate cell damage with the magnitude of the prevailing shear rate or the associated shear stress. Even more complex are the mechanisms of cell damage caused by gas bubbles in sparged bioreactors, bubble columns or air-lift-bioreactors. In the following sections, some basic studies and approaches to describe cell damage mathematically are discussed, focussing mainly on those strategies and equations suitable for bioreactor design and scale-up. Comprehensive reviews can be found in the literature (Chisti 2000, 2001).

4.1.3.1 Anchorage Dependent Cells Grown on Suspended Microcarriers

The impact of shear forces on anchorage-dependent cells in stirred bioreactors was largely studied for microcarrier cultures as anchorage-dependent cells can be grown on the surface of suspendable particles (Fig. 4.8) (Sect. 4.3.1.2). Microcarrier culture is still applied widely for large-scale production of viral vaccines among others. Cells grown on microcarriers experience more severe hydrodynamic forces than do freely suspended cells (for review see Chisti 2001). This is because in the mostly turbulent environment within highly agitated or aerated systems, the length scale of fluid eddies can easily approach the dimensions of microcarriers, resulting in high local relative velocities between the solid and the liquid phases. Additionally, collision among microcarriers and between the impeller and microcarriers may damage attached cells.

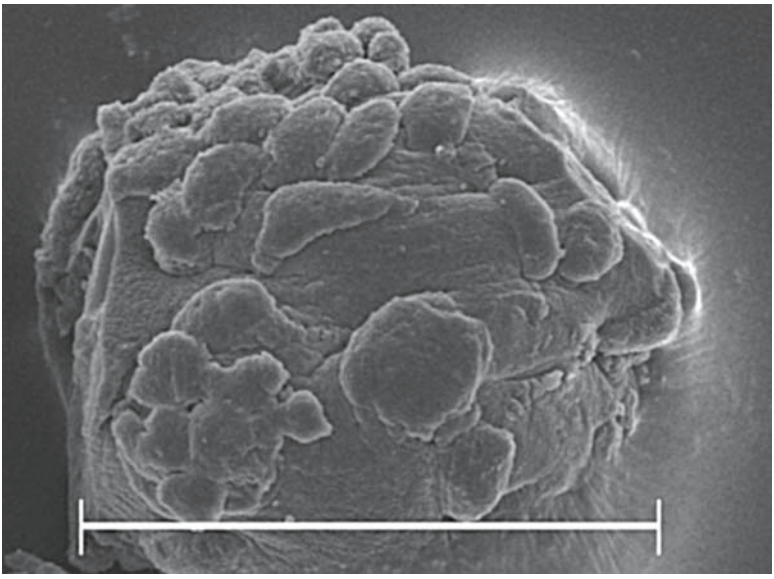

Fig. 4.8 Microcarrier for suspension culture of adherent cells, pig chondrocytes grown on Cytodex 3 (GE Healthcare, bar approx. 150 µm)

In a turbulent flow caused by a stirrer, relatively large eddies are created at first. These eddies break up into smaller ones stepwise, until the energy is completely dissipated. Cherry and Papoutsakis (1986, 1988) distinguished between three different microcarrier-eddy-situations depending on the ratio between eddy size and microcarrier diameter (Fig. 4.9).

Several concepts to describe the complex shear effects on cells in a turbulent flow were suggested and judged by available data on the impact of shear forces on microcarrier cultures in small scale bioreactor systems (compare Fig. 4.10) Among others the concept of an "Integrated Shear Factor" ISF – a measure of the strength of the shear field between the impeller and the spinner vessel walls – was developed to describe shear damage to mammalian cells (Croughan et al. 1987; Sinskey et al. 1981). The ISF is defined as

$$\mathrm{ISF} = \frac{2\Pi n_R d_R}{D_R - d_R} \tag{4.9}$$

with rotation speed n_R, vessel diameter D_R and stirrer diameter d_R. Data from Hu et al. (1985) can be described well. For a range of stirrer vessels (volume 0.25–2.0 L, d_R 3.2–8.5 cm) the viable cell density dropped sharply when the ISF value exceeded 18–20 s^{-1}. Furthermore Croughan et al. (1988) and Croughan and Wang (1989) discussed other concepts such as the correlation between cell damage and impeller tip speed or a time averaged shear rate. Even if in all cases a satisfying

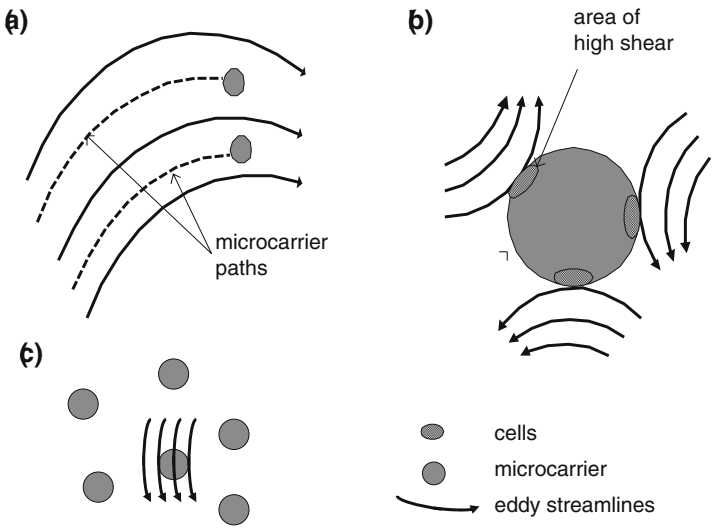

Fig. 4.9 Shear forces on microcarriers in a turbulent flow. Microcarrier-eddy interactions: (**a**) eddies much larger than beads, (**b**) multiple eddies same size as bead, (**c**) eddy size same as interbead spacing (adapted from Cherry and Papoutsakis 1986, modified, with kind permission of Springer)

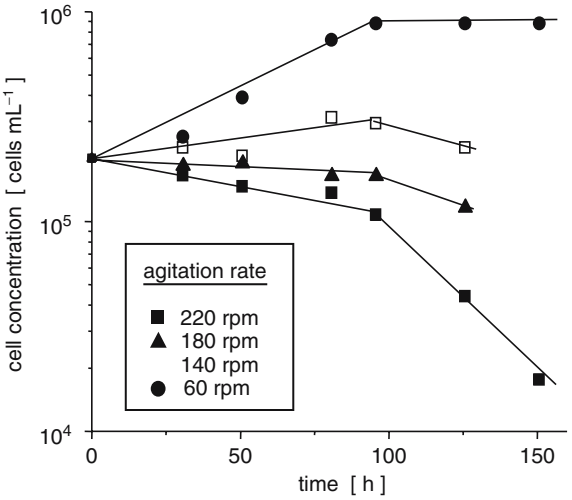

Fig. 4.10 Growth of human FS 4-cells on microcarriers Cytodex 3 in a 250 mL spinner reactor (adapted from Croughan et al. 1987, with kind permission of John Wiley & Sons)

success in correlating cell damage could be obtained, these concepts are regarded as not a relationship for scale-up. For example, if standard stirred tank reactors ($D_R = 3d_R$) are scaled up to a geometrically similar larger vessel, the ISF depends solely on the rotational speed of the impeller (ISF = πn_R). Therefore the rotational speed would be independent of scale and the impeller tip speed $d_R n_R$ would therefore increase with scale. In general it is doubtful whether concepts based on the stirrer speed are appropriate for scale-up of cell damage. Instead, between cell damage and volume specific power input was proposed. This will be discussed in detail in the following sections.

According to Cherry and Papoutsakis (1986, 1988) cells grown on microcarriers within turbulent eddies of the same size as the microcarriers are exposed to the largest shear stress. The energy of the eddies is transferred to the surface of the microcarriers, resulting in high local velocities between the microcarriers and the fluid, and the highest shear rates on the cells. The microcarriers are caused to rotate within these eddies. From Kolmogorov´s theory the length scale l_{Kol} of those smallest eddies are in the order of

$$l_{Kol} = \left(\frac{\upsilon^3}{\varepsilon} \right)^{1/4} \tag{4.10}$$

with the kinematic viscosity ν and ε the energy dissipation rate per unit mass. The Kolmogorov eddy length scale corresponds to the diameter of the smallest eddy generated in the reactor. In a turbulent environment, eddies break down to form smaller eddies. As eddies break down, the energy of the larger eddy is passed down. At the smallest eddy diameters the flow actually becomes laminar, rotation forces

and friction forces are in equilibrium, rotation of eddies stops and fluid flow is characterized by the formation of flow lines. When the Kolmogorov eddy length scale becomes equivalent to the cell diameter, the movement of the flow lines can shear the cells. The Kolmogorov eddy length scale is affected by stirrer speed, liquid properties and impeller design. Croughan et al. (1987) plotted data from Hu et al. (1985) by using the mean energy dissipation rate per unit mass

$$\varepsilon = \frac{P}{\rho_{fl} V} \tag{4.11}$$

with power input P and volume V. As can be seen from Fig. 4.11, for human fibroblasts the number of viable cells decreased rapidly when the length scale declined to approximately below 125 µm. The mean diameter of microcarriers was about 185 µm, or roughly similar to the length scale of the microeddies. Even if this correlation seems to support the underlying theory, the Kolmogorov eddy length scale allows only for a rough estimation of the expected cell damage and is regarded as not suitable for scale-up. For example, if the mean energy dissipation rate per unit mass is increased ten times, the Kolmogorov length scale decreases only by a factor of 0.56. Furthermore this approach cannot be transferred to suspendable cells.

Croughan et al. (1987) further showed that the specific death rate k_d can be linked to the mean energy dissipation rate per unit mass

$$k_d \approx \varepsilon^{3/4}. \tag{4.12}$$

Hülscher (1990) confirmed this relationship for microcarrier cultures as well as for suspendable cells (see below).

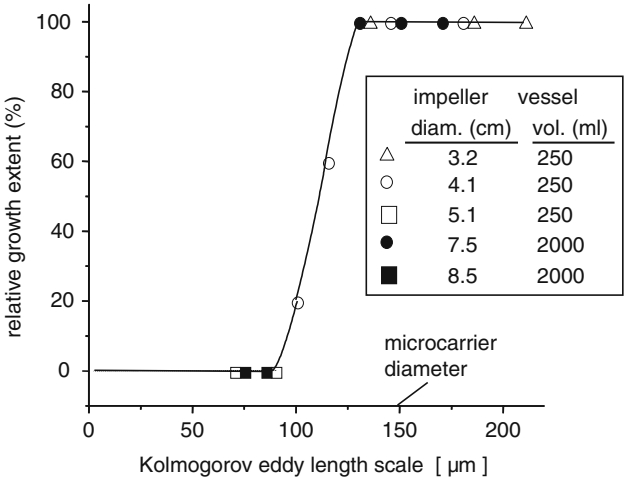

Fig. 4.11 Growth of human FS 4-cells on microcarriers Cytodex 3 in a 250 mL spinner reactor – correlation of growth with Kolmogorov length of eddies (adapted from Croughan et al. 1987, with kind permission of John Wiley & Sons)

4.1.3.2 Non-Anchorage Dependent Cells Grown in Suspension

Similar to shear effects on cells grown on microcarriers, several studies have addressed damage to suspendable cells (mostly hybridom or myeloma, insect cells, or anchorage dependent cells adapted to growth in suspension, e.g. CHO, BHK) in stirred tanks. Again, factors such as cell type, medium, amount of serum, type of stirrer, and type of vessel, among others, have to be considered. A comprehensive overview is given by Chisti (2001). As an example, data from Kramer (1988) are summarized in Table 4.2. In this case, cell damage on suspended hybridom cells grown in a small stirred vessel was first observed at a stirrer speed of 300 rpm; at 580 rpm cell growth stopped completely. Similar results were reported by Shiragami (1997), who observed a maximum specific antibody production rate at ~ 180 rpm in a 250 mL reactor.

The Reynolds number Re is expressed by

$$\mathrm{Re} = \frac{n_R d_R^2 \rho_{fl}}{\eta_{fl}} \tag{4.13}$$

In view of the available studies, damaging effects caused by intense mechanical forces and those associated with aeration or bubble entrainment have to be distinguished (compare Chisti 2001):

- Cell damage in stirred tanks operated at high stirrer speeds can be reduced by applying baffles to prevent vortexing and gas entrainment.
- Cell damage increases significantly in serum- or protein-free medium.
- Intense mechanical forces may cause physical damage to cells, leading to necrosis or lysis, or may induce apoptosis (a genetically controlled cell death) at sublethal stress levels.

Stevens (1994) compared data from different sources on damage to suspended hybridom cells. The mean shear stress and the mean energy dissipation rate per unit mass were calculated for those conditions, where growth rate and death rate were equal. Critical values for the mean shear stress in stirred vessels were between 0.39 and 1.5 Nm^{-2}, significantly lower than those reported for coaxial cylinder Searle viscometer (compare Table 4.1). A good correlation of these data can be obtained

Table 4.2 Cell damage of suspended hybridom cells (data from Kramer 1988) Culture conditions: stirred tank reaktor (volume 750 ml, vessel diameter 15 cm, rushton turbine (four blades), stirrer diameter 5 cm, medium RPMI 1640 + 10% Serum

Stirrer speed [rpm]	200	300	400	500
Re [–]	12,000	18,000	24,000	30,000
ε [W m^3]	26	88	210	410
μ [h^{-1}]	0.047	0.059	0.049	0.034
k_d [h^{-1}]	0	0	0.01	0.034

by plotting the critical mean energy dissipation rate per unit mass vs. the serum content in the medium (Fig. 4.12). The data for different hybridom cell lines agree quite well with those cases with surface aeration and without bubble entrainment. In the case of bubble aeration resulting in foam formation, significantly lower critical values were observed. For bubble aeration, but without free surface (no foam), the critical values were much higher. This proves that effects caused by bubble and foam formation have to be considered separately (see below).

Even if some data from the literature could be used to describe the approach used in Fig. 4.12, this does not provide a concept to be used for the design and scale-up of bioreactors with respect to shear stress. But it attempts to describe the impact of culture conditions on the damage of suspended cells by the mean power input. A similar approach was suggested by Märkl et al. (1987) for microbial cultures in stirred vessels. Strategies for design and scale-up of large-scale reactors will be discussed in Sect. 4.1.3.4.

4.1.3.3 Sparged Bioreactors

Gas sparging or bubbling air or another gas in the culture broth through a sparger located relatively deep within the bioreactor may cause damage to suspended mammalian cells or cells grown on microcarriers. As sparged bioreactors are still the preferred means of cell culture aeration, much effort has been expended on understanding the underlying mechanisms involved in bubble-associated cell damage and the methods available to control such damage (reviewed by Chisti 2000). The basic

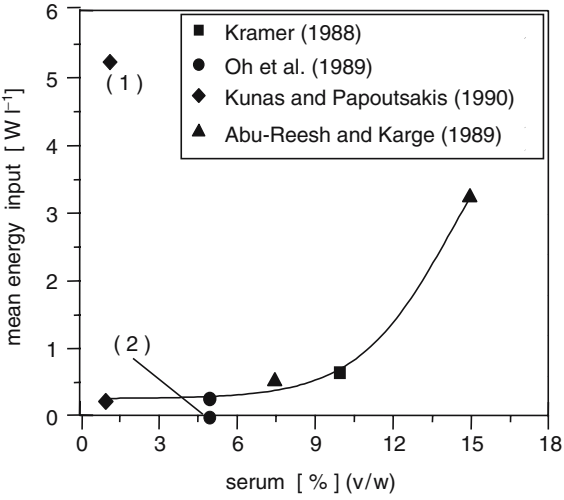

Fig. 4.12 Volume specific energy required for cell death. Mean energy input at 50% of maximal growth versus concentration of serum in the culture medium, (1) bubbles, but without free surface (no foam), (2) surface- and bubble aeration (foam), else: surface aeration

mechanisms have been outlined in Sect. 4.2.1.3. Here aspects relevant for the design and operation of sparged bioreactors (bubble aerated stirred vessels, air-lift bioreactors, bubble column bioreactors) are discussed.

The main mechanisms for cell damage in sparged bioreactors are discussed with reference to a mechanistic analysis suggested by Tramper et al. (1987) and Tramper and Vlak (1988). Assuming a first-order kinetic for cell damage (4.2), the first-order rate constant k_d for cell death was related to all causes of cell death in a sparged bioreactor by

$$k_d = \frac{24 Q V_k}{\pi^2 d_B^3 d_T^2 h_L} \tag{4.14}$$

with the volumetric aeration rate Q, the height of fluid h_L, the vessel diameter d_T, the bubble diameter d_B and a hypothetical killing volume V_k. This approach is based on the idea that cells trapped in the circulation wake of a bubble are carried with the bubble to the surface, where most of the damage takes place. The volume of the bubble wakes is addressed as "killing volume" surrounding the bubbles. From (4.14) some general conclusions can be drawn:

- The specific cell-death rate constant (first-order rate constant) should be proportional to the frequency of bubble generation ($6Q/\pi d_B^3$), the frequency of bubble rupture and the killing volume associated with the bubbles.
- Bubble break-up and foam formation at the culture surface are the principal cause of damage to suspended cells in sparged bioreactors.
- The specific cell-death rate constant should decline with the increasing height of the fluid.
- Events at the sparger and rise stages can be regarded as of minor importance, in particular, bubble coalescence and break-up within the bulk culture.
- Cell damage will increase in direct proportion to the superficial gas velocity in the column or the specific power input.
- Large bubbles should be less damaging than small bubbles.
- Serum or other proteins should have a protective effect.

Most of these statements could be confirmed experimentally (Chisti 2000). Nevertheless the concept of the killing volume itself has some week points. The killing volume V_K seems to be independent of the aeration rate and the height of the fluid, provided that the bubble diameter is not affected. But V_K should increase with bubble diameter indicating increasing cell damage with increasing bubble diameter. This seems to be incorrect, as there are numerous contrary experimental observations in the literature showing reduced cell damage with increasing bubble diameter. [For further discussion of this as well as other concepts of cell damage in sparged bioreactors, see Chisti (2000)].

Cell damage caused by bubbles can be significantly reduced by adding shear-protective substances to the culture medium, including serum and serum proteins (e.g. serum albumin), pluronics or polyethylene glycols among others (Chisti 2000). The protective effect can be physical and/or physiological (biochemical) depending

on the specific agent. The protective effect of serum increases with increasing serum concentration up to 10% v/v serum and seems to be physical and physiological. The physical protective effect can be attributed to reduced plasma-membrane fluidity, increased medium viscosity or a turbulence-dampening effect. The precise nature is not yet clear. Physiological effects seem to take longer to become effective, meaning that a prolonged exposure of cells to serum will reduce their shear sensitivity. In addition to whole serum, serum compounds such as serum albumin also protect cells (e.g. bovine serum albumin (BSA) at >0.4 g L^{-1} (Hülscher et al. 1990)). But despite these shear protecting effects, serum or serum components are mostly avoided in industrial production processes, as discussed earlier (Sect. 2.3).

Alternatively, chemical agents can be used as shear protective agents. The most prominent one is the non-ionic surfactant polyol Pluronic®–F68, a block polymer of poly-oxyethylene and poly-oxypropylene (molar mass 8,358 Da). Typically Pluronic®–F68 is added at 0.5–3 g L^{-1} to the cell culture medium. The protective effect increases with concentration, whereas 0.5 g L^{-1} seems to be a minimum level, and is associated with several, mostly physical mechanisms:

- The attachment of cells to bubbles is reduced; therefore fewer cells are carried to the surface.
- The plasma-membrane fluidity of the cells is reduced.
- The gas–liquid interface is stabilized and therefore the film drainage during bubble rupture is slower.
- The nutritional transport is improved due to a reduced cell-fluid interfacial tension.
- The membrane of the cells is stabilized by incorporating Pluronic®–F68 into the membrane, thus strengthening the cells.

Furthermore, physiological factors, e.g. an effect on the permeability of some cells, have been observed.

Poly-ethyleneglycol (PEG) has been shown to protect some cells but not others. A protecting effect has been found for molecular weights exceeding 1,000 Da and concentrations above 0.25 g L^{-1}. The protective mechanism of PEG seems to be due to an effect on the surface tension and/or the presence of PEG at the gas–liquid interface (Chisti 2000).

Despite the many different protective mechanisms discussed above, the main effect can be attributed to a reduced number of cells adhering to the bubble surface just before its rupture. Additives that rapidly lower the gas-liquid interfacial tension will obviously prevent cell adhesion to bubbles and so reduce cell damage. For a certain culture process, a feasible additive (combination of additives) and an appropriate concentration, as well as the best time for addition, has to be found empirically.

4.1.3.4 Consequences for Reactor Design

For design and operation of sparged and agitated bioreactors some general conclusions can be drawn (Chisti 2000; Fenge and Lüllau 2006; Ma et al. 2006, modified)

- The aeration rate should be kept as low as possible (below 0.1 vvm).
- The sparger should be located such that the rising bubbles do not interact with any impellers.
- The sole purpose of the impeller should be to suspend cells and to mix the fluid gently. Therefore the impeller should be of a type that does not produce excessively high local rates of energy dissipation.
- For air-lift and bubble column bioreactors the aspect ratio (ratio between height and diameter) should be ~14 for small scale and 6–7 for large scale.
- In stirred tanks the mean energy dissipation rate should be below ~ 1,000 W m^{-3}.
- Impeller tip speed should be between 1 and 2 ms^{-1}.
- A suitable additive such as Pluronic®–F68 should be used whenever feasible.

Despite a number of concepts having been suggested in the literature to describe shear effects caused by fluid-mechanical forces or bubbles, none of these concepts allow for a precise layout of large-scale bioreactors (design, operating parameters such as aeration rate, power input or stirrer speed) without additional experiments. Furthermore, experimental findings on a small scale have to be validated on a pilot scale before being transferred to the final industrial scale. A simple strategy for design and scale-up of large scale-reactors based on the concept of a constant power-to-volume-ratio could be as follows:

- Determine the critical mean energy dissipation rate (power input per volume) in a laboratory scale bioreactor geometrically similar to the large scale reactor.
- Calculate the stirrer speed in the large scale bioreactor by considering the mean energy dissipation rate to be constant (e.g. by applying a correlation between the power-number or Newton-number and the Reynolds-number).

In applying this strategy, some restriction should be considered. First an increase in the scale of more than 10:1 might lead to unreasonable values for the stirrer speed. Therefore several scale-up steps from the laboratory to the industrial scale are required and the design criteria have to be evaluated at each step. Furthermore it is not taken into account, that due to an uneven distribution of energy dissipation within a stirred vessel suspended cells or cells grown on microcarriers are exposed to varying levels of shear stress on their way through the vessel. The maximal energy dissipation can differ significantly from the mean energy dissipation, depending on the geometry of the vessel and the stirrer. Additional frequency of exposure to the maximal energy dissipation has to be considered. Henzler and Kauling (1993) have shown some important scale-up relationships (Fig. 4.13). The mechanical stress produced by the liquid increases with the size of the reactor, even if the mean energy dissipation (power input per volume) remains constant. In contrast, the shear produced by the bubbles decreases simultaneously. If the size of the reactor is increased by a factor of 1,000 (from 1 to 1,000 L) the main shear due to aeration decreases by a factor of 10. As cell damage seems to be caused mainly by sparging, this is a very important indication. It suggests that cell damage due to shear stress observed on the laboratory scale is of minor importance in larger reactors. This seems to be one reason why sparging of bioreactors is often regarded as

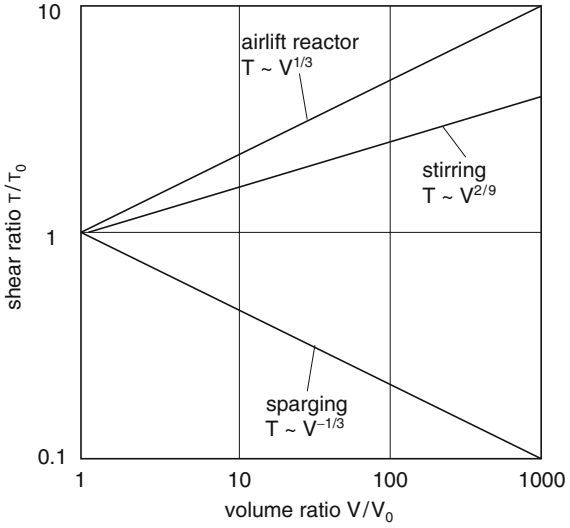

Fig. 4.13 Variation of mechanical stress with increasing reactor volume for *P/V* = constant (adapted from Henzler and Kauling 1993, with kind permission of Springer)

problematic on a laboratory scale, whereas on a large scale it continues to be the preferred and robust method for supplying oxygen to the cell culture.

Varley and Birch (1999) draw some conclusions from research concerned with shear stress on mammalian cells:

- Many suspension cells, especially hybridoma, are not as shear sensitive as thought at first.
- Most cell death is caused by bursting bubbles, even if other reasons for cell death have to be considered and cell death increases when the Kolmogoroff eddy length approaches the size of the cells.
- The range of tolerable aeration rates and stirrer speed for altering mixing is limited.

Implications on design and operation of bioreactors from mammalian cells, especially stirred tanks and air-lift reactors, will be discussed in Sect. 5.1

4.2 Oxygen Supply

4.2.1 Introduction

Mass transfer, including oxygen supply and carbon dioxide removal, is one of the most important factors in operating cell culture bioreactors. Because oxygen is only slightly soluble in medium (approximately 7 mg L^{-1}) and the oxygen

consumption rate (or oxygen uptake rate OUR) is between 3×10^{-10} and 2×10^{-8} mg cell^{-1} h^{-1} (Aunins and Henzler 1993), a typical culture of 2×10^6 cells mL^{-1} would deplete the oxygen dissolved in the medium in under one hour and run out of oxygen rapidly. Therefore it is clearly necessary to supply oxygen during the culture period. Some methods used for this purpose on a small scale are surface aeration, membrane aeration, gas sparging and increase of the partial pressure of oxygen in the headspace or the supplied air (Aunins and Henzler 1993). The scale-up of animal cell cultures is greatly dependent upon the ability to supply sufficient oxygen without causing cell damage. Because of high mass transfer rates and operational simplicity, gas sparging is the preferred method in large scale cell culture. However, cultured animal cells may be damaged by gas sparging (Handa et al. 1987; Kunas and Papoutsakis 1990; Michaels et al. 1996; Zhang et al. 1992a). Cell bubble interactions are generally regarded as the likely cause of this cell damage but the mechanism is not fully understood (Sect. 4.1.3.3) (Chisti 2000; Meier et al. 1999; Wu 1995). It is hypothesized that shear associated with bubble rupture on the bubble surface is the main cause.

The supply of oxygen in the cultivation of animal cells in bioreactors still poses a problem. Even though oxygen consumption rates of animal cell cultures are low compared to cultures of other microorganisms, they must be supplied with a sufficient amount of oxygen. But animal cells are more sensitive to shear stress caused by vigorous mixing and gas sparging. This necessitates a maximum possible oxygen transfer into the liquid phase to keep the mechanical force low (Kunas and Papoutsakis 1990; Fenge et al. 1993; Papoutsakis 1991). In bubble aerated reactor systems, damage to animal cells often occurs due to a wide range of bubble size distribution (Kunas and Papoutsakis 1990; Fenge et al. 1993). It occurs when ascending bubbles force the cells in the medium to the surface (Grima et al. 1997). The stress to the cells is caused by the displosion of bubbles breaking through the surface, resulting in permanent damage (Kunas and Papoutsakis 1990; Papoutsakis 1991).

The size of the bubble appears to be an influential parameter for the tendency of the cells to rise to the surface. Another disadvantage of bubble aeration is that foam could be generated on the surface of the medium, which then could lead to a push-out of the medium out of the bioreactor. But there are several methods available to fight foam production within the vessel (Tan et al. 1994; Zhang et al. 1993). Widely used are silicone based antifoaming agents. The most significant advantage of bubble aeration is its high oxygen mass transfer into water. This high rate is due to a high volume-specific phase surface area and a lower transport resistance compared to membrane procedures.

Because of the relatively high transport resistance, bubble-free aeration systems such as membranes require high membrane surface areas to gain a sufficient oxygen supply into the medium. Also greater effort in installation and maintenance is required in comparison to bubble aeration. Also, the need for sterile operation makes the use of membrane procedures more problematic. In consequence, membrane aeration systems are mostly used in the laboratory and pilot scales (Marks 2003; Henzler and Kauling 1993). Other indirect aeration systems used are

spin filters and vibro mixers. In addition to this, systems with external or perfluorocarbon mediated aeration can be used Gotoh et al. (2001).

But these procedures involve high apparatus costs, which make them unsuitable for large scale production. Also a scale up can be prone to errors. With increase of the inner volume, oxygen transfer progressively becomes more difficult, because the mass transfer efficiency of stirred tank reactors generally decreases as the scale is increased (Marks 2003; Henzler and Kauling 1993). Even though all other aeration methods are technically more complex and lead to less reliability due to the greater number of connection tubes, direct sparging is still the method of choice for the pilot and production scale (Henzler and Kauling 1993; Krahe 2003). Three different shear hypotheses were considered by Henzler and Kauling (1993), who also showed a relation for scale up (Sect. 4.1.3.4). The shear ratio related to increasing volume of the reactor from 1 L to 1 m^3 was calculated and a tenfold decrease of the main shear was found. This finding indicated that shear problems due to bubble aeration observed in the laboratory scale are of minor importance in larger bioreactors (Wu et al. 1995). In recent studies it has been shown that the bubble size has a significant influence on cell damage (Meier et al. 1999). The bigger the cell size the higher the relative speed between the gas bubble and the cell. Three possible causes of cell death are associated with bursting bubbles: bursting bubbles may destroy nearby cells within the suspension due to a shear associated with the burst; cells which are trapped inside a bubble may be damaged by the burst, and a bursting bubble may also damage cells which attached to the bubble during its ascent. The relative effect of each of these is a result of the bubble size and medium properties (Meier et al. 1999; Marks 2003).

Due to the contact of a cell with a bubble, shear stress on the cell membrane is created, which damages the cell. Floating of a cell in foam can also cause cell damage (Wu et al. 1995). Once a foam bubble collapses, the high surface tension results in a destruction of the cell membrane (Ghebeh et al. 2002). Experiments performed by Kunas and Papoutsakis in completely filled bioreactors with microbubbles of sizes between 50 and 300 µm in diameter showed that the cultured hybridomas sustained only very little damage, even when small bubbles were present (Kunas and Papoutsakis 1990). Microbubbles have less relative speed in the fluid, less collision chance and damage ability, due to their higher mean residence time. It was shown by Michaels et al. that it is possible to minimize the frequency of bubble coalescence and breakup events by employing microbubbles for oxygenation at low agitation rates for mixing (Michaels et al. 1996).

As a result of smaller bubble size, the relative surface of the gas in the liquid increases. This leads to a higher mass transfer of oxygen into the liquid. Less gas flow is required to meet the oxygen demand of the living cells. If the reactor is aerated with high oxygen partial pressures and with pulsed aeration profile, most of the bubbles will be completely dissolved before reaching the surface, resulting in less foam. Nowadays nearly every industrial cell culture reactor is equipped with standard ring spargers, spargers or micro spargers. In industrial production with cell cultures the strategy is to use cell lines, which are not so sensitive to cell damage by direct sparging.

4.2.2 Limitations for Oxygen Transfer

Oxygen concentration in media is indicated usually as percentage air saturation, percentage dissolved oxygen, concentration in weight per volume (μg mL^{-1} or mg L^{-1}), p_{O2} or molar units (mmol L^{-1}). Percentage air saturation (identical to percentage dissolved oxygen, % DO) is given by:

$$\% \text{ DO} = (c_L/c^*)\ 100\%,$$

with c_L as the actual oxygen concentration in the medium and c^* as the oxygen concentration in the equilibrium with air (21% oxygen).

Oxygen tension or p_{O2} is the partial pressure of oxygen in the liquid phase in equilibrium with the partial pressure in the gas phase.

The interrelationship between the equilibrium oxygen concentration in media and the partial pressure in the gas phase is given by Henry's law:

$$P_{O2} = c^*\text{He} \tag{4.15}$$

He is Henry's constant which is a function of temperature. Oxygen solubility in pure water between 0 and 36 °C is given by the following equation (Truesdale et al. 1955):

$$c^* = 14.16 - 0.3943T + 0.007714T^2 - 0.0000646T^3. \tag{4.16}$$

With solubility of oxygen c^* in units of mg L^{-1} and temperature T in °C.

The solubility of oxygen in media is also influenced by the presence of electrolytes and organic components so the equilibrium oxygen concentration in medium has to be corrected (Schumpe et al. 1978). Quicker and Schumpe have given an empirical correlation to correct values of oxygen solubility in water for the effects of cations, anions and sugars (Quicker et al. 1981):

$$\text{Log}_{10}(c_0^*/c^*) = 0.5\sum H_i z_i^2 c_{iL} + \sum K_j c_{jL}. \tag{4.17}$$

With:

c_0^*: oxygen solubility at zero solute concentration (mol m^{-3})
c^*: oxygen solubility (mol m^{-3})
H_i: constant for ionic component i (m^3 mol^{-1})
Z_i: valency of ionic component i
c_{iL}: concentration of ionic component i in the liquid (mol m^{-3})
K_j: constant for non-ionic component j in the liquid (m^3 mol^{-1})
c_{jL}: concentration of non-ionic component j in the liquid (mol m^{-3})

Values of H_i and K_j for use in the above equation are listed in literature (Schumpe et al. 1978; Quicker et al. 1981). In a typical fermentation medium oxygen solubility is between 5 and 25% lower than in water as a result of solute effects (Doran 2006).

For RPMI medium the oxygen concentration has been reported to be 0.2 mmol L^{-1} (or 7.1 mg L^{-1} – in equilibrium with air $p_{O2} = 0.21$, $T = 37$ °C) (Oller et al. 1989).

4.2.2.1 Evaluation of Oxygen Consumption and Oxygen Transport Efficiency

High concentrations of oxygen can be toxic for the cells. Effects of different oxygen concentrations on cells are reported in the literature. A good summary is given by Doyle and Griffith (1998) and Ruffieux et al. (1998). Established cell lines function well over a wide range of oxygen concentrations (between 15 and 90% of air saturation). Primary cells are cultivated best at lower oxygen concentrations to simulate the in vivo environment.

The oxygen uptake rate (OUR) or the specific oxygen consumption rate (q) is influenced by the cell type, cell density, proliferative state of the culture, and glucose and glutamine concentration and is a good indicator of cellular activity; under some conditions, it is even a good indicator of the number of viable cells (Doyle and Griffith 1998; Ruffieux et al. 1998; Riley 2006).

For the quantification of the oxygen uptake rate (OUR) and the oxygen transfer rate (OTR), it is necessary to give an unsteady-state mass balance of oxygen within the bioreactor. The mass balance can be written as follows: the change in oxygen concentration over the time in the reactor is equal to the rate of oxygen transfer into the culture (OTR) minus the oxygen consumed by the cells:

$$dc/dt = k_L a(c^* - c_L) - \mathrm{OUR}\ X \tag{4.18}$$

with:
k_La: mass transfer coefficient, which is the product of k_L, the overall mass transfer coefficient from the gas to the liquid phase (two film model), and a, the gas–liquid interfacial area per unit of the reactor liquid volume (s^{-1})
c_L: concentration of oxygen in solution (kg m^{-3})
c^*: equilibrium solubility of oxygen – oxygen saturation (kg m^{-3})
X: cell density (cells L^{-1})
OUR: oxygen uptake rate (kg O_2 10^{-6} cells s^{-1})
t: time (s)
The oxygen transfer rate (OTR) is given by:

$$\mathrm{OTR} = k_L a(c^* - c_L) \tag{4.19}$$

A very common method for measuring the k_La and the OUR is the "dynamic method". The main advantage of the dynamic method is the low cost of equipment needed. There are several different versions of the dynamic method described in the literature. Here only the method with cells in a batch culture is described.

As shown in Fig. 4.14 at some time t_0 the culture is de-oxygenated by stopping the aeration if the culture is oxygen consuming. Dissolved oxygen concentration c_L drops during this period. Before c_L remains c_{crit} the aeration is started and the increase in c_L is monitored as a function of time. Assuming re-oxygenation is fast relative to cell

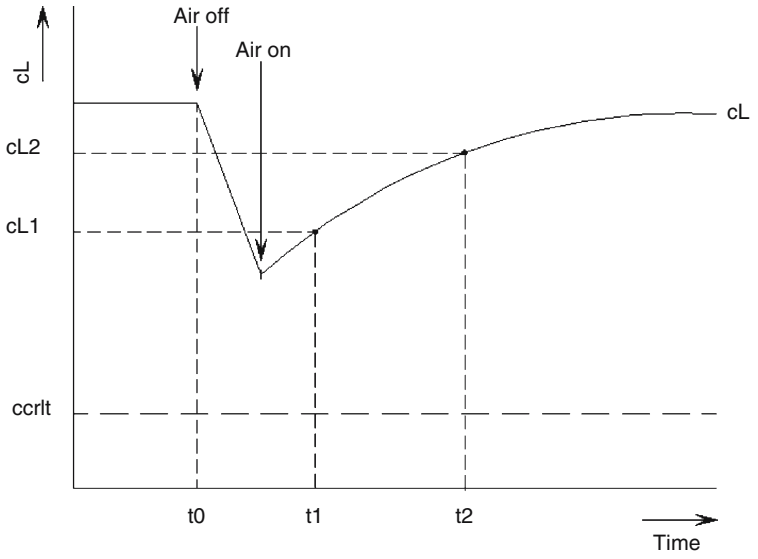

Fig. 4.14 Variation of oxygen tension for dynamic measurement of $k_L a$

growth, the dissolved oxygen level will soon reach a steady state value c_{AL} which reflects a balance between oxygen supply and oxygen consumption in the system.

During the re-oxygenation step the system is not in steady state and we can use the above unsteady-state mass balance (4.19). When $c_L = c_{AL}$, dc/dt = 0 because there is no change in c_L with time. Therefore:

$$\text{OUR X} = k_L a(c^* - c_{AL}). \tag{4.20}$$

Substituting the result into (4.19) and cancelling the term k_La· c* gives:

$$\mathrm{d}c/\mathrm{dt} = k_L a(c_{AL} - c_L). \tag{4.21}$$

Assuming k_La is constant with time, we can integrate (4.21) between t_1 and t_2. The resulting term for k_La is:

$$k_L a = \ln[(c_{AL} - c_{L1}) / (c_{AL} - c_{L2})] / (t_2 - t_1). \tag{4.22}$$

When ln $[(c_{AL} - c_{L1})/(c_{AL} - c_{L2})]$ is plotted against $(t_2 - t_1)$ as shown in Fig. 4.15 the slope is k_La.

Equation (4.22) can be applied to actively oxygen consuming cultures or to systems without oxygen uptake.

In the de-oxygenation period the slope of the dissolved oxygen concentration profile is the oxygen uptake rate (OUR) because (4.18) reduces to

$$\mathrm{d}c_L / dt = -\text{QUR X} \tag{4.23}$$

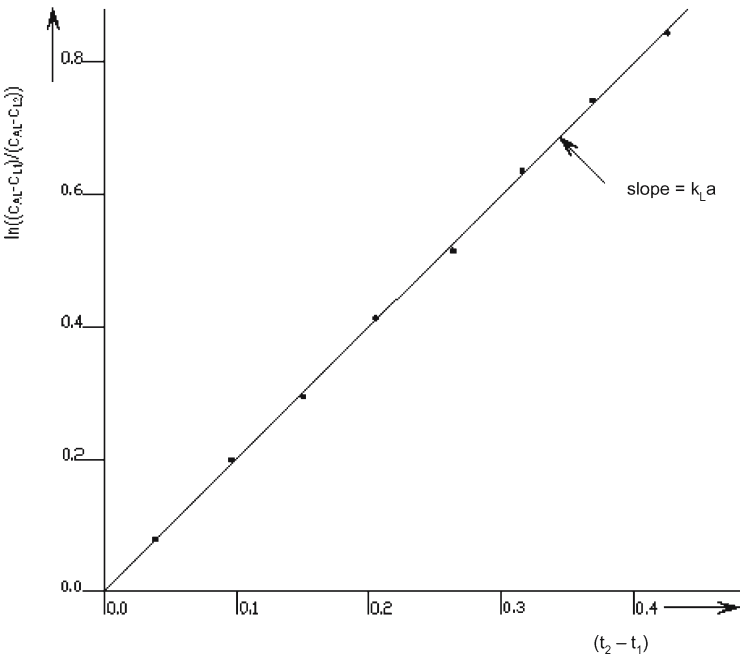

Fig. 4.15 Evaluating $k_L a$ using the dynamic method

for a reactor where the oxygen transfer term can be neglected. The most critical step is the removal of all air bubbles from the reactor.

4.2.3 Oxygen Supply Systems (Aeration Systems)

A culture can be aerated by one, or a combination, of the following methods: surface aeration, direct sparging, indirect and/or membrane aeration (diffusion), medium perfusion, increasing the partial pressure of oxygen, and increasing the atmospheric pressure (Griffith 2000; Varley and Birch 1999). Methods of oxygen supply for submerse fermentation of animal cells can be seen in Fig. 4.16.

4.2.3.1 Surface Aeration

In surface aeration, mass transfer occurs only through the surface of the liquid. To increase the mass transfer by increasing the effective phase interface, a second impeller should be located at the interface or near the liquid interface (Fig. 4.17).

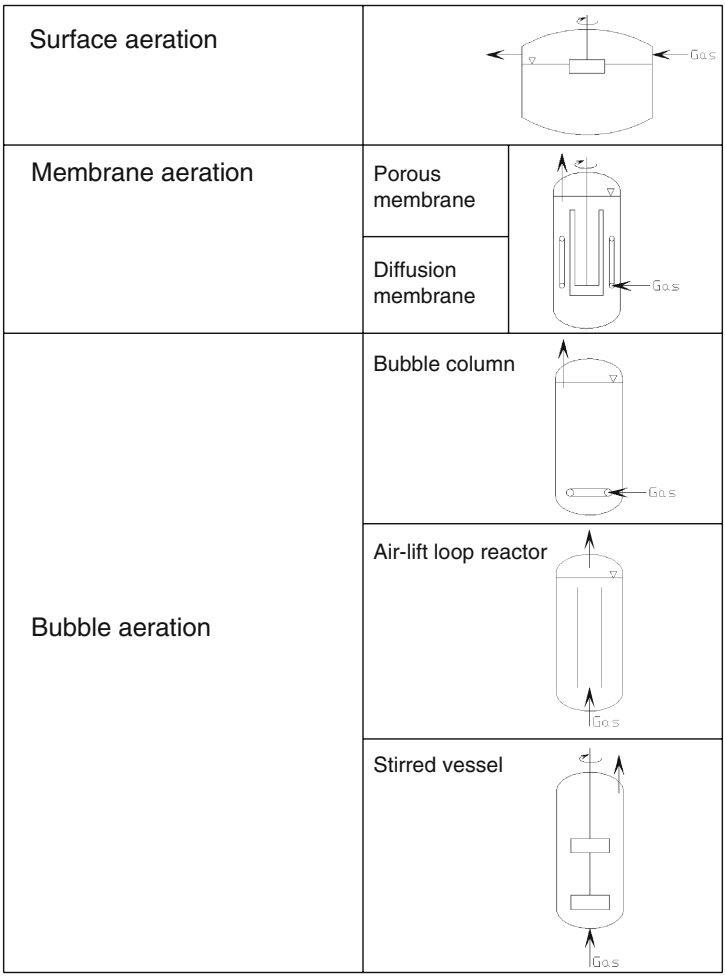

Fig. 4.16 Methods of oxygen supply for submers fermentation of animal cells [adapted from Henzler and Kauling (1993) with kind permission of Springer Science and Business Media]

Alternatively an intensive wave motion could be inserted (wave bioreactor) (Singh 1999; Sect. 5.1.4). The partially submerged second impeller (surface aerator) was seen to increase the mass transfer coefficient four times for laboratory scale stirred reactors (Hu et al. 1986). Because bubble introduction should be avoided, oxygen input cannot be increased indefinitely by surface aeration. Henzler and Kauling (1993) gave correlations in the low power input range based on experimental data for the volumetric mass transfer coefficient k_La, the limiting speed of the impeller located at the interface and for the scale-up.

$$k_L a(H_R/D_R) = f(d_R/D_R)(n_R{}^2 d/g) \tag{4.24}$$

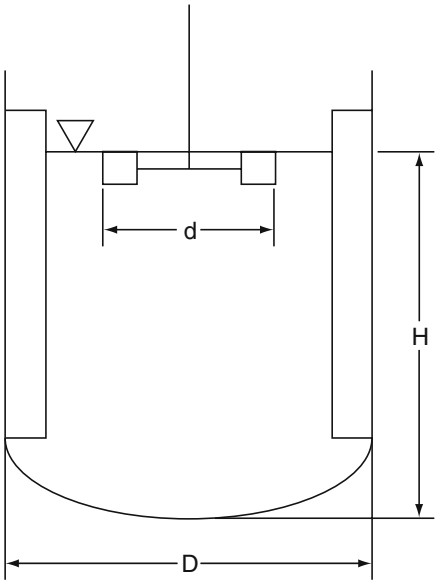

Fig. 4.17 Schematic of a reactor with surface aeration [stirrer at interface – adapted from Henzler and Kauling (1993) with kind permission of Springer Science and Business Media]

with
H_R: filling height of the stirred reactor – impeller located at the interface (m)
D_R: reactor diameter (m)
d_R: impeller diameter (m)
n_R: impeller speed (s^{-1})
g: acceleration due to gravity ($m^2\ s^{-1}$)
and

$$f(d_R/D_R) = [(d_R/D_R) - 0.13]400 \tag{4.25}$$

for $d_R/D_R > 0.15$

Henzler and Kauling (1993) show that even for semi-industrial scale, sufficient oxygenation of cell cultures cannot be provided by the surface of the liquid. Therefore surface aeration is sufficient only for low density cultures in small vessels like T-flasks, roller bottles and bench scale vessels, where a relatively large ratio of air-medium interface to volume exists.

4.2.3.2 Direct Sparging

Direct gas sparging into the medium is the most common and simple way to supply oxygen into the bioreactor (Marks 2003; Varley and Birch 1999; Chalmers 1994). Aeration with spargers gives high oxygen transfer rates caused by large interfacial

area, a, for bubbles (Fenge et al. 1993; Henzler and Kauling 1993; Varley and Birch 1999; Moreira et al. 1995; Nehring et al. 2004). Disadvantages of direct sparging are possible cell damage and foaming of the culture (Kunas and Papoutsakis 1990; Michaels et al. 1996; Chisti 2000; Meier et al. 1999; Wu 1995; Henzler and Kauling 1993; Zhang et al. 1992a,b). Anyway many different cell types have been grown successfully in air-sparged bioreactors such as bubble columns, airlift reactors or agitated/stirred vessels (Doyle and Griffith 1998; Ma et al. 2006).

Interfacial area (a) will also obviously affect $k_L a$. Oxygen transfer rates increase as the size of bubbles decreases. Bubble size will generally be in the region of 4–6 mm for sparging with standard spargers (metal sparger, ring injector) or 0.1–1 mm for sparging with micro spargers (e.g. ceramic) (Varley and Birch 1999; Nehring et al. 2004). The effects of additives including new born calf serum and Pluronic F-68 were found to depend on the size of the bubbles (Henzler and Kauling 1993; Varley and Birch 1999; Moreira et al. 1995). Although it is known that bubble coalescence is important, as it affects bubble size and hence interfacial area and $k_L a$, the effect of fluid properties and surface properties is still not well understood (Varley and Birch 1999).

Correlations based on the most relevant bubbling regimes for animal cell culture are available for predicting the bubble size at the sparger: separate bubble formation and chain bubbling (Varley and Birch 1999).

For separate bubbling:

$$d_s = 1.7\,[\sigma d_o / (\Delta\rho g)]^{1/3} \tag{4.26}$$

where
d_s: Sauter mean diameter (m)
σ: surface tension (kg s^{-2})
d_o: orifice diameter (m)
$\Delta\rho$: density difference (kg m^{-3})
g: acceleration due to gravity (m^2 s^{-1})
For the chain bubbling regime:

$$d_s = 1.17 v_0^{\,0.4} d_0^{\,0.8} g^{-0.2} \tag{4.27}$$

with
v_0: gas velocity at the sparger (m s^{-1})

Equations have been proposed for bubble size for turbulent flow (generally stirred sparged vessels) far from the sparger, both for non-coalescing and coalescing solutions. However, at the low gas flow rates and low agitation rates used in animal cell culture, the bubble size far from the sparger is likely to be equal to the bubble size at the sparger (Varley and Birch 1999).

There are several correlations for the oxygen transfer coefficient in the literature (Henzler and Kauling 1993; Moreira et al. 1995; Ma et al. 2006; Moo-Young and Blanch 1981).

For specified medium, specified reactor dimensions and type of sparger, the mass transfer coefficient $k_L a$ in bubble columns and loop reactors (e.g. airlift) depends only on the superficial gas velocity (Henzler and Kauling 1993).

$$k_L a = C v^{\alpha} \tag{4.28}$$

with
C: constant
v: superficial gas velocity (m s^{-1})
α: exponent (further function of superficial velocity).

The influence of sparger holes/pores is noticeable at low gas velocity in the range desired for the oxygenation of cell cultures (Henzler and Kauling 1993; Nehring et al. 2004). With increasing gas velocity the aeration efficiency ($k_L a/v$) decreases as a result of increasing coalescence, so it makes sense to use oxygen-enriched air to minimize shear due to gas bubbles (Henzler and Kauling 1993). Using special ceramic micro-spargers or increasing gas velocities gives a uniform distribution of the gas over all the sparger holes/pores and a more homogenous bubble size distribution (Figs. 4.18 and 4.19). This leads to reduced coalescence because of the decrease in the local gas hold-up (Henzler and Kauling 1993). Henzler and Kauling (1993) showed that the mass transfer is hindered in protein-containing media by the presence of protein at the interface, especially for smaller bubbles, because of the increased foam formation tendency of protein-containing media and a resulting increase in coalescence of bubbles.

The mass transfer can be enhanced by stirring. Therefore lower gas velocities are necessary in sparged bioreactors with agitation than in bubble column reactors. For industrial animal cell reactors, gas flow rates of 1 vvh (volume gas per volume reactor per hour) for bubble columns and 0.1–1 vvh for aerated and stirred reactors have been reported (Bliem et al. 1991). These lower gas flow rates may reduce the level of required antifoam agents and shear protectants (Czermak and Nehring 1999). For cell culture, the region of low impeller power is of interest. The $k_L a$ is independent of the type and geometry of the impeller if sufficient mixing takes place in the bioreactor. As the viscosity of cell culture media is low, this assumption is usually satisfied (Henzler and Kauling 1993).

For stirred reactors (4.27) becomes the form

$$k_L a = C v^{\alpha} (P/V)^{\beta} \tag{4.29}$$

with
P/V: power input per unit volume of gas dispersion (kg m s^{-3})
β: exponent independent of scale and impeller type.
Table 4.3 gives $k_L a$ values, determined using the dynamic method (Nehring et al. 2004), for standard stirred bioreactors (Braun Biotech/Sartorius) on different scales, equipped with propeller or three-blade segment impeller (both are axial mixing stirrers) and different sparger systems (microsparger – stainless steel, Braun Biotech/Sartorius; microsparger – ceramic, BIM/Applikon Biotechnology; ring sparger – stainless steel, Braun Biotech/Sartorius).

Hydrophilic materials such as porous ceramics are suited to the production of microbubbles (Figs. 4.18 – 4.20) in water-based fluids. The formation of microbubbles (bubbles sizes differ in diameter from 100 to 500 µm (Nehring et al. 2004;

Table 4.3 $k_L a$ values for standard stirred bioreactors (Braun Biotech/Sartorius) in different scale equipped with propeller or three blade segment impeller (both are axial mixing stirrers) and different sparger systems (microsparger – stainless steel, Braun Biotech/Sartorius; microsparger – ceramic, BIM/Applikon Biotechnology; ring sparger – stainless steel, Braun Biotech/Sartorius)

Reactor type	rpm	Aeration System	Sparging rate (vvm)	Medium	$k_L a$ (h^{-1})	References
Biostat ECD 10 L	50	Microsparger 100 µm pores (stainless steel)	0.1	Tap-water	9.3	(Fenge et al. 1993)
Biostat UCD 40 L	20	Microsparger 100 µm pores (stainless steel)	0.1	Tap-water	7.1	(Fenge et al. 1993)
Biostat UCD 35 L	20	Ring sparger 1 mm pores	0.1	Tap-water	4.9	(Fenge et al. 1993)
Biostat B 5 L	50	Microsparger 2–5 µm pores (ceramic – TiO_2)	0.1	RPMI 1640	33.1	(Nehring et al. 2004; Bliem et al. 1991)
Biostat B 5 L	50	Microsparger 100 µm pores (stainless steel)	0.1	RPMI 1640	10.1	(Nehring et al. 2004; Bliem et al. 1991)
Biostat B 5 L	50	Microsparger 2–5 µm pores (ceramic – TiO_2)	0.05	RPMI 1640	30.6	(Nehring et al. 2004; Bliem et al. 1991)
Biostat B 5 L	50	Microsparger 100 µm pores (stainless steel)	0.05	RPMI 1640	9.4	(Nehring et al. 2004; Bliem et al. 1991)
Biostat B 5 L	100	Microsparger 2–5 µm pores (ceramic – TiO_2)	0.1	RPMI 1640	50.4	(Nehring et al. 2004; Bliem et al. 1991)
Biostat B 5 L	100	Microsparger 100 µm pores (stainless steel)	0.1	RPMI 1640	10.4	(Nehring et al. 2004; Bliem et al. 1991)
Biostat B 5 L	100	Microsparger 2–5 µm pores (ceramic – TiO_2)	0.05	RPMI 1640	32.8	(Nehring et al. 2004; Bliem et al. 1991)
Biostat B 5 L	100	Microsparger 100 µm pores (stainless steel)	0.05	RPMI 1640	9.7	(Nehring et al. 2004; Bliem et al. 1991)

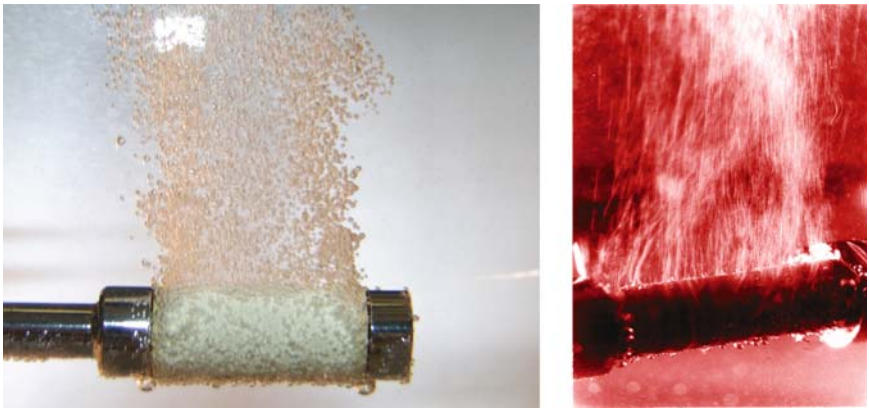

Fig. 4.18 The ceramic sparger tip in buffer and DMEM medium

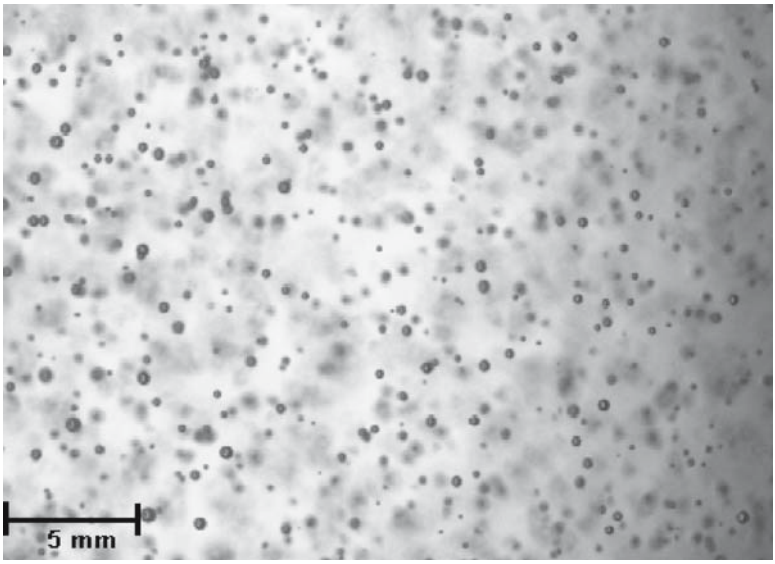

Fig. 4.19 Bubbles in phosphate buffer aerated by a ceramic sparger. Bubbles sizes differ in diameter from 100 to 500 µm (from Nehring et al. (2004) with kind permission of American Chemical Society)

Bliem et al. 1991)) is due to the small contact angle between the water and ceramic. The high k_La-values of the ceramic microsparger aeration system clearly show that a significantly better oxygen transfer into the medium was achieved by the larger phase surface area and in addition by the fact that the gas bubbles remained longer in the bioreactor (Nehring et al. 2004).

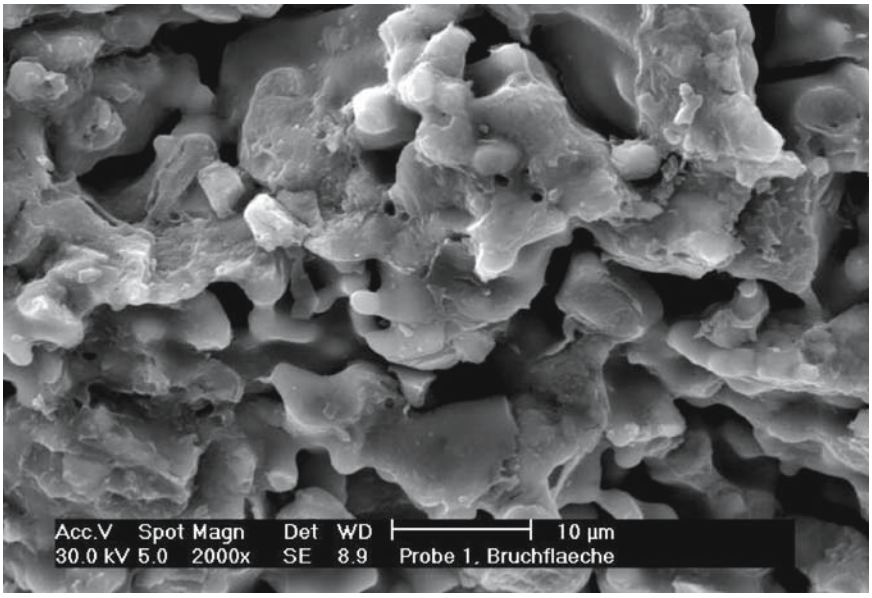

Fig. 4.20 SEM images of the porous structure of a zirconium dioxide microsparger cross section (The image was taken after breaking the ceramic tube across the diameter)

The culture of cells on microcarriers in sparged reactors requires low gas flow rates, small bubble diameter for high oxygen transfer rates, low mechanical agitation and the use of antifoams to avoid shear stress to the anchorage dependent cells and to avoid flotation of the carriers (Doyle and Griffith 1998). By using a ceramic microsparger system, five times higher $k_L a$ values (two microspargers integrated into the baffles) in comparison to stainless steel microspargers (Applikon Biotechnology) were shown for a microcarrier culture (3 g L^{-1} Cytodex 3 microcarrier; DMEM medium) in a 75 L stirred reactor (H/D = 1.5; 2 propeller stirrers with different diameter; 33 rpm) at a very low aeration rate of 0.001 vvm (Czermak and Nehring 2000).

4.2.3.3 Membrane Aeration

Bubble free oxygenation of cell culture media by membrane aeration with open-pore membranes or diffusion membranes can be seen in (Figs. 4.21–4.23) (Aunins and Henzler 1993; Henzler and Kauling 1993; Qi et al. 2003; Schneider et al 1995).

For microporous membranes, the medium is in direct contact with air in the micropores of the membrane. The air–liquid interface in the pores is controlled by pressure and hydrophobic force. For diffusion membranes oxygen diffuses first from the gas phase into the oxygen soluble membrane (very common: silicone rubber) and then into the culture medium.

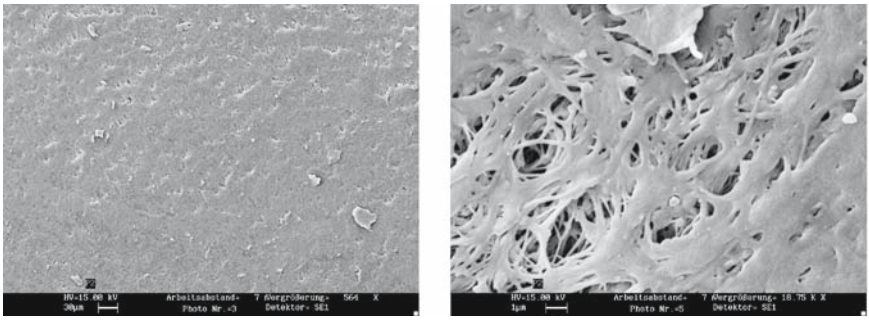

Fig. 4.21 REM cross section of a porous oxygenation membrane (PP)

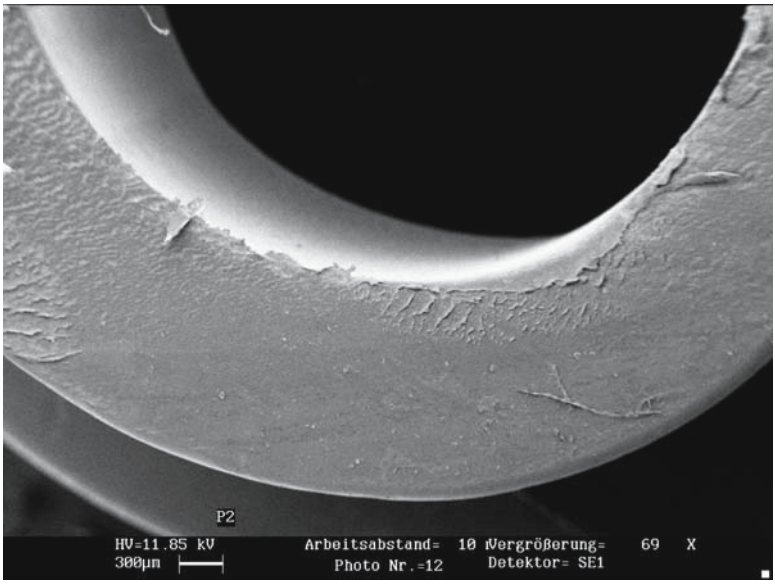

Fig. 4.22 REM cross section of diffusion membrane (silicon tube)

In the case of oxygenation with microporous membranes there is the mass transfer coefficient at the gas–liquid interface k equal to k_L (4.29) (Aunins and Henzler 1993; Henzler and Kauling 1993). In aeration with diffusion membranes, k is an overall mass transfer coefficient at the liquid side coefficient k_L and additional membrane diffusion (tubular membrane):

$$k=1/[(1/k_L+[d_2\ln(d_2/d_1)]/(2D_sHe_w/H_s)] \tag{4.30}$$

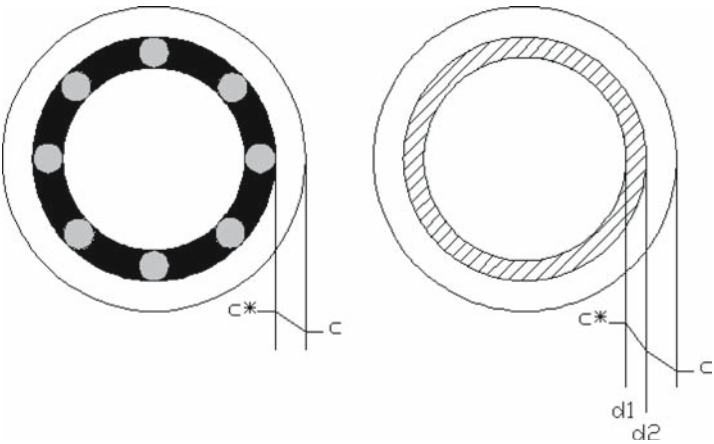

Fig. 4.23 Concentration profiles for oxygen supply via membranes [adapted from Henzler and Kauling (1993)]

with:
k: mass transfer coefficient at the gas–liquid interface (m s^{-1})
k_L: mass transfer coefficient at the liquid-side interface (m s^{-1})
d_2: outer diameter of the membrane tube (m)
d_1: inner diameter of the membrane tube (m)
D_s: diffusion coefficient of oxygen in the membrane (m^2 s^{-1})
He_w: Henry constant of oxygen in water (m^2 s^{-2})
He_s: Henry constant of oxygen in membrane material (m^2 s^{-2})
For the material constant $D_s He_w/He_s$ of silicone the temperature dependence in the range of 10–40 °C is as follows (Henzler and Kauling 1993; Bräutigam 1985):

$$D_s He_w/He_s \sim 7.3\times10^{-9}\exp(0.024T)(\mathrm{m^2\,s^{-1}}) \tag{4.31}$$

For the description of the mass transfer coefficient k_L, it is suitable to use dimensionless relations in the form of Sh = f (Re, Sc) with the Sherwood number $Sh = k_L d_2/D$. Correlations are given by Aunins and Henzler (1993) and Henzler and Kauling (1993).

The main factors which affect the oxygen transfer are the oxygen concentration in the supply gas, the membrane porosity and the surface area of the membrane, as well as the value of k_L influenced by agitation of the medium by a stirrer or by movement of the membranes (dynamic membrane aeration).

The advantages of membrane aeration for cells sensitive to sparging, microsparging and foam formation are superposed by limitations such as the complexity of the process, limited design data, large membrane area, difficulties in maintenance and cleaning. In addition, proteins can foul the membrane potentially altering the hydrophobic properties of the membranes, especially at porous membranes (Aunins and Henzler 1993; Henzler and Kauling 1993; Doyle and Griffith 1998; Ma et al. 2006;

Qi et al. 2003; Schneider et al. 1995). With membrane aeration, oxygen transfer rates comparable to direct sparging are possible, but high gas pressures and flow rates are necessary for it (Aunins and Henzler 1993; Henzler and Kauling 1993; Moreira et al. 1995). Because of the large membrane area required (2–3 m of silicone tubing per litre of medium) membrane aeration is used to small and intermediate scale bioreactors (5–500 L) only (Doyle and Griffith 1998; Ma et al. 2006).

To overcome the limitations of standard membrane aeration (Fig. 4.24), especially with increasing scale, the newly developed dynamic membrane aeration system is of interest (Fig. 4.25) (Frahm et al. 2007; Rampe 2006). The silicone tubes (membranes) are wrapped on a rotor. This membrane carrier is placed in an oscillating circular motion. Therefore the flow of the medium at the membranes and the mass transfer is enhanced. In addition there are no moving gaskets for the gas supply, with the resulting advantages for cleaning, design and scale-up (Frahm et al. 2007).

In Table 4.4 the mass transfer coefficient (for the membrane and the liquid film for oxygen) is listed for different power inputs to show the efficiency increase by oscillating the silicone membrane tubing through the medium (dynamic membrane aeration) compared to a standard membrane aeration system, where the silicone membrane tubing is wrapped in a basket (stator) and fluid flow around the tubing is generated by an anchor stirrer (Frahm et al. 2007). Figure 4.25 shows a dynamic aeration rotor at a 200 L scale. It is easy to scale-up the membrane area by adjusting the number of rotor arms and/or by branching out the rotor arms and therefore the volume specific mass transfer coefficient k_a of the dynamic membrane aeration system is much higher than a comparable standard membrane aeration system with silicone tubing.

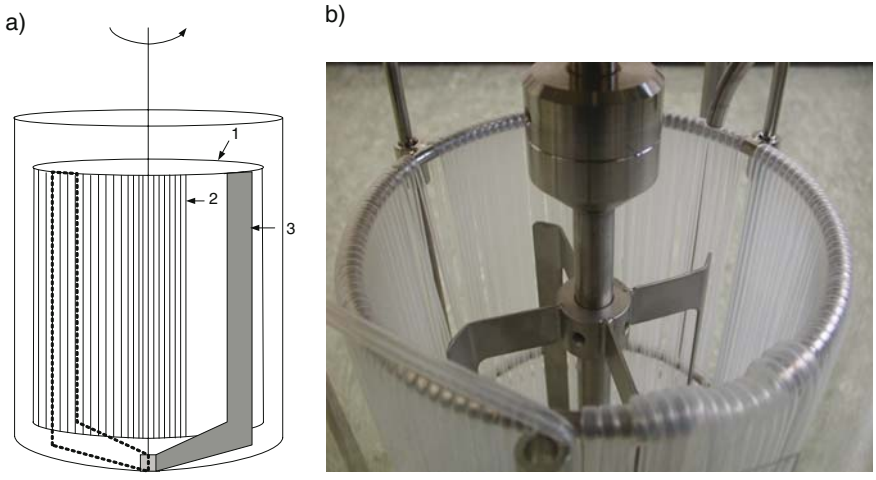

Fig. 4.24 (**a**) Schematic of a standard membrane aeration system (1) membrane basket (2) silicone tubing (3) anchor stirrer (**b**) photograph of membrane basket and anchor stirrer (with courtesy from Bayer Technology Services GmbH, Germany)

Fig. 4.25 Photograph of the dynamic membrane aeration system (DMA) for a 200 L cell culture reactor (with courtesy from Bayer Technology Services GmbH, Germany)

Table 4.4 Mass transfer coefficient for oxygen (membrane and liquid film) in dependence of power input per liquid volume (100 L reactor volume) adapted from (Frahm et al. 2007)

Aeration system	P/V (W m^{-3})	k (m h^{-1})
Dynamic membrane aeration	10	0.075
Membrane stator	10	0.055
Dynamic membrane aeration	100	0.09
Membrane stator	100	0.07

4.2.4 Consequences for Reactor Design and Operation

Ozturk calculated the limit in the cell densities for several aeration systems based on the mass transfer coefficients reported by Henzler and Kauling see Fig. 4.26 [adapted from Ozturk (1996)].

Surface aeration is not sufficient for high density cultures. Membrane aeration as a better method for oxygen delivery at high density cultures can be used inside or outside of the bioreactor, in the form of a basket or gas exchanger, respectively. The mass transfer in membrane aeration depends on the length of tubing per reactor volume. Handling membrane aeration systems increases by reactor size and is not manageable for high density systems larger than to 200 L. Membrane aeration using silicone tubing can provide enough oxygen to support 5×10^7 cells mL^{-1} (Fig. 4.26). In cultures aerated by spargers, higher mass transfer rates and thus higher cell densities can be achieved. Cell lysis and foaming limit the sparging rates to about 0.1 vvm (Ozturk 1996). Selection of a good sparger is important for minimizing the foaming and maximizing the mass transfer rates (Fenge et al. 1993; Nehring et al. 2004; Zhang et al. 1992a,b). The use of micro spargers (such as sintered metal or ceramic), provides more mass transfer area and therefore higher $k_L a$. Micro bubbles can increase the foaming problems by producing more dense foam (Fig. 4.27).

Macro spargers create bubbles greater than 2 mm and are more appropriate for minimizing the foaming (Ma et al. 2006; Ozturk 1996). Though the mass transfer coefficients are lower for macro spargers, and higher gas flow rates should be used to achieve the same cell density as micro spargers. However, Henzler and Kauling

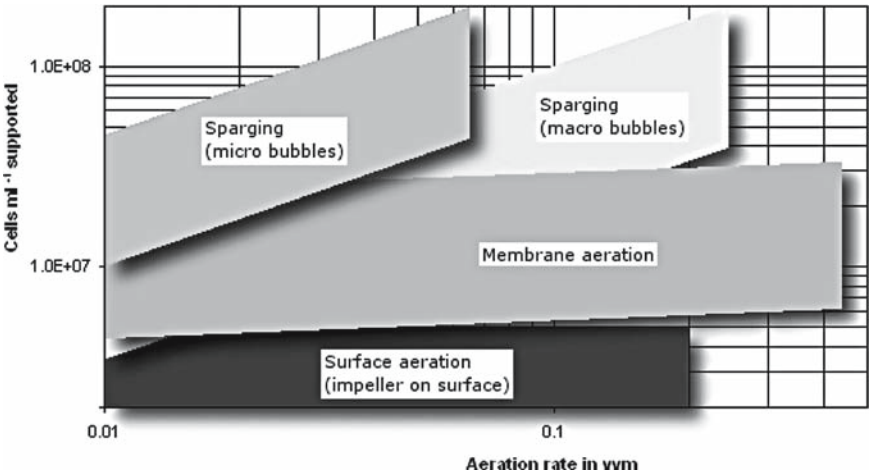

Fig. 4.26 Limitations in cell density based on oxygen delivery in different aeration systems (adapted from Ozturk (1996) with kind permission of Springer Science and Business Media)

Fig. 4.27 5–10 mm foam layer at the medium surface (cell line: CHO-easyC – CHO-K1 derived line, Cell Culture Technologies GmbH, Zürich, Switzerland; CHO-master HP-1 medium; aerated with a ceramic micro sparger Fig. 4.18

(1993) showed that if the size of the reactor is increased, e.g., from V = 1 L to V = 1,000 L, the main shear due to the aeration decreases by a factor of 10. They suggest that problems observed on lab scale with sparger aeration are of minor importance in larger reactors; thus in many cases sparger aeration can be used for oxygenation even in production processes with animal cells. Nehring et al. (2004) compared a microsparging aeration system made of porous ceramic with bubble-free membrane aeration in the cultivation of MDCK cells and in the cultivation of virus infected MDCK cells (2, 5, 30 and 100 L reactor scale). They achieved similar results for cell densities. Antifoaming agents such as Pluronic F-68 and lowering gassing rates and agitation speed (possible when using micro sparger systems) can decrease the problems related to sparging, such as foaming and cell damage (Aunins and Henzler 1993; Nehring et al. 2004; Ozturk 1996; Ma et al. 2004; Dey et al. 1997). However, the introduction of such additives decreases mass transfer and results in problems in the downstream processing (Aunins and Henzler 1993).

4.2.4.1 CO_2 Accumulation

CO_2 plays an important role in cell culture. The solute species of CO_2 in the form of CO_2, HCO_3^-, H_2CO_3 or CO_3^{2-}, and therefore the variation of CO_2 concentrations, influences the pH of the medium when using sodium bicarbonate as the pH buffer. In addition CO_2 is a potentially inhibitory byproduct in cell cultures. So CO_2 accumulation and excessive removal should be avoided (Ma et al. 2006; Ozturk 1996). Aeration removes CO_2 from the system and leads to a more complex gas exchange with respect to the balance between O_2 addition and CO_2 removal. The partial pressure of metabolically produced carbon dioxide (pCO_2) and hence mass transfer of carbon dioxide from solution to the gas bubbles is important in animal cell culture. A rise in pCO_2 can cause a rise in H_2CO_3 and hence a drop in pH. pCO_2 must therefore be carefully monitored and controlled (Marks 2003; Varley and Birch 1999; Ma et al. 2006). The accumulation of CO_2 depends on the mass transfer characteristics of the aeration system. The mass transfer coefficients for CO_2 and O_2 are not very different when using sparger for aeration and CO_2 accumulation is a minor problem. If a micro sparger system is used for aeration, CO_2 stripping can still be a problem. Small bubbles get saturated by the CO_2 more easily than large bubbles and the efficiency of CO_2 removal decreases. While using membrane aeration, CO_2 accumulation is of greater importance. Depending on the material, the mass transfer coefficients for O_2 and CO_2 can be very different. For silicone tubing the CO_2 mass transfer coefficient is measured to be about four times lower than that of O_2 (Ozturk 1996). However, a proper pH control is necessary.

4.3 Immobilization of Cells

Biocatalysts (e.g. cells) are regarded as immobilized when they are restricted in their motility while their metabolic or catalytic activity is maintained (Lundgren and Blüml 1998). *In vivo,* mammalian cells are immobilized in tissues and organs and perfused by lymph, blood, etc. *In vitro,* immobilization is primarily used to increase the stability and the process intensity of the culture. Immobilization of mammalian cells was first described as early as 1923 by Carrel (1923). Since then, different techniques for immobilizing mammalian cells have been proposed, including entrapping cells on a particle surface or in the interstices of a porous particle, encapsulation of cells within gels, or growth of cells within compartments formed by membranes (Lundgren and Blüml 1998; Butler 2004; Davis and Hanak 1997; Davis 2007). These techniques are widely applied, as they offer some solutions to problems inherent in mammalian cell culture:

- Attachment of anchorage-dependent cells is the only way these cells can grow.
- Immobilization in macroporous carriers can protect cells against shear stress, promoting the use of serum- or protein-free medium (Lüdemann et al. 1996, Sect. 5.1.2).

- Cell densities in immobilized systems are considerably higher compared to those without immobilization (e.g., suspension culture approx. 10^6–10^7 cells mL^{-1}, immobilized culture approx. 10^7–10^8 cells mL^{-1}, tissue approx. 10^9 cells mL^{-1}) and allow for smaller reactor volumes.
- Immobilization techniques enable preliminary separation of (extracellular) products and cells, easing requirements for downstream.
- Immobilization systems are preferably run in perfusion mode (Sect. 4.4), where the medium feed rate is not dependent on the growth rate of the cells and higher volume-specific productivities can be obtained.

Besides these advantages of immobilization techniques, several problems have to be solved depending on the specific system:

- Materials have to be selected according to the requirements of the cells and the culture system. Especially in the case of adherent cells, they have to promote cell attachment and spreading, a complex mechanism as shown in Fig. 2.1 (Sect. 2.2.1).
- All techniques involving the growth of cells in a three-dimensional structure, mass transfer effects, especially nutrient and oxygen supply, as well as removal of toxic metabolites and carbon dioxide, have to be considered.

In the following sections, the different techniques for cell immobilisation are briefly discussed, as this has been done extensively by a number of reviews and text books (Lundgren and Blüml 1998; Butler 2004; Davis and Hanak 1997; Kelly et al. 1993; Howaldt et al. 2005; Ozturk and Hu 2006; Hübner 2007). Special attention is paid to mass transfer aspects to give a deeper understanding of the underlying mechanisms and resulting consequences. The main focus is on solid and macroporous carriers for immobilization of mammalian cells as well as on encapsulation techniques. Membrane-based bioreactor concepts are discussed in Sect. 5.1.3 for production of biopharmaceuticals and in Part II, Chap. 2 for tissue engineering.

4.3.1 Carriers for Cell Immobilization

4.3.1.1 General Aspects

The development of carriers to support cell growth was initially driven by the idea to provide a large-scale production system for adherent cells, e.g., for vaccine production. In the early sixties facilities for vaccine production used batteries of roller bottles. Scale-up was possible by increasing the number of roller bottles used. The high labour intensity of this technology is quite obvious. An important breakthrough was the development of the so called “microcarrier” by van Wezel (1967) in the beginning of the seventies, a solid particle with a 100–200 µm structure, on which the cells could grow. As the microcarriers are suspendable in stirred tanks, it became possible to work with large scale suspension reactors (nowadays up to 4,000 L (Lundgren and Blüml 1998). The great success of this technology led to the development of a large number of different microcarriers for suspension

culture and furthermore for different reactor systems, especially for fixed-bed and fluidized-bed reactors (Lundgren and Blüml 1998). The desired features of a carrier can be defined according to Lundgren and Blüml (1998) as well as Pörtner and Märkl (1995):

- Autoclavable
- Available in large batches for industrial customers
- Available with documents required for approval (Drug master or regulatory support files)
- High batch-to-batch consistency
- Suitable for a large number of cell lines (adherent and non-adherent cells)
- Good long-term stability
- High surface-to-volume ratio (large multiplication steps)
- Material of non-biological origin (minimal viral risks)
- Macroporous for high cell density and shear force protection
- Efficient diffusion from the medium into the center of the carriers
- Non-toxic, non-immunogenic matrix
- Size appropriate to reactor system
- Simple immobilization and harvesting of cells
- Mechanical stability
- Uniform size distribution
- Reusable
- Possibility to count cells
- Transferable between vessels (ease of scale-up)
- Transparent

Even if an "ideal" carrier does not exist, the above list gives some arguments for selecting a carrier or evaluating different suppliers. Although for research purposes aspects such as good growth conditions might be mainly important, for production processes, other aspects related to the approval of the process and maintaining the process for the lifespan of the product have to be considered.

Depending on the intended culture system, the properties of the carriers, especially the size, vary significantly (from 10 µm to 5 mm). In Fig. 4.28 different carriers are grouped according to size. The term "microcarrier" is traditionally used basically for those carriers used in suspension culture with an ideal size of 150–500 µm. Larger carriers are used for fluidized and fixed bed reactors due to the higher sedimentation rate. For fluidized bed reactors, carriers having a size of 0.6 to 1 mm are used. For fixed-bed cultures, larger carriers (3–5 mm) are better, to prevent blocking of free channels between the carriers. Obviously larger carriers will have limitations in terms of mass-transfer-effects, especially with respect to oxygen supply, because of the poor solubility of oxygen in the medium and the high uptake rate of the cells. This will be discussed later in this chapter.

A wide variety of different materials has been suggested for carriers (Lundgren and Blüml 1998; Pörtner and Platas Barradas 2007; Pörtner et al. 2007) including dextran, collagen, polymers, glass, and ceramic (among others), as they have a great impact on parameters such as toxicity, hydrophobicity, micro- and macroporosity,

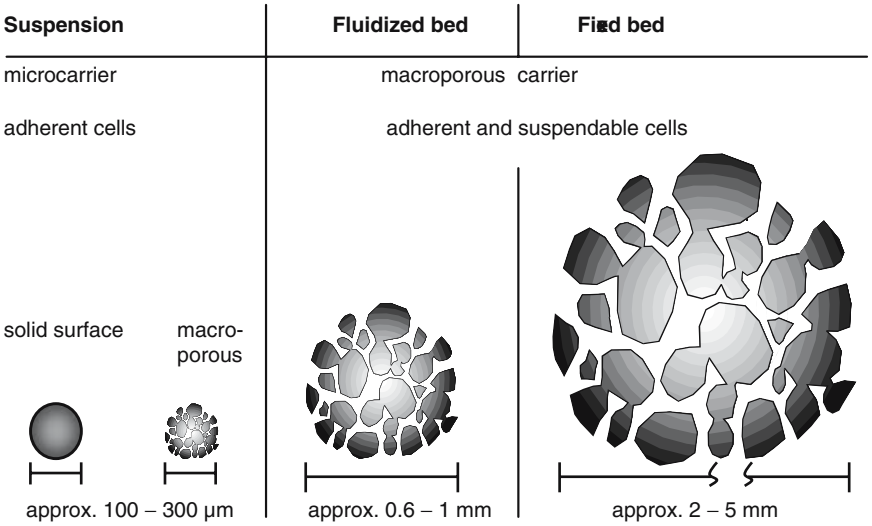

Fig. 4.28 Carrier for immobilization of mammalian cells

mechanical stability, mass-transfer, specific gravity, and shape. Different shapes are available, such as fibers, flat discs, woven discs, and cubes, though the sphere is the most common. The surface is usually positively or negatively charged to ensure cell attachment. The density of the electrostatic charge on the surface is critical to allow cell attachment and growth. Non-charged carriers are also available, which are normally coated with collagen or gelatine (denatured collagen) or have fibronectin or fibronectin peptides coupled on the surface. While carriers consisting of gelatine may be autoclaved, this is not the case for protein-coated carriers.

The density of the carriers is determined by the intended application. Smooth microcarriers for suspension culture have a density just above the medium (1.02–1.04 g cm^{-3}), while materials used for macroporous carriers have densities between 1.04 and 2.5 g cm^{-3}. Lundgren and Blüml (1998) suggest the use of sedimentation velocity as a better parameter to judge the suitability of a carrier for a specific reactor type, especially for fluidized bed reactors, as this includes not only the specific density but also the size and shape of the carrier. Sedimentation velocities lower than 30 cm min^{-1} do not create sufficient mixing for efficient nutrient supply throughout the carrier. For adherent cells tending to form bridges between the carriers higher sedimentation rates (150–250 cm min^{-1}) are recommended.

The surface of most carriers can be either solid or microporous. In the case of microporosity, the pore size is not sufficient to allow cells to grow in the inner parts of the carrier. Micropores are intended to take up larger molecules, up to a molecular weight of approximately 100 kda, to allow the cells to create a micro-environment on the beads and to support cell attachment and growth.

A carrier is considered macroporous if the average pore size is between 30 and 400 µm, allowing for cell growth within the carriers. The porosity of these carriers, defined as the ratio between the volume of the pores and the total carrier volume (as percentage) is normally between 60 and 99%. Macroporous carriers are suitable for immobilizing adherent as well as non-adherent cell lines. Furthermore they allow cells to grow in a three-dimensional, almost tissue-like structure at higher densities compared to solid or microporous carriers. The tissue-like growth stabilizes the cell population, protects against shear stress and decreases the need for external growth factors, so that the use of serum-free or protein-free media becomes easier. As the stability of the culture is improved at high cell density (Sect. 4.4), macroporous carriers are preferably used for long-term continuous culture. Due to the high cell density, the different culture technologies applied for macroporous carriers (stirred tanks for macroporous microcarriers, fixed bed and fluidized bed reactors) are generally run at high perfusion rates. This provides a sufficient nutrient supply as well as removal of toxic metabolites. Furthermore, the residence time of an extracellular product at 37 °C is reduced and it can quickly be separated from the cells and cooled.

Besides these advantages, some disadvantages of carriers have also to be considered (Lundgren and Blüml 1998):

- Some carriers have to be prepared before use.
- Scale-up of a culture using cells harvested from microcarriers is more complex than expansion of a suspension culture.
- Cell harvest from macroporous carriers can be difficult.
- Cell count, especially in the case of macroporous carriers, requires special techniques.
- For larger macroporous carriers, mass transfer limitations have to be considered.

Despite the large number of carriers and support materials suggested in the literature, only very few are on the market and even fewer fulfill industrial standards for large-scale manufacturing (Lundgren and Blüml 1998). In the following sections, some typical examples are discussed and recommendations for use in culture given.

4.3.1.2 Microcarrier for Suspension Culture

The term “microcarriers” denotes small beads, either solid or macroporous (Fig. 4.29), having a diameter of approximately 100–300 µm and a density of 1.02–1.04 g cm^{-3}, slightly higher than that of the growth medium. When first developed in the late 1960s by van Wezel (1967), microcarrier culture introduced new possibilities and suspension culture of anchorage-dependent cells in high density became possible (Lundgren and Blüml 1998; Nilsson et al. 1986; van der Velden-de Groot 1995). Nowadays beads made of DEAE-Sephadex, DEAE-polyacrylamide, polyacrylamide, polystyrene, cellulose fibers, hollow glass, gelatin or gelatin-coated dextran beads are in use (Lundgren and Blüml 1998; Shuler and Kargi 2002). In microcarrier

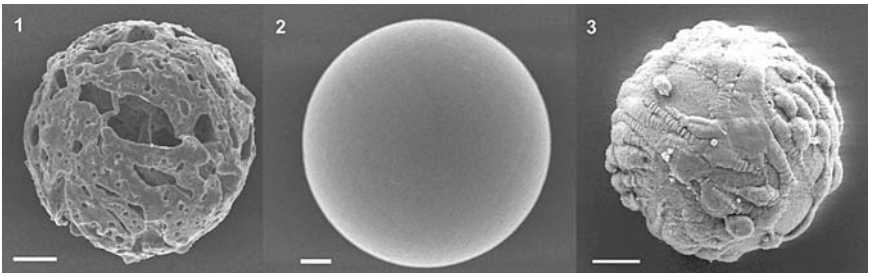

Fig. 4.29 Microcarrier for suspension culture of anchorage dependent cells. (1) Cultisphere (Percell Biolytica, Gelatin), bar 20 µm; (2) Cytodex 3 (GE Healthcare, Gelatin-Dextran), bar 10 µm; (3) Cartilage cells grown on Cytodex 3, bar 20 µm

culture, cells grow as monolayers on the surface of small spheres (Fig. 4.29) or three-dimensional within the pores of macroporous structures. The carriers are usually suspended in culture medium by gentle stirring.

On smooth solid microcarriers, cells grow on the outer surface until a monolayer is formed. Each microcarrier can accommodate approximately 100–200 cells. To reach an optimal growth on all individual microcarriers, an even distribution of cells is required. For most cell lines, more than7 cells per carrier are required during inoculation to ensure that the population of unoccupied microcarriers is <5% and the use of the available surface area is maximized (Butler 2004). For laboratory scale, it is often recommended to establish a microcarrier culture with 1–3 g (dry weight) of microcarriers per liter with initial cell densities of $1–2\times10^5$ cells mL^{-1} (might be lower in serum containing medium) and by using a certain start-up strategy (e.g., intermittent stirring to allow for attachment of cells on carriers). Final cell densities are in the range of 2×10^6 cells mL^{-1} with a multiplication factor of approximately 10–20 (Handbook GE Healthcare). In microcarrier culture usually a serum supplement of 5–10% is added to the medium for general purpose culture, as anchorage-dependent cells require certain adhesion factors contained in serum. For certain types of cell, the concentration of serum supplement can often be reduced. Furthermore, serum- or protein-free media supplemented with certain factors including fibronectin, transferring, insulin or epidermal growth factors, as well as shear protecting agents such as serum albumin, are probably suitable for microcarrier culture (Handbook GE Healthcare).

On the industrial scale, higher multiplication factors (up to 100) can be achieved by optimizing the cell-carrier-system for ease of scale-up (Lundgren and Blüml 1998). The larger the multiplication factor in each step of scale-up to final production volume, the fewer the scale-up steps required. For a multiplication factor of 100 a 1-L suspension would be appropriate to inoculate a 100 L-reactor. A further increase of the scale might be possible by a technique named "bead-to-bead transfer" or "colonization". Basically the microcarrier culture is scaled-up just by adding more microcarriers and more media (Butler 2004). Lundgren and Blüml (1998) reported on a 1:1,000 dilution with Chinese Hamster Ovary Cells (CHO) that do not attach well to the carriers or that detach easily during mitosis. In this case a 1 L-suspension could

inoculate a 1,000 L-reactor. If this technique cannot be applied and harvesting of cells from the beads is required, specific techniques for breaking the cell-surface and cell-cell interactions and separation of cells and microcarriers have to be applied.

4.3.1.3 Macroporous Carrier for Fluidized Bed and Fixed Bed Culture

Suitable carriers for the immobilization of mammalian cells in fixed bed and fluidized bed must fulfil certain requirements such as high surface to volume ratio, simple and non-toxic immobilization, optimal diffusion from the bulk phase to the centre of the carrier, mechanical stability, and pH stability. They should be steam sterilisable, reusable and suitable for adherent and non-adherent cells (reviewed by Pörtner and Märkl 1995; Pörtner and Platas 2007; Pörtner et al. 2007). A large number of macroporous carriers and support materials for immobilization have been suggested, including glass (natron, borosilicate), cellulose, collagen, synthetic materials, e.g., polypropylene and polyurethane, and ceramic. Most of these carriers proved to be suitable for a large number of cell types (e.g., hybridom, CHO, hepathocytes etc., see Sect. 5.1.2). In some cases (e.g., carriers made of glass or cellulose) coating with gelatine was recommended to support the growth of strictly adherent cells (unpublished data, Lüllau et al. 1994). The modification of the surface is a critical parameter. Anchorage-dependent cells, especially primary or non-established cell lines, have proved to be much more sensitive to the carrier surface than established cell lines (e.g. hybridom, CHO, L293, NIH3 T3). This has to be taken into account during the selection of a suitable carrier for each specific cell line. Examples are shown in Figs. 4.30 and 4.31. As already mentioned, only very few carriers are on the market and even fewer fulfill industrial standards for large-scale manufacturing.

The cell density within a carrier depends on several parameters such as diameter of the carrier, porosity, cell type, etc. In general, the number of immobilized cells in the carrier increases with decreasing carrier diameter (Fig. 4.32). Therefore smaller carriers are preferable (e.g., 0.6–1 mm for fluidized bed). But in the case of fixed reactors, smaller carriers create narrow free channels, which can be blocked by cells growing in these channels. Therefore, diameters of 3–5 mm are an appropriate choice for fixed-bed reactors (Pörtner and Platas, 2007). Further recommendations regarding design and operation of fixed bed and fluidized bed reactors are given in Sect. 5.1.2.

Fig. 4.30 Macroporous carriers for fixed bed and fluidized bed. I: Fibra-Cel™ (New Brunswick); II: glass carrier SIRAN® (QVF); III: ceramic carrier SPONCERAM® (Zellwerk)

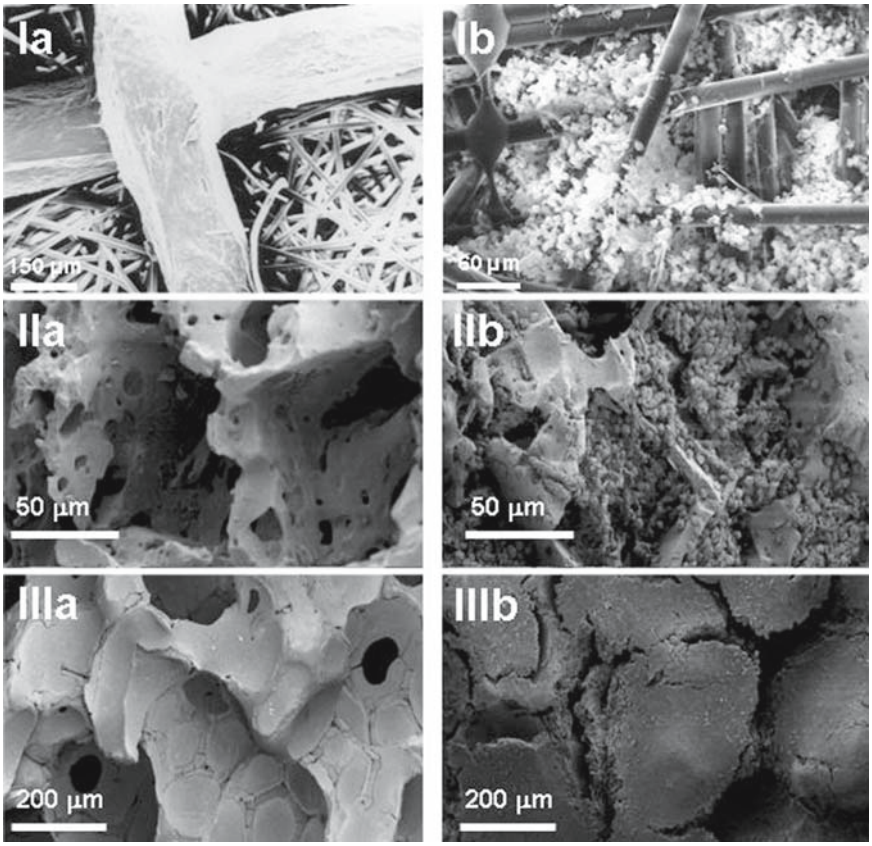

Fig. 4.31 SEM of macroporous carriers for fixed bed and fluidized bed. I: Fibra-Cel™ (New Brunswick), Ia: native carrier, Ib: CHO-K1 cells growing on the carrier. II: glass carrier SIRAN® (QVF), IIa: native carrier, IIb: hybridom cells growing within the carrier. III: ceramic carrier SPONCERAM® (Zellwerk). IIIa, native carrier surface, IIIb: hepatoblastoma cells growing within the carrier

4.3.1.4 Mass Transfer Effects in Macroporous Carriers

Within macroporous carriers a sufficient supply of immobilised cells with nutrients and removal of inhibiting metabolites are essential. On one hand, oxygen supply has to be addressed, as the solubility of oxygen in culture medium (approx. 0.2 mmol L^{-1}, if the medium is in equilibrium with air) is far lower than the concentration of other nutrients (e.g. glucose 18–25 mmol L^{-1}). Therefore, the supply of necessary oxygen to immobilised cells is an important criterion for selection of a macroporous carrier. On the other hand, removal of carbon dioxide is also an important aspect, as increased levels of carbon dioxide might reduce the pH to unfavourable conditions.

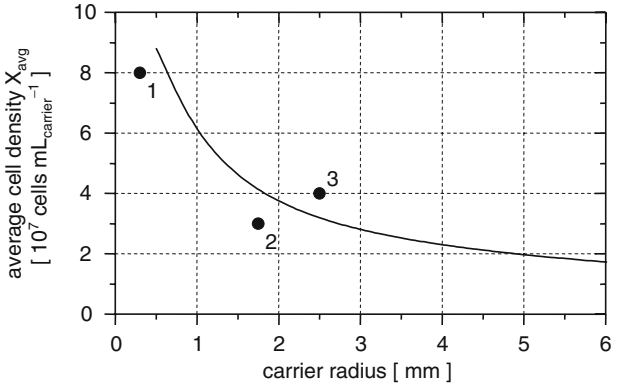

Fig. 4.32 Average cell density X_{avg} as a function of the carrier size (radius) for SIRAN carrier. The symbols indicate experimental data by (1) Yoshida et al. (1993), (2) Pörtner et al. (1995) and (3) Looby et al. (1990). The line shows a model calculation suggested by Fassnacht (2001) using a cell density of 1.75×10^8 cells mL^{-1} for those areas of the carrier loaded with cells

In the following sections, oxygen supply within a macorporous carrier will be addressed to provide a deeper understanding of the mechanisms involved in mass-transfer limitation. Here, only internal effects are considered, and effects due to a boundary layer around the carriers are ignored (Fig. 4.33). It can be assumed that mass transfer within the carriers is mainly diffusive. Some carriers, especially those having a very high porosity (>90%) can be perfused at an early stage of cultivation. But during the progress of the culture the free pores will be closed by growing cells and extracellular matrix. For a spherical particle the oxygen concentration c_{O2} within the particle can be described by the following differential equation:

$$\frac{\mathrm{d}^2 c_{o_2}}{\mathrm{d}r^2} + \frac{2}{r}\frac{\mathrm{d}c_{o_2}}{\mathrm{d}r} - \frac{Xq_{o_2,\max}}{D_e}\frac{c_{o_2}}{k_{o_2} + c_{o_2}} = 0 \tag{4.32}$$

with radius r, diffusiv coefficient D_e, cell density X, maximal cell specific oxygen uptake rate $q_{o2,max}$, Monod-constant k_{o2}, if the cells are distributed homogeneously within the carrier, oxygen can be considered as the limiting substrate, and diffusion can be described by Fick's law. This equation can be solved with the following boundary conditions: for $r = 0 \rightarrow \mathrm{d}c_{o2} / \mathrm{d}t = 0$, and $r = r_P$ (radius of the particle) $\rightarrow$ c_{o2} $(r_P) = c_{o2,Fl}$ (oxygen concentration in the bulk fluid). The diffusive coefficient is assumed to be $D_e = 2.56\times10^{-9}$ m^2 s^{-1}, as suggested by Kurosawa et al. (1989) for oxygen limitation within alginate beads. The cell specific oxygen uptake rate can be described by a Monod-equation. From Miller et al. (1987) and own unpublished data, the Monod-constant k_{o2} is seen to be approximately 0.001 mmol L^{-1}. As this value is very low compared to the oxygen concentration in the medium, it can be ignored in the first place and oxygen uptake can be regarded as following a zero order reaction. Furthermore the term Xq_{o2},max can be combined and replaced by

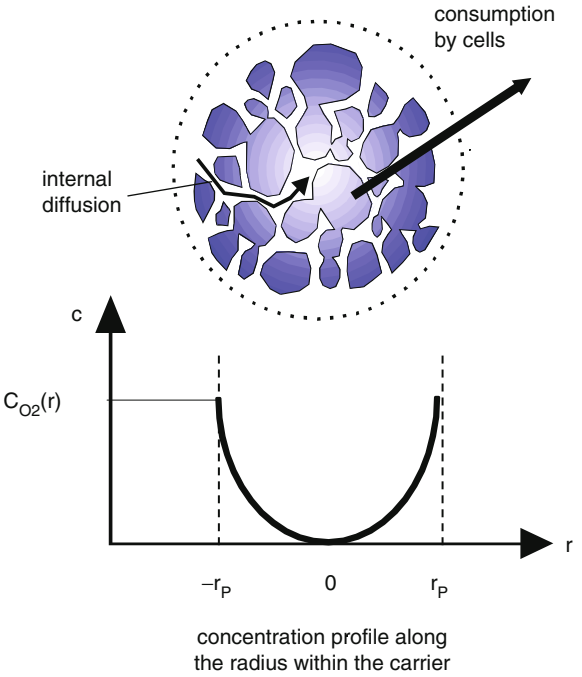

Fig. 4.33 Modeling of oxygen profil in a carrier loaded with cells neglecting the boundary layer effects

the term OUR, the volume specific oxygen uptake rate of a carrier loaded with cells, leading to

$$\frac{\mathrm{d}^2 c_{o_2}}{\mathrm{d}r^2} + \frac{2}{r}\frac{\mathrm{d}c_{o_2}}{\mathrm{d}r} - \frac{OUR}{D_e} = 0 \tag{4.33}$$

This equation was solved numerically by a fifth-order Runge–Kutta-method for different values of the oxygen concentration in the fluid and different volume-specific uptake rates. As can be seen from Fig. 4.34, severe oxygen limitation has to be expected, especially for larger particles ($r_P = 2\,\mathrm{mm}$) and higher volume-specific uptake rates. These theoretical considerations are supported by NMR studies described by Fassnacht (2001) (Fig. 4.35) and underline the statements made earlier, regarding an appropriate carrier size in fixed bed and fluidized bed reactors.

Besides solving the mass balance equation for the biocatalyst, a good estimation of the degree of mass transfer limitation within a biocatalyst can be obtained from the Thiele-Modulus Φ and the effectiveness factor η_i for internal mass-transfer-resistance. The Thiele-Modulus (Thiele 1939) describes the ratio between the maximum conversion within a biocatalyst and the maximum mass transfer to the biocatalyst. There are several definitions of the Thiele-Modulus in the literature.

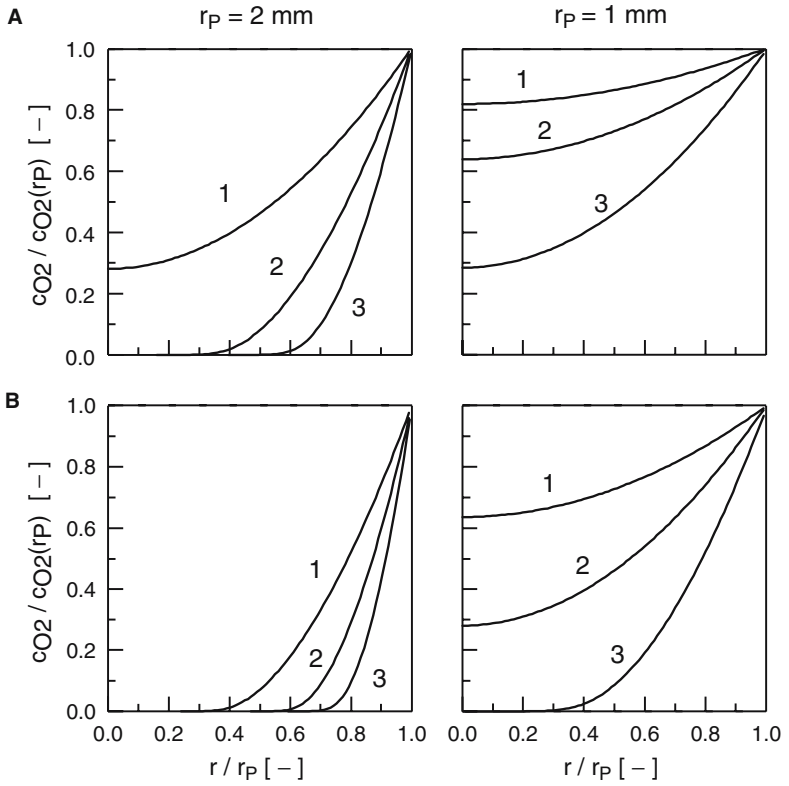

Fig. 4.34 Oxygen profile in a spherical carrier loaded with cells. Oxygen concentration $C_{O2}(r_p)$ in the bulk medium: 1–200 µmol L^{-1}, 2–100 µmol L^{-1}, 3–50 µmol L^{-1}. Volumetric oxygen uptake rate OUR: A – 2 mmol L^{-1} h^{-1}, B – 4 mmol L^{-1} h^{-1}

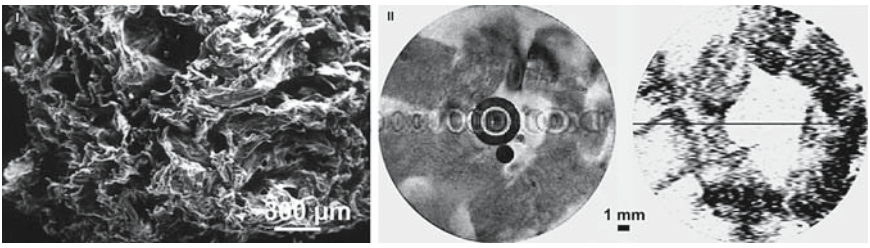

Fig. 4.35 I – SEM of CellSnow (Biomaterials), a macorporous cellulose carrier (approx. 5 × 5 mm). II – Cross-section of an NMR fixed-bed (2 mm slice thickness) reactor with CHO-K1 cells immobilized on CellSnow. On the left a spin echo image is shown. The *darker* parts show the cubic-shaped carriers, and the lighter parts indicate the interstitial space. The center shows the cross-section of the tube leading to the bottom of the bed. The small black circle located below the center is the glass capillary that contains a standard for 31P spectra. On the right a STEAM image of the same slice. This image shows viable cells at a dark color because of the low apparent diffusion coefficient of the intracellular water. Extracellular water is not detected and remains white. The black dashed circles indicate the cross-section of a single carrier showing that cell growth is only possible to a critical depth of approx. 0.7 mm (adapted from Fassnacht 2001)

In general, separate equations are required for different reaction kinetics and catalyst geometries. An overview is given by Doran (2006). For the case discussed above, a spherical particle and a zero-order kinetic for oxygen uptake, the Thiele-Modulus Φ_0 can be calculated as follows:

$$\phi_0 = \frac{r_P}{3\sqrt{2}} \sqrt{\frac{OUR}{D_e c_{O_2}}}. \tag{4.34}$$

The Thiele-Modulus Φ_0 was calculated for different values of the carrier radius, the oxygen uptake rate and the oxygen concentrations c_{fl} in the medium (Fig. 4.36). As expected, the Thiele-Modulus increases with increasing oxygen uptake rate, increasing carrier radius and decreasing oxygen concentration in the bulk medium.

An effectiveness factor of the carrier η_i can be defined as the ratio of the average observed reaction rate throughout the carrier to the rate without mass-transfer resistance:

$$\eta_i = \frac{\text{average reaction rate throughout the carrier}}{\text{rate without mass-transfer resistance}}$$

The effectiveness factor can also be interpreted as the ratio of the average reaction rate to the reaction rate on the surface of the carrier. For a spherical particle and a zero-order kinetic for oxygen uptake, the following equations can be used to calculate $\eta_{i0} = f(\Phi_0)$:

for $0 < 0 < 0.577 \rightarrow \eta_{i0} = 1$.

for $\Phi_0 < 0.577$.

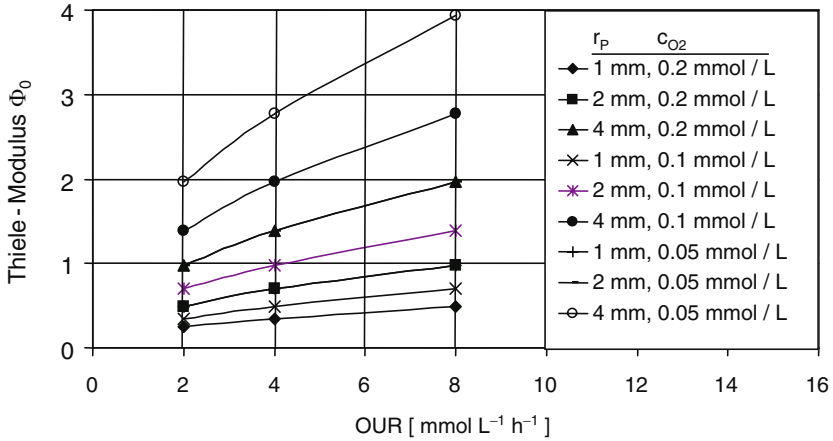

Fig. 4.36 Effectivity of oxygen supply in carriers with immobilized cells. Thiele-Modulus Φ_0 vs. volume specific oxygen uptake rate OUR calculated for different values of carrier radius r_P and different concentrations c_{O2} in the medium

$$\eta_{i0} = 1 - \left[\frac{1}{2} + \cos\left(\frac{\Psi 4\pi}{3}\right)\right]^3, \tag{4.35}$$

where

$$\Psi = \arccos\left(\frac{2}{3\phi_0^2} - 1\right). \tag{4.36}$$

The effectiveness factor η_{i0} was calculated according to these equations for different values of the carrier radius, the oxygen uptake rate and the oxygen concentrations c_{O2} in the medium (Fig. 4.37). As expected, all data points can be described by one curve. It confirms that calculation of the Thiele-Modulus and the effectiveness factor provides a good estimation of the degree of mass-transfer-limitation based on available process parameters, without solving the exact mass balance equations.

4.3.2 Encapsulation

Microencapsulation is another method for the immobilization of mammalian cells (Butler 2004; Hübner 2007; Huebner and Buchholz 1999). Basically, it can be used to protect cells against hazardous environmental conditions. The capsules can be cultivated in suspension reactors similar to microcarriers. Even direct aeration in combination with higher aeration rates, high agitation rates or stirrer speeds can be used without damaging the cells. The fragile nature of the microcapsule is

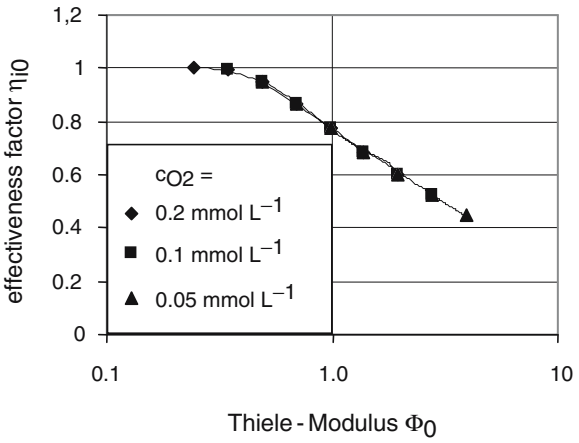

Fig. 4.37 Effectivity of oxygen supply in carriers with immobilized cells. Effectiveness factor η_{i0} vs. Thiele-Modulus Φ_0 calculated for carrier radius 1, 2 and 4 mm, oxygen uptake rate 2, 4 and 8 mmol L^{-1} h^{-1} and different oxygen concentrations c_{O2} in the medium

detrimental to scale-up and long-term operation. Handling of the cells is simplified, as medium exchange can be easily performed without cell loss. Furthermore, within the capsules, a microenvironment favourable for the cells can develop. Autocrine growth factors can accumulate and in an ideal case the cells switch directly to exponential growth after immobilisation, without a significant lag phase. This is probably the most important aspect.

The three basic encapsulation systems available are the bead, the coated bead and the membrane-coated hollow sphere (Hübner 2007; Murtas et al. 2005; Sielaff et al. 1995). Typical size for beads made of polysine-alginate is 300–500 µm, and the molecular weight cut-off of these capsule membranes is 60–70 kDa (Shuler and Kargi 2002). The simplest way to encapsulate cells in solid alginate beads is shown in Fig. 4.38. Immobilization in Ca-alginate beads often leads to problems when the cells release organic acids such as lactate into the medium or when phosphate ions exist as buffering agents in the medium and compete for the binding with the calcium ions. This difficulty led to the development of the coated beads, where additional polyelectrolyte layers, which are also stable in the presence of other ions, are applied to the beads. So the dissolving of the bulb core later on could be done without any problem, and the production of pure polyelectrolyte immobilisates without a solid bead core was a consequent improvement. Common polymers and appropriate

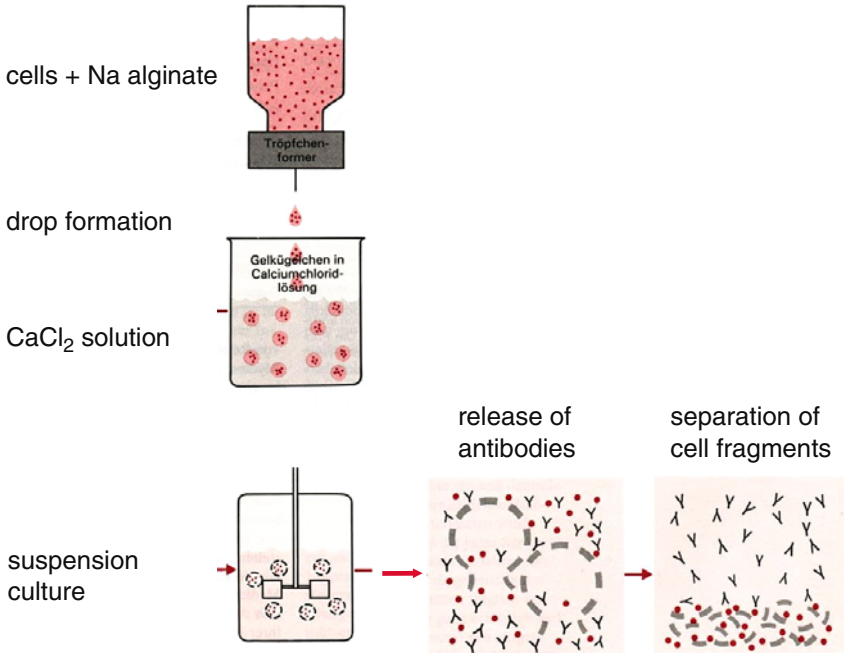

Fig. 4.38 Encapsulation of non-anchorage dependent, suspendable hybridom cells for production of monoclonal antibodies in calcium alginate

encapsulation devices as well as their application have already been described (Huebner and Buchholz 1999).

Cells grow within capsules upto tissue-like cell density before their growth seems to be stopped by space limitations. Cell densities of 10^8 cells per millilitre are standard. These values can only be reached, though, when the nutrient supply of the cells is adequate and the diameter of the capsules is not too large. Again, the sufficient oxygen supply is usually most critical (see above). Cells with a high consumption rate can only be cultivated in relatively small capsules (<1 mm) whereas cells with a lower consumption rate can be cultivated in larger capsules.

4.4 Culture Modes

4.4.1 Principles of Culture Modes

For all biotechnological processes, process strategies for the operation of bioreactors can be classified as discontinuous mode (batch, repeated batch or fed-batch), continuous mode (chemostat, perfusion) or dialysis mode. The basic principles of these modes and some general aspects of their application are discussed here briefly, as this is basic knowledge in biochemical engineering [Doran (2006), among others]. In Sect. 4.4.2 examples of cultivations performed with a specific cell line to provide a deeper understanding of the characteristics of different culture modes are given.

4.4.1.1 Batch and Fed-Batch

A batch culture as shown in Fig. 4.39a is characterized by the growth of cells without further addition of substrate (balance equations in Table 4.5). Before inoculation an appropriate amount of substrates (e.g., a culture medium as mentioned in Sect. 2.3) is provided in the culture system. After inoculation the cells start to grow by converting substrates and oxygen into cell mass and metabolites (including the desired product such as monoclonal antibodies or a recombinant protein). At first the cells go through a lag phase with reduced cell growth. Then exponential growth follows until either substrates are consumed or inhibiting metabolites have accumulated (decline phase and death phase). Cell death due to substrate limitation or metabolite inhibition is mainly induced by apoptosis, a genetically controlled cell death program (Sect. 2.5.2.1). During the cultivation additional compounds such as air or oxygen for aeration, acid or base for pH-control or anti foam agents to prevent foaming have to be added. Therefore in a strict sense a batch culture cannot be regarded as a “closed system”.

Batch cultures are regarded as simple and reliable and are often applied in the lab as well as on an industrial scale. Nevertheless the productivity of batch cultures

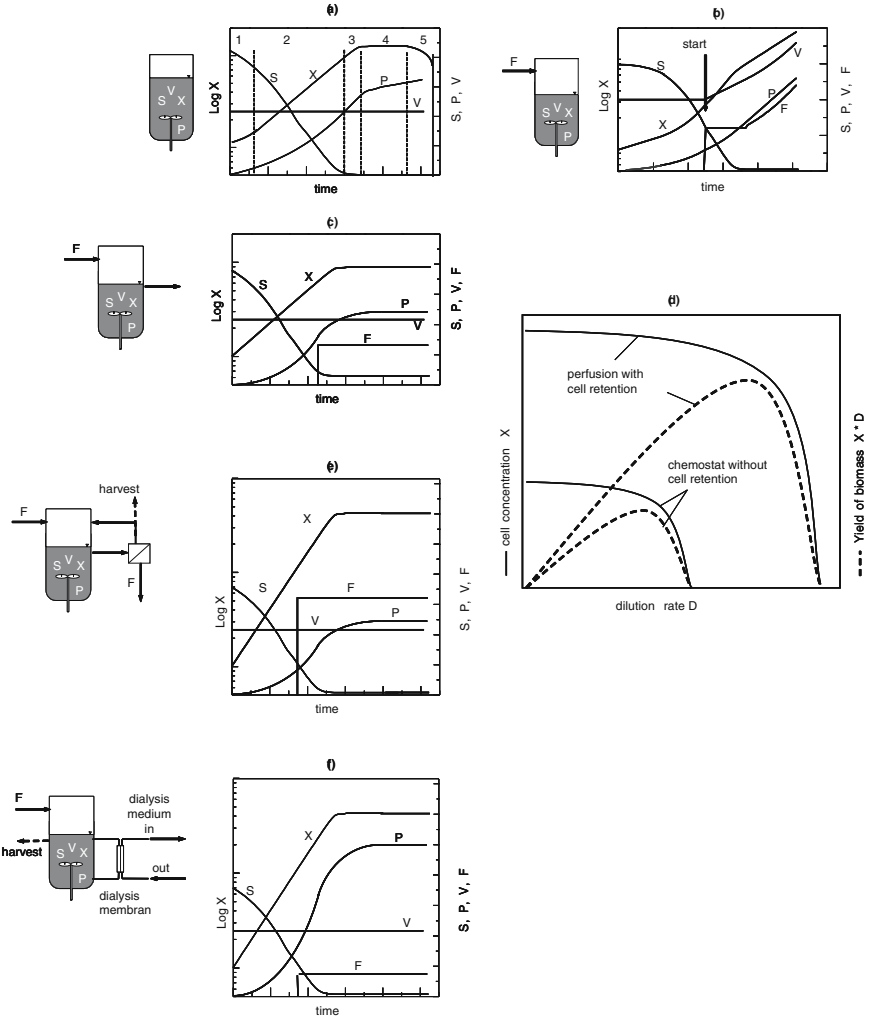

Fig. 4.39 Principles of culture modes (**a**) batch, (**b**) fed-batch, (**c**) chemostat, (**d**) cell concentration and yield vs. dilution rate for chemostat and perfusion, (**e**) perfusion with cell retention, (**f**) dialysis (F: feed rate, P: product, S: substrate, V: volume, X: cell conc.)

is limited by the initial concentration of substrates. On one hand, the solubility of certain medium compounds is limited. On the other hand, too high substrate concentrations my induce substrate inhibition or a high cell specific substrate uptake rate leading to increased production of inhibiting metabolites. Furthermore a batch culture runs at a high volume specific productivity only for a short period of time when a high cell concentration is reached and substrates are not yet consumed completely. After harvest the bioreactor has to be cleaned and refurbished before the cycle is repeated (Krahe 2003).

Table 4.5 Balance equations for batch and fed-batch mode

Concentration of total cells X_t	$\frac{dX_t}{dt} = \left(\mu - \frac{F}{V}\right) X_V$	(4.37)
Concentration of viable cells X_v	$\frac{dX_v}{dt} = \left(\mu - k_d - \frac{F}{V}\right) X_V$	(4.38)
Concentration of dead cells X_d	$\frac{dX_d}{dt} = \left(k_d \frac{F}{V}\right) X_V$	(4.39)
Substrate concentration c_S	$\frac{dS}{dt} = \left(\frac{F}{V}\right)\left(c_{S0} - c_S\right) - q_s X_V$	(4.40)
Product concentration c_P	$\frac{dc_p}{dt} = \left(\frac{F}{V}\right) c_p + q_p X_V$	(4.41)
Volume V	$\frac{dV}{dt} = F$	(4.42)

Concentration of total cells X_t, concentration of viable cells X_v, concentration of dead cells X_d, substrate concentration c_S, product concentration c_P, volume V, flow rate F, cell specific rates: growth rate μ, death rate k_d, substrate uptake rate q_S, metabolite production rate q_P. For batch mode the flow rate F = 0

A first step to improve the efficiency of a batch process can be seen in a so-called "repeated batch". Here the main part of the cultivation broth is harvested at the end of the exponential growth phase. The remaining part is used as inoculum for the next run. The culture system is filled with fresh medium and the process is newly started. This procedure can be repeated several times.

The limited productivity of a batch culture can be further overcome by means of a fed-batch (Fig. 4.39b, balance equations Table 4.5). Here the culture system is initially filled to one-third or half only and started as a batch. As soon as substrates are consumed or have reached growth limiting values, fresh medium is added, mostly in concentrated form. Cell and product yield can be significantly improved by applying a fed-batch strategy, where nutrients are added after depletion according to an appropriate feeding protocol (Pörtner et al. 2004). The main advantages of a fed-batch compared to a batch are a longer growth phase, higher cell and product concentrations and a higher product yield. On the other hand a larger effort for equipment and control is required. Several control strategies are available for fed-batch culture, which are discussed in detail in Sect. 4.4.4.

4.4.1.2 Chemostat without Cell Retention

In chemostat culture, also named "Continuous Stirred Tank Reactor" (CSTR), fresh medium is continuously pumped to the culture system and spent medium is

removed. The volume of the culture broth remains constant. The spent medium (harvest) contains all medium compounds including the cells. An alternative to the chemostat is the "turbidostat", where the cell concentration is kept constant by controlling the dilution rate. The time course of a chemostat culture is shown in Fig. 4.39c, the balance equations are given in Table 4.6. Again cultivation is started as batch. When substrate concentrations are below critical values, feeding of fresh medium and harvest of spent medium are started. After some time all process parameters become constant (average values – steady state), if homogeneous mixing within the culture system can be assumed.

During steady state the values for cell concentration, as well as substrate and product (metabolite) concentration, depend on the flow rates for medium supply and harvest, expressed by the dilution rate D (4.42). As shown in Fig. 4.39d, a constant or increasing cell concentration (depending on the death rate of the cells) can be observed with increasing dilution rate. But when the dilution rate approaches the maximal growth rate of the cells, the cells cannot compensate for wash-out and the cell concentration decreases. At $D > D_{crit}$ (4.47) the cells are washed out of the culture system completely. Substrate concentration is very low at low dilution rates and increases close to the critical dilution rate. The course of the product concentration looks similar to the cell concentration. Chemostat cultures without cell retention are a valuable tool for research (e.g., kinetic studies) (Pörtner and Schäfer 1996; Sect. 2.5), but not for production scale due to low cell and product concentration. Multi-stage chemostat cultures have been suggested to improve the yield of this culture mode (van Lier et al. 1994).

Table 4.6 Balance equations for chemostat culture

Dilution rate	$D = \frac{F}{V}$	(4.43)
Concentration of total cells X_t	$\frac{dX_t}{dt} = (\mu - D) X_V$	(4.44)
Substrate concentration c_S	$\frac{dc_S}{dt} = (c_{s0} - c_s) D - q_s X_V$	(4.45)
Product concentration c_P	$\frac{dc_p}{\mathrm{dt}} = -c_p D + q_p X_V$	(4.46)
Steady state ($dX/dt = 0$; $dc_S/dt = 0$)	$\mu = D$	(4.47)
Max. dilution rate $D_{crit.}$ (for monod type kinetic)	$D_{crit.} = \mu_{max} \frac{c_{s0}}{k_s + c_{s0}}$	(4.48)

4.4.1.3 Perfusion with Cell Retention

The drawbacks of a continuous chemostat culture can be overcome to some extent by retaining the cells in the culture system and perfusing the system continuously with medium. This can be done by connecting cell retention devices (e.g., settlers, spin filters, and centrifuges among others) to a suspension bioreactor or by immobilizing the cells (e.g., fixed bed or fluidized bed bioreactor). The specific techniques are discussed in detail in Chap. 5. Similar to a chemostat, here fresh medium is pumped continuously to the culture system and spent medium (harvest) is removed with the same flow rate. But as the cells are retained in the bioreactor, significantly higher flow rates can be applied leading to higher cell concentrations within the bioreactor, as shown in Fig. 4.39d and e.. Therefore higher volume specific productivities can be expected. The critical perfusion rate $D_{\text{crit,perf}}$ can be calculated from

$$D_{\text{crit,perf}} = D_{\text{crit,chemostat}} \frac{1}{1+\alpha_{\text{perf}} - \alpha_{\text{perf}}\beta_{\text{perf}}} \tag{4.49}$$

with the critical dilution rate in the chemostat $D_{\text{crit,chemostat}}$, recirculation rate α_{perf} (ratio of feed and recirculated medium) and rate of concentration β_{perf} (ratio of cell concentration within the bioreactor and the recirculated medium).

Continuous perfusion presents several advantages (Voisard et al. 2003; Geserick et al. 2000; Lüllau et al. 2003; Bödeker et al. 1994). Among these are the ability to grow cells to a very high density, the ease of handling media exchanges for the purpose of fresh feed and product harvest, the easy removal of metabolites and other inhibitors, and the prospect of easy scale up. When dealing with adherent cells, perfusion reactor design becomes slightly simpler (e.g. fixed bed and fluidized bed) due to immobilization of cells within macroporous carriers compared to microcarrier suspension culture (Pörtner and Platas Barradas 2007).

4.4.1.4 Dialysis Culture

Non-porous dialysis membranes allow for simultaneous enrichment of cells and high molecular weight compounds. According to Strathmann (1979) dialysis in liquid media is defined as transport of a solved compound from one homogeneous phase, through a membrane, into a second homogeneous phase, driven by a concentration gradient between the two phases. Mass transfer through the membrane can be described in terms of Fick's law:

$$S = P_{\text{mem}} A(c_1 - c_2) \tag{4.50}$$

The molecular flow S is caused by the concentration gradient of a specific compound c_1–c_2 across the membrane and is proportional to the membrane area A and the permeability coefficient P_{mem}. The permeability coefficient depends on the specific compound, the type of membrane and other process parameters (boundary layers on both sides of the membrane, fluid velocity, stirrer speed, etc.). If process

parameters are maintained constant, a relationship can be found between the permeability coefficient and the molecular weight of the compound, similar to that between the diffusion coefficient and the molecular weight. Therefore the permeability coefficient decreases with increasing molecular weight (Pörtner and Märkl 1998). At high values of the molecular weight, the mass transport over the membrane ceases. Usually membranes are characterised by a specific "cut-off", meaning that above this molecular weight, no mass transport over the membrane occurs. The basic principle of a dialysis process, as well as the time course of important process parameters, is shown in Fig. 4.39f. The dialysis process can be run as batch, fed-batch or continuously. An overview of the numerous process strategies available for dialysis cultures can be found in Pörtner and Märkl (1998) and Pörtner (1998).

4.4.2 Examples of Different Culture Modes

In the following sections, the characteristic features of batch, fed-batch and continuous cultures (chemostat, perfusion and dialysis) are discussed to provide a better understanding of these culture modes with respect to mammalian cells. All experiments were performed with one cell line, a hybridoma cell line producing an IgG-1 monoclonal antibody (data from Pörtner 1998 and Fassnacht 2001, if not mentioned otherwise). The intention is not to benchmark the different culture modes on the basis of, e.g., cell concentration, time–space yield or antibody concentration. Recommendation as to which culture mode should be used for a specific process has to consider the respective process, the desired complexity of the process control and for how long the same cell line will be used.

4.4.2.1 Batch and Fed-Batch

Batch processes (Fig. 4.40) usually start with an initial cell density of approximately $1–2 \times 10^5$ cells mL^{-1} and last 1–2 weeks. The required initial cell density depends on the type of cell and can be higher in serum- and protein-free media compared to serum containing medim (Lee et al. 1992; Lüdemann et al. 1996). Final cell densities are in the range of $2–5 \times 10^6$ cells mL^{-1}, depending on the medium. Therefore during a batch culture the cell number increases only approximately ten times (Griffiths 1992). Metabolites (lactate, ammonia) do not usually accumulate to inhibiting values in a batch culture, as in most cell culture media, the substrate concentrations (e.g., glucose and glutamine) are quite low and consumed quite rapidly.

A typical example of a fed-batch process is shown in Fig. 4.41 (data from Pörtner et al. 1996). In this case the appropriate feed rate was determined by model simulation before starting the feeding pumps ("a priori"). Data at time 24 h were used as start values for simulation of the expected time course for cells, glutamine

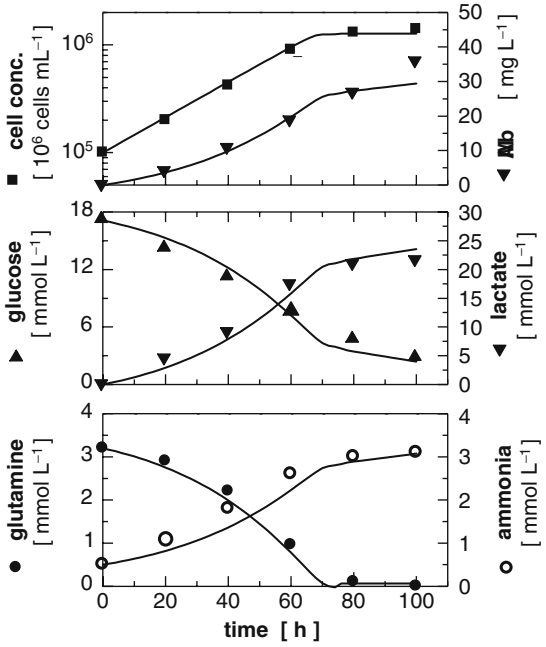

Fig. 4.40 Batch culture of hybridom cell line IV F 19.23 in T-25 flask (data from Pörtner 1998)

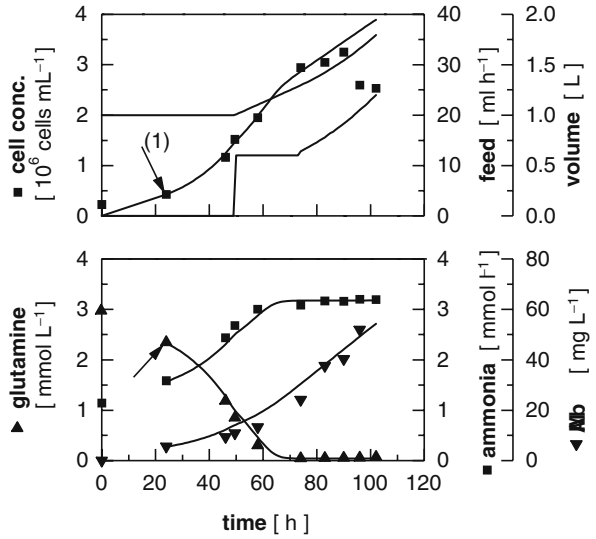

Fig. 4.41 Fed-batch culture with hybridom cell line IV F 19.23 - model based process control (data from Pörtner et al. 1996), suspensions reactor 2 L, 2 rushton turbine (110 rpm), surface aeration; (1) start values for model prediction

ammonia, glucose, lactate and monoclonal antibody (MAb) according to the following strategy: At a calculated glutamine concentration of 1 mmol L^{-1} (t = 50 h) the feed pump was started with a constant pump rate (12 mL h^{-1}). At a calculated glutamine concentration of 0.04 mmol L^{-1} (t = 73 h) the pump rate was increased to maintain this concentration. The "a priori"– determined course of the culture could predict the course of the culture quite well. The maximum cell concentration was 3.2×10^6 cells mL^{-1}, the final MAb-concentration was 54 mg L^{-1}. This example gives a basic idea of the complexity of fed-batch-processes. Other process strategies are discussed in Sect. 4.4.3.

4.4.2.2 Chemostat

As mentioned earlier, in chemostat culture a "steady state" is obtained, if the medium flow rates (feed, harvest) are kept constant. Figure 4.42 shows the relationship between the steady state concentrations for cells, glutamine, glucose, lactate, ammonia and monoclonal antibodies (MAb). Similar data were shown by others for hybridom cells (Miller et al. 1988; Hiller et al. 1991). As expected, the cell

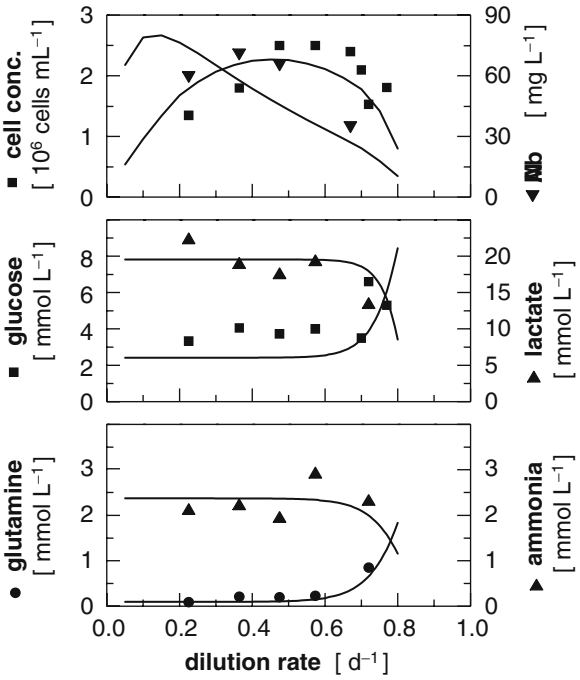

Fig. 4.42 Chemostat culture of hybridom cell line IV F 19.23 (data from Pörtner 1998) suspensions reactor 400 ml, paddle impeller (35 rpm), surface aeration

concentration first increases with the increasing dilution rate. The low cell densities at very low dilution rates are mainly due to cell death caused by apoptosis. Later, for dilution rate D approaching the maximal growth rate, the cell concentration decreases and finally becomes zero for $D > D_{crit}$. A similar course can be found for antibody concentration. Substrate concentrations, especially for glutamine as the limiting substrate in this case, remain at very low values at low dilution rates and increase at dilution rates approaching the maximal growth rate. Ammonia and lactate did not reach limiting concentrations (Pörtner and Schäfer 1996).

In general, the maximal cell and product concentrations obtained in chemostat cultures are quite low and in a similar range as those found in batch culture. Therefore chemostat cultures are a valuable tool for kinetic studies, especially as reliable data at very low substrate concentrations can be obtained. For industrial applications usually cell and product yield are regarded as too low (Griffiths 1992; Werner et al. 1992).

4.4.2.3 Continuous Fixed Bed Culture with Cell Retention

Cultivation of the hybridom cell line in a 100 ml fixed-bed reactor applying oxygen concentration above air saturation (compare Sect. 5.1.2) is shown in Fig. 4.43 (data from Fassnacht 2001). After inoculation, the cells started to proliferate in the fixed-bed, which can be seen in the decreasing glucose and increasing lactate concentrations. A high dilution rate D_{FB} of 10 mL medium per ml fixed-bed per day was used to minimize substrate limitation. A first steady-state was obtained on the fifth day after inoculation at a dissolved oxygen concentration of air saturation at the entry of the fixed-bed. This steady-state was controlled by oxygen limitation,

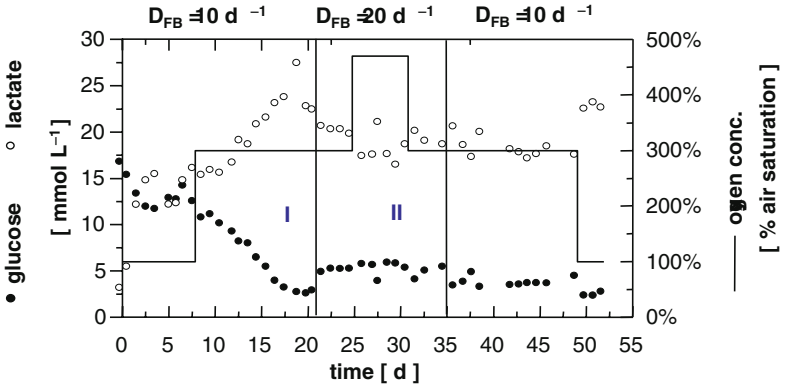

Fig. 4.43 Fixed bed culture of hybridom cell line IV F 19.23 – variation of dissolved oxygen concentration (data from Fassnacht 2001) fixed bed 100 ml, axial flow, conditioning vessel 1 L, macroporous carrier SIRAN®, steady state values for phase I: $c_{Gln} = 0.52$ mmol L^{-1}, $c_{MAb} = 30.7$ mg L^{-1}; phase II: $c_{Gln} = 1.36$ mmol L^{-1}, $c_{MAb} = 20.2$ mg L^{-1}

as indicated by the high steady-state glucose concentration and a steady-state glutamine concentration of 2.46 mmol L^{-1} (data not shown). The dissolved oxygen concentration was raised to 300% air saturation on the eighth day. This resulted in an increase of the glucose consumption rate and a new steady-state was reached on the 21st day. The glutamine concentration dropped to 0.52 mmol L^{-1} (data not shown), and the steady-state antibody concentration was 30.7 mg L^{-1}. The low glucose and glutamine concentrations suggest that the steady-state was now controlled by substrate limitation. Therefore, the dilution rate D_{FB} was increased to 20 d^{-1}. This increased the glucose consumption rate significantly, and a new steady-state was obtained with a corresponding non-limiting glutamine concentration of 1.36 mmol L^{-1} and an antibody concentration of 20.2 mg L^{-1}. However, setting the dissolved oxygen concentration to oxygen saturation (477% air saturation) on the 26th day did not result in a further increase of the glucose uptake rate indicating that the system was also not controlled by oxygen limitation and that the maximal possible performance was reached. The oxygen concentration was again reduced to 300% air saturation and the dilution rate to 10 d^{-1}, and the same steady-state was reached on day 46 as on the 21st day, with a glutamine concentration of 0.49 mmol L^{-1}. The shown examples underline the potential of long- term cultivation, especially long-term stability in bioreactor systems with cell retention.

4.4.2.4 Continuous Dialysis Culture

Dialysis offers an efficient process strategy for the removal of inhibiting metabolites and a simultaneous retention of cells and macromolecular products. It also allows for a number of different strategies (batch, fed-batch, continuous) for decoupling the flows of high molecular and low molecular substrates, low molecular metabolites and high molecular products. Pörtner and coworkers (Lüdemann 1997; Pörtner et al. 1997; Schwabe et al. 1999; Frahm et al. 2003) used a "nutrient-split" feeding strategy based on suggestions made by Ogbonna and Märkl (1993). The medium is divided into a buffer solution containing all mineral salts and a medium concentrate containing all relevant substrates (glucose, glutamine, other amino acids, etc.). The medium concentrate can be fed directly to the cells with significantly reduced flow rates, whereas the buffer solution is used as dialysis medium (compare Fig. 4.39f).

Figure 4.44 shows as continuous dialysis culture run with the above mentioned "nutrient-split" – feeding strategy in a membrane-dialysis-bioreactor (data from Lüdemann (1997)). The bioreactor is discussed more in detail in Sect.. 5.1.1.1. The process was started as batch culture. Continuous perfusion of the cell chamber was switched on at t = 74 h with a perfusion rate of D_i = 0.11 d^{-1}. At t = 163 h the perfusion rate was set to D_i = 0.145 d^{-1}. For the dialysis chamber perfusion was started at t = 123 h with a perfusion rate D_a = 0.163 d^{-1}. The viable cell concentration increased to a maximum value of 1.1×10^7 cells mL^{-1} at t = 140 h and levelled of at 7.5×10^6 cells mL^{-1}. Antibody concentration increased up to 650 mg L^{-1}.

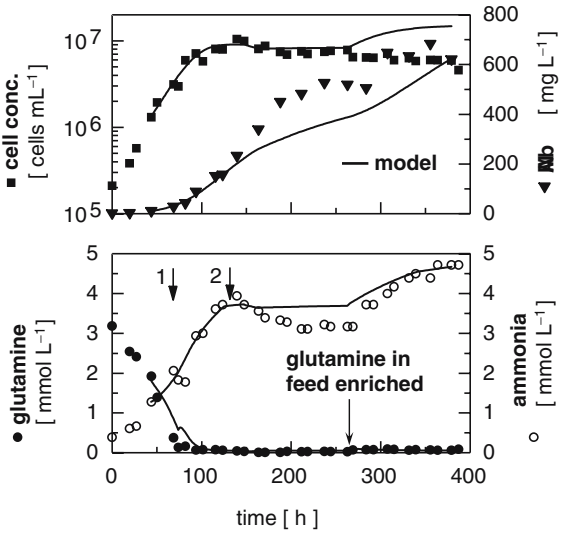

Fig. 4.44 Culture of hybridom cell line IV F 19.23 in Membrane-Dialysis-Reactor – "Nutrient-Split" feeding (data from Lüdemann 1997), suspension culture, dialysis chamber 4.9 L, culture chamber 1.3 L, 2 rushton turbines (110 rpm), membrane and bubble aeration, 1: start feed, 10× medium concentrate, $D_i = 0.11\,d^{-1}$ until $t = 163\,h$, then $D_i = 0.145\,d^{-1}$; 2: start dialysis, buffer, $D_a = 0.163\,d^{-1}$

4.4.2.5 Comparison of Different Culture Modes

The examples discussed above allow for some general conclusions regarding yield and efficiency of different culture modes, even if the used cell line cannot be regarded as "industrial-like" and optimal process parameters were not chosen in all examples. The main results are summarized in Table 4.7. As expected, the lowest cell and product concentrations were obtained in batch culture. The low efficiency, expressed by a high medium requirement per mg monoclonal antibody, is mainly due to high cell specific substrate uptake rates during exponential growth. Only the utilization level of the substrates is high, as most of the substrates are consumed totally. For the fed-batch culture cell and product concentration are significantly higher. Due to the applied process strategy to control glutamine at a very low level (Kurokawa et al. 1994) the cell specific substrate uptake rates and therefore the medium requirement could be kept low (Sect. 4.4.3). During chemostat the product concentration was quite low and the medium requirement high, as cell and product concentration are determined by the relationship between cell-specific growth rate and perfusion rate. In perfusion mode, shown here by fixed bed cultivation with cell retention, growth rate and perfusion rate are not coupled. Therefore a significantly higher product yield could be obtained, even if product concentration was similar to chemostat culture and lower compared to fed-batch culture. Furthermore Table 4.7 shows a significantly higher product concentration and product yield for the dialysis culture due to simultaneous retention of cells and product. The "nutrient-split"-feeding strategy

Table 4.7 Experimental results for different culture modes with hybridom cell line IV F 19.23 (* estimated from the glucose uptake rate)

Culture system	Batch	Fed-batch	Chemostat	Perfusion (fixed bed)	Membran-dialyse-reactor, continuous, "nutrient-split" feeding
Perfusion rate [d^{-1}]	–	Calculated "a priori"	0.7	10	D_i : 0.145; D_a : 0.163
Cell conc. [cells mL^{-1}]	2×10^6	3.2×10^6	2.4×10^6	$5\times10^{7*}$	6×10^6
MAb-conc. [mg L^{-1}]	35	54	35	30	650
MAb-yield [mg L^{-1} d^{-1}]	8.4	12.7	26.4	300	94.3
Utilisation level glucose [%]	88.6	100	76	80	90
Utilisation level glutamine [%]	100	100	86	83	99.6

further improves the efficiency of this culture mode. Drawbacks of the dialysis technique can be seen in the higher efforts for equipment and process control (Pörtner and Märkl 1998). The above discussion focuses on data obtained in lab-scale culture systems. Implications on the industrial scale will be addressed in Sect. 4.4.4.

4.4.3 Process Strategies for Fed-Batch

The research on fed-batch strategies for suspension cultures of mammalian cells is motivated by the industrial relevance of this process (Glaser 2001; Wrotnowski 2000) (see below). However, despite intensive research carried out in this field during the past few years (reviewed by Pörtner et al. 2004, Wlashin and Hu 2006), it is still difficult to evaluate the performance and suitability of different strategies. In cell culture operations, normally only a few variables are available on-line (e.g., DO, pH, and temperature), and cultivation strategies have to rely on off-line measurements that either have significant time delay or are usually obtained at the end of the cultivation. Conventional control of substrates is therefore rarely applied and alternative procedures are required.

As a simple feeding strategy, pre-defined fixed feed trajectories can be applied. Usually the feed rate has to be increased during the process (e.g., using an exponential or linear profile), as the number of cells and consequently the demand for substrate(s) increases. As there is no feedback or re-adjustment during the process, this control strategy cannot react to changes occurring during the actual process with the risk of suboptimal feeding. However, the fixed feed trajectories can be refined, based on the results of the preceding cultivation. Consequently, it allows improvement on a

cultivation-to-cultivation basis. This is subject to the condition that any culture conditions influencing nutrient uptake of the cells remain unchanged.

On-line characterization is a basic approach describing the metabolism and physiological state of cells. The physiological state of the cells determines the uptake of nutrients and the production of metabolites. Metabolic activity is difficult to measure directly, but respiration and energy conversion rates can be monitored by oxygen mass balance (Eyer et al. 1995; Kyung et al. 1994) or spectroscopic analysis of NAD/NADH + H^+ (Siano and Muthrasan 1991). A strategy described by Zhou et al. (1995) and Zhou and Hu (1994) determined the physiological state of the cells on-line during cultivation by the oxygen uptake rate (OUR). This strategy showed a high potential for sustaining optimal growth and reducing the formation of toxic metabolites (ammonia and lactate). Mass spectrometry analysis of exhaust gas was further used to determine OUR (Kyung et al. 1994).

Model-based control with model-aided cultivation is one of the most promising approaches in cell culture (Barford et al. 1992; Hansen et al. 1993). In the following, two concepts using process models are illustrated: The first is the *"a priori"-determination* of feed trajectories based on a kinetic model (Fig. 4.41). The model and the calculated feed trajectories remain unchanged once the cultivation has been started. The second is the *adaptive, model-based OLFO-controller*. These concepts react to changes during the cultivation and adapt the model and the feed trajectories accordingly.

The "a priori" determination of feed trajectories, based on a kinetic model, requires intensive kinetic studies of the used cell line. Before starting the feeding phase of the cultivation, feed trajectories are calculated on the basis of the kinetic model. This concept can be considered an extension of the pre-defined feed trajectories concept. In both cases, the trajectories are determined before the cultivation but originate in this case from kinetic studies. Furthermore, the intention of the "a priori" determination of feed trajectories is to predict the death phase and calculate the feed trajectories accordingly. Fixed feed trajectories cause overfeeding during the death phase. Of course, given stable cell lines and culture conditions, the overfeeding can be reduced by adjusting the fixed feed trajectories before the next cultivation. However, the "a priori" determination of feed trajectories allows a more sophisticated control of the death phase in comparison to the fixed feed trajectories. Controlling fed-batch processes with "a priori" simulation of process parameters based on a kinetic model (open loop) demands the ability for accurate prediction, especially at low substrate concentrations when the risk of apoptotic cell death is high. The calculation of optimal feed trajectories (Lee et al. 1999; Ryszcuk and Emborg 1997) using kinetic models shows that small deviations between calculated growth and death rates and actual values have a large effect on the reliability of the trajectories. The parameters of the kinetic models, structured or unstructured, are usually derived from previous experiments and thus the trajectories cannot consider actual culture conditions or changes in metabolism. The feed trajectories obtained from simulation might not result in the expected productivity (de Tremblay et al. 1993).

Alternatively model-based, adaptive control has been suggested, e.g., the open-loop-feedback-optimal (OLFO)-controller (discussed by Pörtner et al. 2004). Major

elements of the OLFO-controller are a process model, model parameter identification and an optimization part. They permit adaptation of model parameters and prediction of the future process course of the culture as well as its optimization. Strategies based on the use of expert systems, fuzzy control and neural networks have already been applied in microbial processes but not often investigated for mammalian cell culture.

An overriding goal of the control strategies introduced above was to minimize the production of toxic metabolites such as ammonia and lactate to extend the growth phase. This requires the control of glutamine and glucose at low concentrations so that under these conditions the cell-specific metabolite production is reduced. On the other hand, cell death by apoptosis may be introduced at too low concentrations. Therefore an "intelligent" control strategy has to find an optimum between these two extremes.

Pörtner et al. (2004) compared four different fed-batch strategies including *fixed feed trajectories*, control via *oxygen uptake rate OUR* (stoichiometric feeding), "*a-priori" determination* of feed trajectories based on a kinetic model and the *OLFO-control* strategy. The intention was not to benchmark the different control strategies on the basis of, e.g., time-space-yield or antibody concentration. Recommendation as to which control strategy should be used for a specific process has to consider the respective process, the desired complexity of the process control and for how long the same cell line will be used. However, the illustration of the different strategies points out the different characteristics of each strategy, thus facilitating the choice.

Table 4.8 summarizes the characteristics of the different feeding strategies. A recommendation based on these findings would favour fixed feed trajectories for an established process with a well-characterized and stable production cell line. An adaptive, model-based control strategy could be the method of choice during cell line development or for rapid production of small amounts of the product for clinical trials, because of its universal character and because it does not require intensive process development. From our experience only very few batch experiments are required to adapt the kinetic model. As the OLFO-controller can detect changes in the cell metabolism during a culture, it can adapt the model parameters and the feed trajectories. Our studies illustrate that the adaptive, model-based OLFO-controller is a valuable tool for the fed-batch control of hybridom cell cultures (Frahm et al. 2002). Because of its universal character, it can be transferred to different cell lines or adapted to different boundary conditions (e.g., enhanced fed-batch cultivation using dialysis (Frahm et al. 2003)). More sophisticated optimization criteria, e.g., optimization of final antibody concentration, time-space yield of antibody or another performance measure, can be implemented (Frahm et al. 2005).

4.4.4 Process Strategies Applied in Industrial Processes

Until now, batch and fed-batch strategies are being applied quite frequently on industrial scale (Kelly et al. 1993; Otzturk 2006) due to the several reasons discussed

Table 4.8 Comparision of the characteristics of the feeding strategies (from Pörtner et al. 2004)

	Fixed feed trajectory	Control via oxygen uptake rate (OUR)	"A priori" determination of feed trajectories based on a kinetic model	Model-based adaptive OLFO-control
Possibility of feedback during cultivation	No	Yes, using OUR parameter	No	Yes, using several parameters
Applicability for control at limiting substrate concentrations	No for non-stable cell lines/varying culture conditions (no feedback)	Yes (online feedback via OUR)	No for non-stable cell lines/varying culture conditions (no feedback)	Moderate (feedback in intervals)
Risk of substrate limitation	High for non-stable cell lines/varying culture conditions	Low	Moderate/high for non-stable cell lines/varying culture conditions	Low
Suitable for the the whole process	No, problematic during decline phase/death phase	No, problematic during decline phase/death phase	Yes, problematic during decline phase/death phase only for not well characterized and unstable production cell line and varying culture conditions,	Yes
Risk of overfeeding	High at the end of the cultivation	High at the end of the cultivation	Moderate at the end of the cultivation	Low
Complexity	Low	Low	Moderate/high	High
Time for implementation (from a first cultivation to satisfactory results)	Moderate	Low	High	Low/moderate
Time expense during cultivation	None	Low	None	High
Operating expense when changing to a different cell line	Moderate	Low/none	High	Low
Possibiltiy of fine-tuning	Yes, from cultivation to cultivation	No/marginal	Yes, from cultivation to cultivation	Yes, during a cultivation and from cultivation to cultivation
Suggested application area	Established process, well characterized and stable production cell line and culture conditions	All areas, method is sub-optimal for optimizing the process performance	Well characterized and stable production cell line and culture conditions, higher effort than fixed feed trajectories	Cell line development, rapid production of small amounts of product (e.g. clinical trials)

already. The drawbacks of discontinuous modes such as large reactor volumes, high maintenance (cleaning, sterilization, etc.) can be overcome to some extent by using a continuous mode, especially perfusion with cell and/or product retention (Table 4.9). There are a growing number of reports on stable perfusion cultures even on an industrial scale lasting several months (Kompala and Ozturk 2006; Bohmann et al. 1995; Fassnacht et al. 1999; Fussenegger et al. 2000). The main advantage of perfusion cultures can be seen in the reduced bioreactor size (approximately one-tenth of a suspension reactor without cell retention). Nevertheless there are some difficulties in the perfusion concept. Further equipment such as the retention device itself, pumps for feeding, harvest and medium circulation, and storage tanks for feed and harvest are required. The amount of media needed to complete a moderate to long-term run can be excessively large. A further possible drawback of continuous cultivation is the possibility of variability over the time of the run. Batch or fed-batch cultivations are much shorter in duration and have fewer chances for random occurrences to happen. This is important in dealing with cGMP (current manufacturing practice) conditions that dictate precise reproducibility or evidence of a minimum of non-effects of minor deviations. In the meantime there is a growing number of pharmaceutical products in the market, produced successfully from perfusion systems. Among these are block busters such as Kogenate-FS® (Bayer Health Care) or Remicade® (Centocor) (Kompala and Ozturk 2006). Previous concerns such as getting the processes approved are not longer an issue and it can be expected that due to an increasing pressure on production costs, more perfusion processes will be installed in the future.

The process that is becoming more and more important for the production of small quantities of recombinant proteins is transient transfection (Meissner et al. 2001; Derouazi et al. 2004; Baldi et al. 2005). Non-transfected cells (most commonly HEK-293, COS and BHK cells) are first cultivated usually in batch-mode to a certain cell density and then transfected with DNA encoding for a certain protein. Usually the cells are genetically not stable and soon lose their expression ability, but can produce a certain amount of protein within one batch. Originally it was used just as a preliminary test of gene expression. New developments show that large scale production up to 100 L is possible (Blasey et al. 1996; Girard et al. 2002).

Table 4.9 Comparision of batch and continuous perfusion (adapted from Griffiths 1992)

		Batch	Perfusion
Equipment	Process stability	+	−
	Sterility	+	±
Process control	Handling	+	±
	Labour	−	+
	Duration	−	+
	Development	+	−
Economics	Productivity	−	+
	Cost/unit	−	+
Licencing	Batch-definition	+	±
	Cell stability	+	?

4.5 Monitoring and Controlling in Animal Cell Culture

The production of specific products using bioprocesses requires the monitoring and controlling of a number of parameters (Table 4.10). To maintain these parameters, either of a physical or chemical nature, is crucial for a high productivity of the bioprocess. Non-optimal conditions within the bioreactor could result in a decreased product formation and a less efficient process.

The most common parameters chosen to be monitored and controlled during a bioprocess are temperature, agitation rate, pH, pO_2 and pCO_2. If one of these values differs from the specific desired set point, corrective action has to be taken (Krahe 2003; Chmiel 2006). In addition to this, other parameters like metabolite concentrations in the culture medium or the cell shape and viability can be used to provide information about the state of the process (Riley 2006). This chapter gives an overview of the methods to monitor the parameters mentioned above and how to control them appropriately during the process.

Cell line identification will not be discussed in detail in this chapter. Protocols for this purpose can be found, e.g., in J. R. W. Masters, (Masters 2000) or A. Doyle and J.B. Griffiths, (Doyle and Griffith 1998).

4.5.1 Temperature

The parameter temperature is very critical for a bioprocess and in animal cell cultures and must be maintained at the desired set point within a tight range of about ± 0.5 °C. A higher variation in temperature often leads to production rates far from the optimum due to slow cell metabolism (temperature below lower limit) or rapid

Table 4.10 Parameters measured or controlled in bioreactors

Physical	Chemical	Biological
Temperature	pH	Biomass concentration
Pressure	Dissolved O_2	Enzyme concentration
Reactor weight	Dissolved CO_2	Biomass composition (such as DNA, RNA, protein, ATP/ADP/AMP, NAD/NADH levels)
Liquid level	Redox potential	Viability
Foam level	Exit gas composition	Morphology
Agitator speed	Conductivity	
Power consumption	Broth composition (substrate product, ion concentrations, etc.)	
Gas flow rate		
Medium flow rate		
Culture viscosity		
Gas hold-up		

cell death (temperature above higher limit) (Hartnett 1994). To measure the temperature within the system, resistance temperature devices (RTD) are preferred (PT-100 or PT-1000) due their high accuracy and reproducibility. The device contains a metal conductor which changes resistance with changing temperature. This principle is used to determine the actual temperature within the system. Another method is the application of thermocouples, which are cheaper but also less accurate (Riley 2006; Doyle and Griffith 1998).

However, independent of the device used, the measured temperature and resulting electrical signal must be compared to the chosen set point and eventually corrective action must be taken. For this, the electrical signal obtained by the RTD or thermocouple is amplified and transmitted to a controller, where it is compared to the set point value. Depending on the actual state of the system and the desired temperature value, heating or cooling of the system is induced. For small scale and large scale bioreactors, a heating and cooling action using PID (proportional integral derivative) control provides an adequate control (Storhas 1994).

4.5.2 pH

Cells and their metabolism are very sensitive to changes in H^+-ion concentration and so pH. Therefore a control of pH in a very tight range of ±0.1 around the set point is necessary to ensure high productivity of a bioprocess (Krahe 2003; Chmiel 2006).

Measurement of pH requires a combination of two electrodes, one measuring electrode and one reference electrode. These two electrodes are usually combined in one device, a pH probe. The electrode for measuring has a glass membrane, where a potential develops, which varies with hydrogen ion concentration within the medium to be measured. This potential is then compared to a constant potential built up at the reference electrode to determine the actual pH in the medium to be measured.

Depending on the process, there are two ways to control the pH in the culture medium (Krahe 2003; Riley 2006; Doyle and Griffith 1998). If a medium containing sodium-bicarbonate is used, then the introduction of CO_2 into the medium can be used to control the pH.

$$CO_{2_{(aq)}} + H_2O <-> H^+ + HCO_3^-$$

Phosphates in the medium also aid buffering and, for some cells lines, HEPES ([N-2-hydroxyethylpiperazine-*N*]ethansulphonic acid) can be added to provide further buffering. If a medium containing no sodium-bicarbonate is used, a liquid base (e.g. KOH or NaOH) or acid (e.g. HCl) is used to control the culture pH. In this case, the medium should have at least some buffer capacity to avoid oscillation around the set point. The problem with this method is that the addition could result in a dilution of the medium and so nutrient levels, which then could result in lower productivity. Another problem, which could occur if base and acid are simply

added by dripping on the culture's liquid surface, is cell death due to bad mixing (Langheinrich and Nienow 1999).

4.5.3 Oxygen Partial Pressure

Oxygen is usually used by animal cell cultures for the production of energy from organic carbon sources. Therefore it is a very important substrate but unfortunately, oxygen solubility in aqueous medium is relatively low and can result in oxygen limitations of the culture and thus affect cell growth rate and metabolism. The solubility of oxygen at 1 bar pressure and air saturation is only about 6–8 mg L^{-1}, depending on the liquid temperature and composition (Sect. 4.2). The oxygen consumption rate depends on the specific cell line used, growth rates, carbon sources, etc. (Doyle and Griffith 1998).

It is difficult to measure the dissolved oxygen in the cell culture medium directly; one can use the partial pressure to determine the actual dissolved oxygen concentration. At equilibrium, the partial pressure p_{O2} of oxygen in the medium is proportional to the concentration of oxygen in the vapor phase above the medium c_{O2} [Sect. 4.2 (4.15)].

The most commonly applied device to quantify the dissolved oxygen concentration in a cell culture medium is a so called polarographic Clark-electrode (Clark 1955; Cammann et al. 2002; Chmiel 2006). Here, the oxygen diffuses from the culture medium across an oxygen-selective membrane and is then reduced at a negatively polarized platinum electrode. This cathode is connected to a reference silver anode by an electrolyte solution (KCl).

$$\text{Cathode: } O_2 + 2\,H_2O + 4\,e^- + 4\,OH^-$$

$$\text{Anode: } Ag + KCl + AgCl + K^+ + e^-$$

The electrons produced by the reduction of oxygen produce current, which is directly proportional to the oxygen concentration in the medium.

Relatively new devices to determine the amount of oxygen in cell culture medium are optodes (Klimant et al. 1995; Wolfbeis 1991; Wolfbeis (2000); Wittmann et al. 2003). An optode uses dynamic quenching effects. Therefore pulsed monochromatic light is carried in an optic fiber to the oxygen sensor and excites the immobilized fluorophore (e.g., ruthenium complexes). The excited complex fluoresces and emits energy at a higher wavelength. The collision of an oxygen molecule with a fluorophore in its excited state leads to a non-radiative transfer of energy. This internal conversation decreases the fluorescence signal. The degree of quenching correlates with the oxygen concentration (Figs. 4.45–4.47). It is possible to measure either the fluorescence lifetime or the luminescence intensity. The detection of the fluorescence lifetime as oxygen dependent is not affected by external light sources, changes in the pH, ions or salinity. Changes of the optical properties of the sample like opacity, coloration or the refractive index falsify the fluorescence intensity, but not the lifetime.

The kinetics of this process follows the Stern–Volmer relationship:

$$(\tau_{l0}/\tau_{l}) - 1 = K_{SV} c_{O2}$$

where τ_{l0} and τ_{l} are the fluorescent lifetimes in the absence and presence, respectively, of oxygen, K_{SV} is the Stern–Volmer quenching constant and c_{O2} is the oxygen concentration.

Optodes do work in the whole region 0–100% oxygen saturation in water, but are most sensitive at low oxygen concentrations. During the measurement no oxygen is consumed, as, for e.g., by the use of a Clark-electrode (Wittmann et al. 2003).

As mentioned before, the actual value is compared to a desired set point and, if needed, corrective action is taken. To maintain the desired set point, air or pure oxygen is usually sparged directly into the culture, depending on the required oxygen transfer rates and the achievable flow rates. In the laboratory also, oxygenation by membranes is a widely used technique and ensures bubble-free aeration (Sect. 4.2).

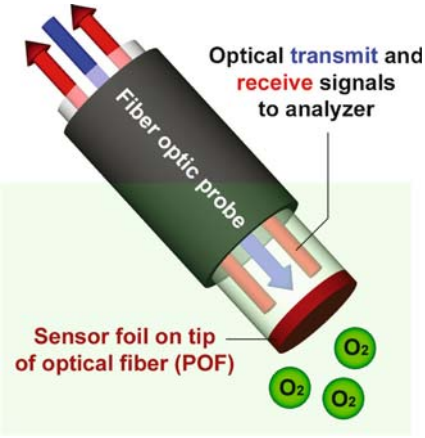

Fig. 4.45 Principle of an optode (with permission and by courtesy of Presens Sensing GmbH, Germany)

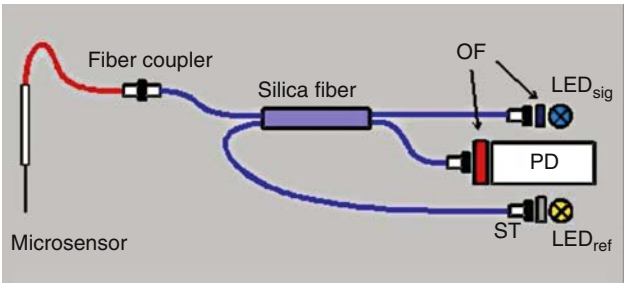

Fig. 4.46 Schematic of the assembly of measurement based on an optode (with permission and by courtesy of Presens Sensing GmbH, Germany)

Fig. 4.47 Single channel instrument for the measurement of oxygen using an optode (with permission and by courtesy of Presens Sensing GmbH, Germany)

4.5.4 Carbon Dioxide Partial Pressure

Not only the concentration of dissolved oxygen but also the concentration of dissolved carbon dioxide within the cell culture medium is very important. The concentration of carbon dioxide in the vapor leaving a bioreactor can also be used to calculate specific respiration rates and cell activity. The latter can easily be measured utilizing infrared (IR) analyzers (Riley 2006; Chmiel 2006). Dissolved carbon dioxide can now be measured in situ utilizing a fiber optic chemical sensor (Riley 2006; Wolfbeis 1991; Chu and Lo 2008; Pattison et al. 2000; Ge et al. 2003). For example, this kind of sensor uses hydroxypyrenetrisulfonate (HPTS) to quantify the dissolved carbon dioxide in the medium. The protonated and un-protonated forms have distinct excitation maxima at 396 and 460 nm, respectively, which allow a ratiometric measurement of pH and thus carbon dioxide concentration (Fig. 4.48). The company YSI Incorporated has developed an in situ device model, 8,500, utilizing this method to quantify dCO_2 (Fig. 4.49), but these devices have not been established widely in the industry yet.

4.5.5 Metabolites and Products

One goal in animal cell cultures is always to maintain suitable culture conditions with regard to nutrients to achieve fast cell growth, high cell viabilities and high product yields. With a good understanding of the cell metabolism and it needs, selective feeding strategies can be utilized to improve productivity and lower culture costs. The carbohydrate glucose and the amino acid glutamine are the two key

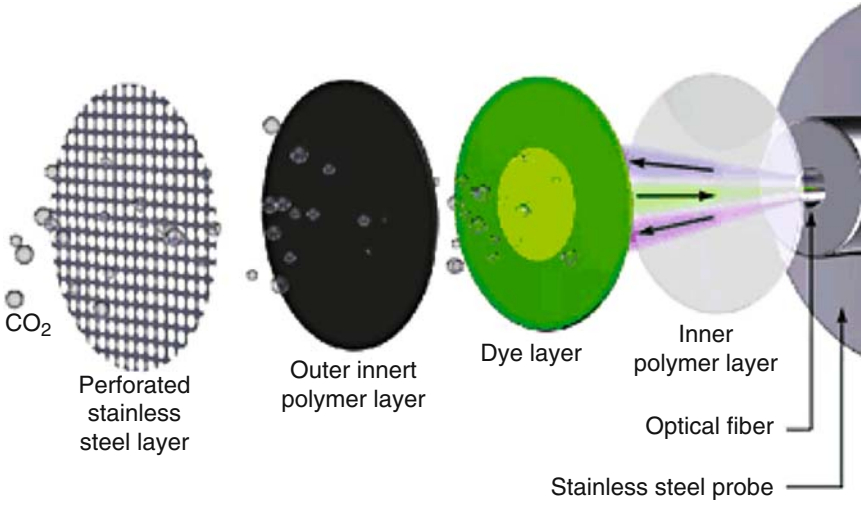

Fig. 4.48 Principle of a fiber optic chemical sensor for the dissolved carbon dioxide measurement (with permission and courtesy of YSI Incorporated, Yellow Springs, USA)

Fig. 4.49 Fiber optic sensor (**a**) and device (**b**) for the dissolved carbon dioxide measurement (with permission and courtesy of YSI Incorporated, Yellow Springs, USA)

nutrients in animal cell cultures, while ammonia and lactate are the two main metabolic byproducts. In addition to insufficient supply of nutrients, byproduct formation can have a negative effect and inhibit cell growth and product formation. Therefore it is very important to monitor and control the concentrations of both nutrients and byproducts in the medium during the process (Riley 2006; Chmiel 2006; Doyle and Griffith 1998).

One approach to quantify nutrient and byproduct concentrations is the use of biosensors. Biosensors are devices which utilize a specific enzymatic reaction to obtain an electrical signal which is proportional to the concentration of the analyte to be quantified. Due to the enzymatic nature of the sensor, a separate sensor has to be used for each analyte. These sensors are most commonly used offline, meaning a sample is taken aseptically from the culture and analyzed outside the system, but

automatic on-line sampling devices are also available if preferred. In all cases the enzymatic reaction, e.g., an oxidase reaction, results in a product that can be easily detected, e.g., hydrogen peroxide.

The following example is based on the YSI Model 2700 Select Biochemistry Analyzer (YSI Incorporated; Yellow Springs, OH). Here a three-layer membrane placed on the face of the probe contains an immobilized enzyme in the middle layer. Once the sample is injected into the buffer-filled sample-chamber, the analyte diffuses through the first membrane and is oxidized after contact with the enzyme to H_2O_2 (Reaction 1) (Fig. 4.50).

$$Glucose + O_2 \xrightarrow{Glucose\ oxidase} Gluconic\ acid + H_2O_2$$
$$Lactate + O_2 \xrightarrow{Lactate\ oxidase} Pyruvate + H_2O_2$$
$$Glutamine + O_2 \xrightarrow{Glutamate\ oxidase} \alpha - ketoglutarate + NH_3 + H_2O_2$$

Hydrogen peroxide is capable of diffusing through the second membrane and is oxidized at the platinum electrode (Reaction 2).

$$H_2O_2 \xrightarrow{Platinum\ anode} 2H^+ + O_2 + 2e^-$$

Due to the free electrons produced, a current occurs, which is linearly proportional to the concentration of the analyte in the sample once a dynamic equilibrium between H_2O_2 production in and diffusion out of the enzyme layer is established. This current is then used to calculate the analyte concentration in the sample.

Ozturk used this kind of analyzer to monitor glucose and lactate during batch and perfusion culture of hybridoma cells by using cell free samples from a circulation

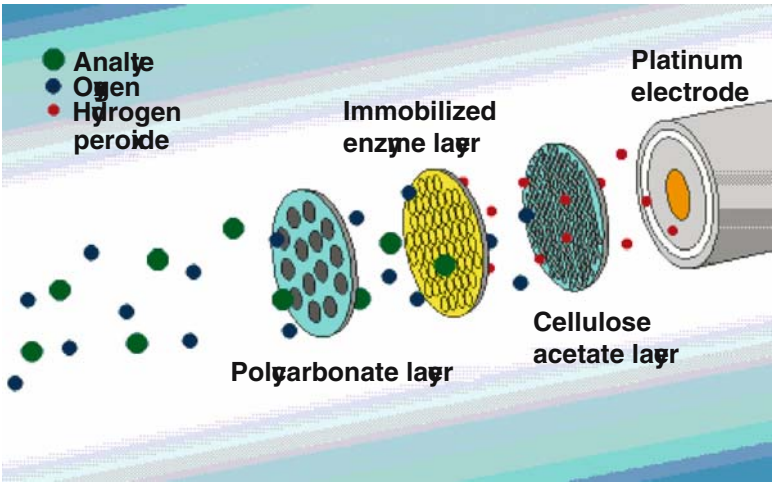

Fig. 4.50 Schematic of the sensing principle of the biosensor (with permission and courtesy of YSI Incorporated, Yellow Springs, USA)

loop of the bioreactor including a 0.45 µm hollow fiber membrane filter (Ozturk et al. 1997).

Another approach to quantify nutrient and byproduct concentrations is the flow injection analysis (FIA). A liquid sample is injected into a stream of aqueous carrier stream and forms a pulse which can then be detected, based on changes in different physical parameters (e.g., absorbance, fluorescence, chemi-luminescence, etc.). Because each sensor can only detect one analyte, the sample flow is often split into different channels for a broader range of analytes to be monitored (Riley 2006; Chmiel 2006).

4.5.6 Cell Density and Viability

Cell density can be measured utilizing different methods, either offline or online. Offline methods require aseptic sampling prior to the cell density determination. The sample is diluted appropriately and often counted with a hemocytometer (Doyle and Griffith 1998; Butler 2004).

Additionally, the dye trypan blue is generally used to determine cell viability. The dye penetrates the broken membranes of dead cells and dyes them blue, binding to the proteins present in the cytosol (Butler 2004). The membranes of viable cells inhibit the dye entering the cytosol and so these cells do not get dyed blue. A recent method to determine cell density and viability is the use of automated counters. These devices, e.g., Vi-Cell Cell Viability Analyzer (Beckman Coulter, Inc., Fullerton, CA) are usually based on the trypan blue method and can help to quantify the determined data more rapidly and are less subjective. If needed, such a device can also be connected directly to a fermenter and samples taken and analyzed automatically (autosampler). Other online methods use probes inserted into the vessel and measure the absorbance of the culture with a Vertical Cavity Surface-Emitting Laser (VSCEL) at a wavelength of 850 nm (TruCell2 probe, Finesse, Inc., Santa Clara, CA). Using this method, it is possible to determine only the total cell density within the culture, but not the percentage of dead cells.

A number of indirect methods of cell density and viability determination are also available but will not be discussed in detail in this chapter. These methods include total protein determination, e.g., the Bradford-assay, or DNA determination, e.g., the DAPI-assay. Methods to determine the percentage of viable cells within the culture include the tetrazolium assay, the lactate-dehydrogenase determination or adenylate energy charge determination. Also the rate of protein or nucleic acid synthesis can be used to determine cell viability (Doyle and Griffith 1998; Butler 2004).

In addition to this, methods for cell line identification are also available. Karyotpying, antibody labeling, isozyme analysis or DNA fingerprinting is utilized to detect cross-contaminations and mutations within a culture. Protocols for these techniques can be found in, e.g., Doyle and Griffiths, 1998.

4.5.7 Agitation

It is very important to maintain a specific rate of agitation within the system. Agitation ensures homogeneity of nutrients and oxygen in the medium and also helps to distribute additions like base or acid evenly in the culture medium (Krahe 2003; Chmiel 2006). If the agitation rate is too high, cell death could occur due to shear stress. Therefore it is very important to know what shear stress the cultivated cells can resist without a decrease in protein production or cell viability. Efficiency and shear stress can be significantly different for different types of impellers. The impeller speed can be measured by all standard speed controllers, e.g. electronic tachometer.

4.6 Questions and Problems

- Summarize briefly the main fluid-mechanical and biological aspects of cell damage.
- What kind of reaction system can be used to investigate shear effects on anchorage dependent cells? Explain the basic characteristics of this system.
- What is an acceptable wall shear stress for adherent growing cells for an exposure time of 24 h?
- Describe fluid dynamic effects on anchorage dependent cells grown on microcarriers in suspension culture.
- What is described by the Kolmogorov-eddy-length? Is this parameter suitable of estimation of shear effects on anchorage dependent cells grown on microcarriers in suspension culture?
- Which effects are responsible for cell damage in bubble columns? Which is the most important one?
- Discuss the consequences of shear effects on reactor design.

4.6.1 Problem

During a cell culture fermentation a system answer for the oxygen concentration in the culture medium was plotted by the "dynamic method" (see figure: *x*-axis: time in seconds, *y*-axis: oxygen concentration in the liquid in mg L^{-1}).

Define the dynamic method and give the mass balances.

Calculate the oxygen uptake rate (OUR) of the culture, the $k_L a$ and the oxygen saturation concentration c^* by approximation using the experimental data (Fig. 4.51).

4.6.2 Problem

The surface area of a culture grown in a spinner culture vessel is 100 cm^2 and the culture medium volume is 100 ml. The oxygen consumption by the cells is 2×10^{-8} mg $cell^{-1}$ h^{-1}. At the end of the log phase of growth the cell concentration reached

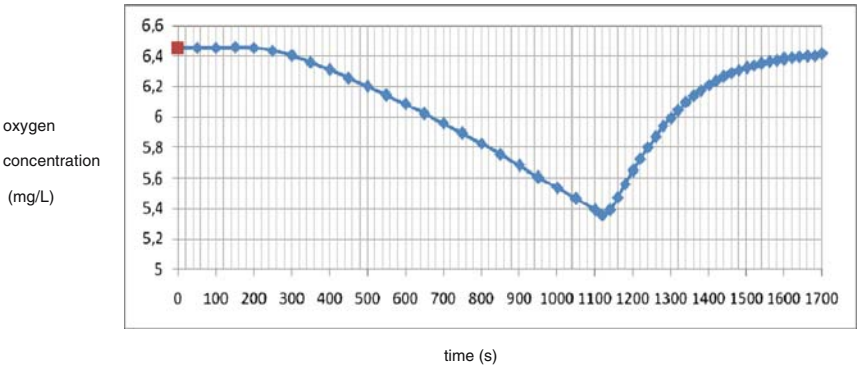

Fig. 4.51

2.5×10^6 cells mL^{-1}. Oxygen is supplied in the form of air pumped into the head space of the vessel and its rate of transfer across air/medium interface has been determined to be 0.17 mg per cm^2 and hour.

It is proposed to use a scaled up version of this spinner culture. The culture volume is to be increased tenfold. The vessel that is to be used has a cross sectional area of 200 cm^2.

What problems do you foresee in supplying oxygen to this culture (calculate the oxygen demand of the up-scaled culture) and how would you solve this problem?

- Which types of membranes can be used for bubble-free aeration of suspension reactors? Enumerate the advantages and disadvantages of bubble-free aeration systems.
- Explain techniques for immobilization and encapsulation of mammalian cells.
- Define the terms “microcarrier” and “macrocarrier” with respect to preferred reactor system.
- Name properties of an “ideal” microcarrier.
- Explain mass-transfer effects in macroporous carriers. Give the fundamental equations for a heterogeneous reaction within a spherical particle.
- What is described by the Thiele-modulus?
- List the advantages and disadvantages of batch and perfusion systems.
- Explain briefly the principles of culture modes.
- Sketch for a chemostat the relationship between cell density, substrate concentration and product concentration as a function of the dilution rate for “steady state”. Explain briefly the term “wash-out point”.
- Explain briefly the strategies used to determine feeding rates in fed-batch cultures
- Name important aspects, when perfusion culture has an advantage compared to batch/fed-batch culture.

- Sketch the scheme for the mass transfer across a dialysis membrane. In which respect does the permeability coefficient of a dialysis membrane depend on the molecular weight of a certain substance?

List of Symbols

A	membrane area
b	width
c	concentration
C	constant
c^*	equilibrium solubility of oxygen – oxygen saturation
c_0^*	oxygen solubility at zero solute concentration
c_1, c_2	concentrations of both sides of a dialysis membrane
c_{AL}	concentration of oxygen at steady state
c_{crit}	critical oxygen concentration
c_{iL}	concentration of ionic component i in the liquid
c_{jL}	concentration of non-ionic component j in the liquid
c_L	concentration of oxygen in solution
c_{O2}	concentration of oxygen
c_P	product concentration
c_S	substrate concentration
c_{S0}	substrate concentration in feed
D	dilution rate in chemostat and perfusion mode
D_a	dilution rate in outer chamber of membrane dialysis reactor
d_B	bubble diameter
$D_{crit.}$	critical (maximal) dilution rate
D_e	diffusive coefficient
D_i	dilution rate in inner chamber of membrane dialysis reactor
d_1	inner diameter of the membrane tube
$d_{i,cou}$	diameter of inner cylinder in couette viscometer
d_2	orifice diameter
DO	dissolved oxygen
d_o	outer diameter of the membrane tube
D_R	vessel diameter
d_R	impeller diameter
D_s	diffusion coefficient of oxygen in the membrane
d_s	Sauter mean diameter
d_T	bubble column vessel diameter
F	liquid flow rate
g	acceleration due to gravity
h	height
He	Henry constant
He_s	Henry constant of oxgen in membrane material

He_w	Henry constant of oxgen in water
H_i	constant for ionic component i
h_L	height of fluid in bubble column
H_R	filling height of the stirred reactor – impeller located at the interface
ISF	integrated shear factor
k	mass transfer coefficient at the gas liquid interface
k_d	cell specific death rate
K_j	constant for non-ionic component j in the liquid
k_L	mass transfer coefficient at the liquid-side interface
k_La	mass transfer coefficient, which is the product of k_L, the overall mass transfer coefficient from the gas to the liquid phase (two film model), and a the gas–liquid interfacial area per unit of the reactor liquid volume
k_{O2}	monod-constant for oxygen
k_S	Monod-constant for substrate limitation
K_{SV}	Stern–Volmer quenching constant
l_{Kol}	Kolmogorov length scale
M_d	torque
n_R	rotation speed
OTR	oxygen transfer rate
OUR	oxygen uptake rate
P	power input
P/V	power input per unit volume
P_{mem}	permeability coefficient of a dialysis membrane
p_{O2}	partial pressure of oxygen in the gas phase
Q	volumetric aeration rate
$Q_{O2,max}$	maximal cell specific oxygen uptake rate
q_P	cell specific production rate
q_S	cell specific substrate uptake rate
r	radius
Re	Reynolds number
$r_{i,cou}$	inner radius of a couette viscometer
r_P	particle radius
r_Z	cell radius
Ta	Taylor number
S	molecular flow
t	time
T	temperature
U	flow velocity in flow chamber
U_T	peripheral speed in couette viscometer
V	volume
v	superficial gas velocity
v_0	gas velocity at the sparger
V_k	hypothetical killing volume.
w	gap width
X_t	total cell concentration

X	cell density
X_d	concentration of dead cells
X_v	concentration of viable cells
Y	length scale in flow chamber
Yz	valency of ionic component i
α	exponent (further function of superficial velocity)
β	exponent independent of scale and impeller type
α_{perf}	recirculation rate in perfusion culture, ratio between feed and recirculated flow
β_{perf}	concentration factor in perfusion culture, ration between biomass, concentration in the reactor and in recirculated flow
γ	shear rate
η_{fl}	fluid viscosity
η_i	effectiveness factor for internal mass transfer resistance
Φ_0	Thiele-Modulus for zero-order kinetic
μ	cell specific growth rate
μ_{max}	maximal cell specific growth rate
$\Delta\rho$	density difference
ε	energy dissipation rate per unit mass
ν	kinematic fluid viscosity
ρ_{fl}	fluid density
σ	surface tension
σ_Z	surface tension of cell membrane at cell burst
τ	shear stress
τ_{crit}	critical shear stress
τ_w	wall shear stress
τ_{l0}	fluorescent lifetimes in the absence of oxygen
τ_l	fluorescent lifetimes in the presence of oxygen

References

Abu-Reesh I, Kargi F (1989) Biological responce of hybridoma cells to defined hydrodynamic shear stress. J Biotechnol 9: 167–178

Augenstein DC, Sinskey AJ, Wang DIC (1971) Effect of shear on the death o two strains of mammalian cells. Biotechnol Bioeng 40: 1004–1010

Aunins JG, Henzler HJ (1993) Aeration in cell culture bioreactors. In: Rehm HJ, Reed G (eds) Biotechnology, Vol 3, 2nd ed, pp 219–281. VCH, Weinheim

Baldi L, Muller N, Picasso S, Jacquet R, Girard P, Thanh HP, Derow E, Wurm FM (2005) Transient gene expression in suspension HEK-293 cells: application to large-scale protein production. Biotechnol Prog 21: 148–153

Barford JP, Phillips PJ, Harbour C (1992) Enhancement of productivity by yield improvements using simulation techniques. In: Murakami H et al. (eds) Animal Cell Technology: Basic & Applied Aspects. Kluwer, Netherlands, pp 397–403

Blasey HD, Aubry JP, Mazzei GJ, Bernard AR (1996) Large scale transient expression with COS cells. Cytotechnol 18: 183–192

Bliem R, Konopitzky K, Katinger H (1991) Industrial animal cell reactor systems: aspects of selection and evaluation. Adv Biochem Eng 44: 2–26
Bödeker BGD, Newcomb R, Yuan P, Braufman A, Kelsey W (1994) Production of recombinant factor VIII from perfusion cultures: I. Large-Scale fermentation. In: Spier RE, Griffiths JB, Berthold W (eds) Animal cell technology: products of today, prospects for tomorrow, pp 580–583. Butterworth-Heinemann, London
Bohmann A, Pörtner R, Märkl H (1995) Performance of a membrane dialysis bioreactor with radial-flow fixed bed for the cultivation of a hybridoma cell line. Appl Microbiol Biotechnol 43: 772–780
Born C, Zhang Z, Al-Rubeai M, Thomas CR (1992) Estimation of disruption of animal cells by laminar shear stress. Biotechnol Bioeng 40: 1004–1010
Bräutigam HJ (1985) Untersuchungen zum Einsatz von nicht porösen Kunststoffmembranen als Sauerstoffeintragssystem. Dissertation, TU Hamburg-Harburg
Butler M (2004) Animal Cell Culture and Technology – The Basics. Oxford University Press, New York
Cammann K et al. (2002) Chemical and biochemical sensors. In: Ullmann's Encyclopedia of Industrial Chemistry, Wiley-VCH, New York
Carrel A (1923) A method for the physiological study of tissues. J Exp Med 38: 407
Chalmers JJ (1994) Cells and bubbles in sparged bioreactors. Cytotechnol 15: 311–320
Cherry RS (1993) Animal cells in turbulent fluids: Details of the physical stimulus and the biological response. Biotechnol Adv 11: 279–299
Cherry RS, Papoutsakis ET (1986) Hydrodynamic effects on cells in agitated tissue culture reactors. Bioproc Eng 1: 29–41
Cherry RS, Papoutsakis ET (1988) Physical mechanisms of cell damage in microcarrier cell culture bioreactors. Biotechnol Bioeng 32: 1001–1014
Chisti Y (2000) Animal-cell damage in sparged bioreactors. Trends Biotechnol 18: 420–432
Chisti Y (2001) Hydrodynamic damage to animal cells. Crit Rev Biotechnol 21: 67–110
Chmiel H (2006) (ed). Bioprozesstechnik, 2nd ed., Spektrum Akademischer Verlag, Elsevier, Amsterdam
Chu C-S, Lo Y-L (2008) Fiber-optic carbon dioxide sensor based on fluorinated xerogels doped with HPTS, pp 120–125. Sensors Actuators B 129
Clark LC (1955) US Patent 2913386
Croughan MS, Hamel JF, Wang DIC (1987) Hydrodynamic effects on animal cells grown in microcarrier cultures. Biotechnol Bioeng 29: 130–141
Croughan MS, Hamel JF, Wang DIC (1988) Effects of microcarrier concentration in animal cell culture. Biotechnol Bioeng 32: 975–982
Croughan MS, Wang DIC (1989) Growth and death in overagitated microcarrier cell cultures. Biotechnol Bioeng 33: 731–744
Czermak P, Nehring D (1999) DE 19953137 A1
Czermak P, Nehring D (2000) DE 20053137 A2
Davis J (2007) Hollow fibre cell culture. In: Pörtner R (ed) Animal Cell Biotechnol – Methods and Protocols. Humana Press, Clifton, UK
Davis JM, Hanak JA (1997) Hollow-fiber cell culture. Meth Mol Biol 75: 77–89
de Tremblay M, Perrier M, Chavarie C, Archambault J (1993) Fed-batch culture of hybridoma cells: comparison of optimal control approach and closed loop strategies. Bioprocess Eng 9: 13–21
Derouazi M, Girard P, Van Tilborgh F, Iglesias K, Muller N, Bertschinger M, Wurm FM (2004) Serum-free large-scale transient transfection of CHO cells. Biotechnol Bioeng 87: 537–545
Dey D, Boulton-Stone JM, Emery AN, Blake JR (1997) Experimental comparisons with a numerical model of surfactant effects on the burst of a single bubble. Chem Eng Sci 52: 2769–2783
Diamond SL, Sharefkin JB, Diefenbach C, Frasier-Scott K, McIntire LV, Eskin SG (1990) Tissue plasminogen activator messenger RNA levels increase in cultured human endothelial cells exposed to laminar shear stress. J Cell Phys 143: 364–371
Doran P (2006) Bioprocess Engineering Principles. Academic Press, London
Doyle A, Griffith JB (1998) Cell and Tissue Culture: Laboratory Procedures in Biotechnology, p 192. Wiley, Chichester

Eyer K, Oeggerli A, Heinzle E (1995) On-line gas analysis in animal cell cultivation: II. Methods for oxygen uptake rate estimation and its application to controlled feeding of glutamine. Biotechnol Bioeng 45: 54–62

Fassnacht D (2001). Fixed-Bed Reactors for the Cultivation of Animal Cells. Fortschritt-Berichte VDI. VDI Verlag GmbH, Düsseldorf, Germany

Fassnacht D, Rössing S, Singh RP, Al-Rubeai M, Pörtner R (1999) Influence of *Bcl-2* on antibody productivity in high cell density perfusion cultures of hybridoma. Cytotechnol 30: 95–105

Fenge C, Klein C, Heuer C, Siegel U, Fraune E (1993) Agitation, aeration and perfusion modules for cell culture bioreactors. Cytotechnol 11: 233–244

Fenge Ch, Lüllau E (2006) Cell culture bioreactors. In: Ozturk SS, Hu WS (eds) Cell Culture Technology for Pharmaceutical and Cell-Based Therapies. Taylor & Francis, New York

Frahm B, Kirchner S, Kauling J, Brod H, Langer U, Bödeker B (2007) Dynamische Membranbegasung im Bioreaktor zur Intensivierung der Sauerstoffversorgung empfindlicher Zellinien. Chemie Ing Tech 79: 1052–1058

Frahm B, Lane P, Atzert H, Munack A, Hoffmann M, Hass VC, Pörtner R (2002) Automated, adaptive, model-based control by the open-loop-feedback-optimal (OLFO) controller for the effective fed-batch cultivation of hybridoma cells. Biotechnol Prog 18: 1095–1103

Frahm B, Lane P, Märkl H, Pörtner R (2003) Improvement of a mammalian cell culture process by adaptive, model-based dialysis fed-batch cultivation and suppression of apoptosis. Bioproc Biosys Eng 26: 1–10

Frahm B, Lane P, Munack A, Pörtner R (2005) Optimierung und Steuerung von Zellkultur-Fed-Batch-Prozessen mittels einer Kollokationsmethode. Chem Ing Tech 77: 429–435

Frangos JA, Eskin SG, McIntire LV, Ives CL (1985) Flow effects on prostacyclin production by cultured human endothelial cells. Science 227: 1477–1479

Frangos JA, McIntire LV, Eskin SG (1988) Shear stress induced stimulation of mammalian cell metabolism. Biotechnol Bioeng 32: 1053–1060

Fussenegger M, Fassnacht D, Schwartz R, Zanghi JA, Graf M, Bailey JE, Pörtner R (2000) Regulated overexpression of the survival factor bcl-2 in CHO cells increases viable cell density in batch culture and decreases DNA release in extended fixed- bed cultivation. Cytotechnol 32: 45–61

Ge X, Kostov Y, Rao G (2003) High-stability non-invasive autoclavable naked optical CO_2 sensor. Biosensors Bioelectronics 18: 857–865

Geserick C, Bonarius HP, Kongerslev L, Hauser H, Mueller PP (2000) Enhanced productivity during controlled proliferation of BHK cells in continuously perfused bioreactors. Biotechnol Bioeng 69: 266–274

Ghebeh H, Gillis J, Butler M (2002) Measurement of hydrophobic interactions of mammalian cells grown in culture. J Biotechnol 95: 39–48

Girard P, Derouazi M, Baumgartner G, Bourgeois M, Jordan M, Jacko B, Wurm F (2002) 100-liter transient transfection. Cytotechnol 38: 15–21

Glaser V (2001) Current trends and innovations in cell culture. Gen Eng N 21: 11

Gotoh T, Mochizuki G, Kikuchi K (2001) Perfluorocarbonmediated aeration applied to recombinant protein production by virus-infected insect cells. Biochem Eng J 7: 6978

Griffith B (2000) Scaling up of animal cell cultures. In: Masters JRW (ed) Animal Cell Culture. 3rd ed, p 19–66. Oxford University Press, New York

Griffiths JB (1992) Animal cell culture proceses – batch or continuous? J Biotechnol 22: 21–30

Grima EM, Christi Y, Moo-Young M (1997) Characterization of shear rates in airlift bioreactors for animal cell culture. J Biotechnol 54: 195–210

Handa A, Emery AN, Spier RE (1987) On the evaluation of gas–liquid interfacial effects on hybridoma viability in bubble column bioreactors. Dev Biol Stand 66: 241–253

Hansen HA, Madson NM, Emborg C (1993) An evaluation of fed-batch cultivation methods for mammalian cells based on model simulations. Bioproc Eng 9: 205–213

Hartnett T (1994) Instrumentation and control of bioprocesses. In: Lydersen BK, D'Elia NA, Nelson KL (eds). Bioprocess Engineering: Systems, Equipment, and Facilities. Wiley, New York

Henzler HJ, Kauling OJ (1993) Oxygenation of cell cultures. Bioproc Eng 9: 61–75

Hiller GW, Aeschlimann AD, Clark DS, Blanch HW (1991) A kinetic analysis of hybridoma growth and metabolism in continuous suspension culture on serum-free medium. Biotechnol Bioeng 38: 733–741

Howaldt M, Walz F, Kempken R (2006) Kultur von Tierzellen. In: Chmiel H (ed) Bioprozesstechnik. Elsevier – Spektrum Akademischer Verlag

Hu WS, Meier J, Wang DIC (1985) A mechanistic analysis of the inoculum requirements for the cultivation of mammalian cells on microcarriers. Biotechnol Bioeng 27: 585–595

Hu WS, Meier J, Wang DIC (1986) Use of surface aerator to improve oxygen transfer in cell culture. Biotechnol Bioeng 28: 122–125

Hübner H (2007) Cell encapsulation. In: Pörtner R (ed) Animal Cell Biotechnol – Methods and Protocols. Humana Press, Clifton, UK

Huebner H, Buchholz R (1999) Microencapsulation. In: Flickinger MC, Drew SW (ed) Encyclopedia of Bioprocess Technology: Fermentation, Biocatalysis and Bioseparation, pp 1785–1798. Wiley, Hoboken, NJ

Hülscher M (1990) Auslegung von Airlift-Schlaufenreaktoren für die Kultivierung von Tierzellen im Hinblick auf Zellschädigung. Dissertation Universität Dortmund

Hülscher M, Pauli J, Onken U (1990) Influence of protein concentration on mechanical cell damage and fluid dynamics in airlift reactors for mammalian cells. Food Biotechnol 4: 157–166

Jordan M (1993) Die Rolle von Serum bei der hydrodynamischen Belastung von tierischen Zellen im Bioreaktor; Möglichkeiten der Serum Reduktion. Dissertation an der ETH Zürich, Schweiz

Kelly BD, Chiou TW, Rosenberg M, Wang DIC (1993) Industrial animal cell culture. In: Stephanopolous G (ed) Biotechnology, Vol 3 (Bioprocessing), VCH Verlagsgesellschaft, Weinheim, Germany

Klimant I, Meyer V, Kühl M (1995) Fiber-optic oxygen microsensors, a new tool in aquatic biology. Limnol Oceanogr 40: 1159–1165

Kompala DS, Ozturk SS (2006) Optimization of high cell density perfusion bioreactors. In: Ozturk SS, Hu WS (eds) Cell Culture Technology For Pharmaceutical and Cell-Based Therapies. Taylor & Francis, New York

Krahe M (2003) Biochemical Engineering. Reprint from Ullmann's Encyclopedia of Industrial Chemistry, Vol 6. VCH Publishers, Weinheim, Germany

Kramer HW (1988) Der Einfluβ von Scherkräften in Bioreaktoren auf Proliferation und Syntheseleistung tierischer Zellen. Dissertation ETH Zürich, Nr. 8565

Kretzmer G (1994) Entwicklung optimaler Prozeßbedingungen zur Produktion von rekombinanten Proteinen mit adhärenten Säugerzellen. Habilitationsschrift Universität Hannover

Kunas KT, Papoutsakis ET (1990) Damage mechanism of suspended animal cells in agitated bioreactors with and without bubble entrainment. Biotechnol Bioeng 36: 476–483

Kurokawa H, Park YS, Iijima S, Kobayashi T (1994) Growth characteristics in fed-batch culture of hybridoma cells with control of glucose and glutamine concentrations. Biotechnol Bioeng 44: 95–103

Kurosawa H, Matsumura M, Tanaka H (1989) Oxygen diffusity in gel beads containing viable cells. Biotechnol Bioeng 34: 926–932

Kyung YS, Peshwa MV, Gryte DM, Hu WS (1994) High density culture of mammalian cells with dynamic perfusion based on on-line oxygen uptake rate measurements. Cytotechnol 14: 183–190

Langheinrich C, Nienow AW (1999) Control of pH in large scale, free suspension animal cell bioreactors: alkali addition and pH excursions. Biotechnol Bioeng 66: 171–179

Lee GM, Kaminski MS, Palsson BO (1992) Observations consistent with autocrine stimulation of hybridoma cell growth and implications for large-scale antibody production. Biotechnol Lett 14: 257–262

Lee JH, Lim HC, Yoo YJ, Park YH (1999) Optimization of feed rate profile for the monoclonal antibody production. Bioproc Eng 20: 137–146

Looby D, Racher AJ, Griffiths JB, Dowsett AB (1990) The immobilization of animal cells in fixed bed and fluidized porous glass sphere reactors. In: de Bont JAM et al. (eds) Physiology of Immobilized Cells, pp 255–264. Elsevier, Amsterdam

Lüdemann I (1997) Nutrient-Split-Fütterungsstrategie für suspendierte und immobilisierte nicht-adhärente tierische Zellen. VDI-Verlag, Düsseldorf

Lüdemann I, Pörtner R, Schaefer C, Schick K, Šrámková K, Reher K, Neumaier M, Franék F, Märkl H (1996) Improvement of the culture stability of non-anchorage-dependent animal cells grown in serum-free media through immobilization. Cytotechnol 19: 111–124

Ludwig A, Kretzmer G, Schügerl K (1992) Determination of a "critical shear stress level" applied to adherent mammalian cells. Enz Microbiol Technol 14: 209–213

Lüllau E, Biselli M, Wandrey C (1994) Growth and metabolism of CHO-cells in porous glass carriers. In: Spier RE, Griffiths JB, Berthold W (eds) Animal Cell Technology: Products of Today, Prospects of Tomorrow, pp 252–255. Butterworth-Heinemann, London

Lüllau E, Kanttinen A, Hassel J, Berg M, Haag-Alvarsson A, Cederbrant K, Greenberg B, Fenge C, Schweikart F (2003) Comparison of batch and perfusion culture in combination with pilot-scale expanded bed purification for the production of soluble recombinant beta-secretase. Biotechnol Prog 19: 37–44

Lundgren B, Blüml G (1998) Microcarriers in cell culture production. In: Subramanian G. (eds) Bioseparation and Bioprocessing – A Handbook. Wiley-VCH, New York

Ma N, Chalmers JJ, Aunins JG, Zhou W, Xie L (2004) Quantitative studies of cell-bubble interactions and cell damage at different Pluronic F-68 and cell concentrations. Biotechnol Prog 20: 1183–1191

Ma N, Mollet M, Chalmers JJ (2006) Aeration, mixing and hydrodynamics in bioreactors. In: Ozturk SS, Hu WS (eds) Cell Culture Technology for Pharmaceutical and Cell-Based Therapies. Taylor & Francis, New York

Märkl H, Bronnenmeier R, Wittek B (1987) Hydrodynamische Belastbarkeit von Mikroorganismen. Chem Ing Tech 59: 907–917

Marks DM (2003) Equipment design considerations for large scale cell culture. Cytotechnol 42: 21–33

Masters JRW (2000) (ed). Animal Cell Culture. 3rd ed., Oxford University Press, New York, 2000

McQueen A, Meilhoc E, Bailey JE (1987) Flow effects on the viability and lysis of suspended mammalian cells. Biotechnol Lett 9: 831–836

Meier SJ, Hatton TA, Wang DIC (1999) Cell death from bursting bubbles: role of cell attachment to rising bubbles in sparged reactors. Biotechnol Bioeng 62: 468–478

Meissner P, Pick H, Kulangara A, Chatellard P, Friedrich K, Wurm FM (2001) Transient gene expression: recombinant protein production with suspension-adapted HEK293-EBNA cells. Biotechnol Bioeng 75: 197–203

Michaels JD, Mallik AK, Papoutsakis ET (1996) Sparging and agitation-induced injury of cultured animal cells: do cell to-bubble interactions in the bulk liquid injure cells? Biotechnol Bioeng 51: 399–409

Miller WM, Wilke CR, Blanch HW (1987) Effects of dissolved oxygen concentration on hybridoma growth and metabolism in continuous culture. J Cell Phys 132: 524–530

Miller WM, Wilke CR, Blanch HW (1988) A kinetic analysis of hybridoma growth and metabolism in batch and continuous suspension culture. Effect of nutrient concentration, dilution rate and pH. Biotechnol Bioeng 32: 947–965

Moo-Young M, Blanch HW (1981) Design of biochemical reactors – mass transfer criteria for simple and complex systems. Adv Biochem Eng 19: 1–70

Moreira JL, Cruz PE, Santana PC, Feliciano AS (1995) Influence of power input and aeration method on mass transfer in a laboratory animal cell culture vessel. J Chem Tech Biotechnol 62: 118–131

Murtas S, Capuani G, Dentini M, Manetti C, Masci G, Massimi M, Miccheli A, Crescenzi V (2005) Alginate beads as immobilization matrix for hepatocytes perfused in a bioreactor: a physico-chemical characterization. J Biomater Sci Polym Ed 6: 829–846

Nehring D, Czermak P, Luebben H, Vorlop J (2004) Experimental study of a ceramic microsparging aeration system in a pilot scale animal cell culture. Biotechnol Prog 20: 1710–1717

Nilsson K, Buzsaky F, Mosbach K (1986) Growth of anchorage dependent cells on macroporous microcarrier. Bio/Technology 4: 989–990

Ogbonna JB, Märkl H (1993) Nutrient-split feeding strategy for dialysis cultivation of *Escherichia coli*. Biotechnol Bioeng 41: 1092–1100
Olivier LA, Truskey GA (1993) A numerical analysis of forces exerted by laminar flow on spreading cells in a paralled plate flow chamber assay. Biotechnol Bioeng 42: 963–973
Oller AR, Buser CW, Tyo MA, Thilly WG (1989) Growth of mammalian cells at high oxygen concentrations. J Cell Sci 94: 43–49
Otzturk SS (2006) Cell culture technology – an overview. In: Ozturk SS, Hu WS (eds) Cell Culture Technology For Pharmaceutical and Cell-Based Therapies. Taylor & Francis, New York
Ozturk SS, Thrift JC, Blackie JD, Naveh D (1997) Real time monitoring and control of glucose and lactate concentrations in a mammalian cell perfusion reactor. Biotechnol Bioeng 53: 372–378
Ozturk SS (1996) Engineering challenges in high density cell culture systems. Cytotechnol 22: 3–16
Ozturk SS, Hu WS (eds) (2006) Cell Culture Technology For Pharmaceutical and Cell-Based Therapies. Taylor & Francis, New York
Papoutsakis ET (1991) Fluid-mechanical damage of animal cells in bioreactors. Tibtech 9: 427–437
Pattison RN, Swamy J, Mendenhall B, Hwang C, Frohlich BT (2000) Measurement and control of dissolved carbon dioxide in mammalian cell culture processes using an in situ fiber optic chemical sensor. Biotechnol Prog 16: 769–774
Pörtner R (1998) Reaktionstechnik der Kultur tierischer Zellen. Shaker, Aachen
Pörtner R, Lüdemann I, Märkl H (1997) Dialysis cultures with immobilized hybridoma cells for effective production of monoclonal antibodies. Cytotechnol 23: 39–45
Pörtner R, Märkl H (1995) Festbettreaktoren für die Kultur tierischer Zellen. BIOforum 18: 449–452
Pörtner R, Märkl H (1998) Dialysis cultures. Appl Microbiol Biotechnol 50: 403–414
Pörtner R, Platas Barradas OBJ (2007) Cultivation of mammalian cells in fixed bed reactors. In: Pörtner R (ed) Animal Cell Biotechnology – Methods and Protocols. Humana Press, Clifton, UK
Pörtner R, Platas Barradas OBJ, Fassnacht D, Nehring D, Czermak P, Märkl H (2007) Fixed bed reactors for the cultivation of mammalian cells: design, performance and scale-up. Open Biotechnol J 1: 41–46
Pörtner R, Schäfer Th (1996) Modelling hybridoma cell growth and metabolism – A comparision of selected models and data. J Biotechnol 49: 119–135
Pörtner R, Schilling A, Lüdemann I, Märkl H (1996) High density fed-batch cultures for hybridoma cells performed with the aid of a kinetic model. Bioproc Eng 15: 117–124
Pörtner R, Schwabe JO, Frahm B (2004) Evaluation of selected control strategies for fed-batch cultures of a hybridoma cell line. Biotechnol Appl Biochem 40: 47–55
Pörtner R, Shimada K, Matsumura M, Märkl H (1995) High density culture of animal cells using macroporous cellulose carriers. In: Beuvery EC et al. (eds) Animal Cell Technology: Developments Towards the 21st Century, pp 835–839. Kluwer, The Netherlands
Qi HN, Goudar CT, Michaelis JD, Henzler HJ, Jovanovic GN, Konstantinov KB (2003) Experimental and theoretical analysis of tubular membrane aeration for mammalian cell bioreactors. Biotechnol Prog 19: 1183–1189
Quicker G, Schumpe A, König B, Deckwer WD (1981) Comparison of measured and calculated oxygen solubilities in fermentation media. Biotechnol Bioeng 23: 635–650
Rampe M (2006) Scale-up und Weiterentwicklung eines effizienten Membranbegasungssystems für Bioreaktoren. Thesis, University of Applied Sciences Giessen
Riley M (2006) Instrumentation and process control. In: Ozturk SS, Hu WS (eds) Cell Culture Technology for Pharmaceutical and Cell-Based Therapies, p 276. CRC Press, Boca Raton
Ruffieux PA, von Stockar U, Marison IW (1998) Measurement of volumetric (OUR) and determination of specific (qO_2) oxygen uptake rates in animal cell cultures. J Biotechnol 63: 85–95
Ryszcuk A, Emborg C (1997) Evaluation of mammalian fed-batch cultivations by two different models. Bioproc Eng 16: 185–191
Schneider M, Reymond F, Marison IW, von Stockar U (1995) Bubble-free oxygenation by means of hydrophobic porous membranes. Enzyme Microb Technol 17: 839–847
Schumpe A, Adler I, Deckwer WD (1978) Solubility of oxygen in electrolyte solutions. Biotechnol Bioeng 20: 145–150

Schwabe JO, Pörtner R, Märkl H (1999) Improving an on-line feeding strategy for fed-batch cultures of hybridoma cells by dialysis and "nutrient-split' -feeding. Bioproc Eng 20: 475–484
Shiragami N (1997) Effect of shear rate on hybridoma cell metabolism. Enz Microb Technol 13: 913–919
Shiragami N, Unno H (1994) Effect of shear stress on activity of cellular enzyme in animal cell. Bioproc Eng 10: 43–45
Shuler ML, Kargi F (2002) Bioprocess Engineering – Basic Concepts. Prentice-Hall PTR, Englewood Cliffs, NJ
Siano SA, Muthrasan R (1991) NADH Fluorescence and oxygen uptake responses of hybridoma cultures to substrate pulse and step changes. Biotechnol Bioeng 37: 141–159
Sielaff TD, Hu MY, Amiot B, Rollins MD, Rao S, McGuire B, Bloomer JR, Hu WS, Cerra FB (1995) Gel-entrapment bioartificial liver therapy in galactosamine hepatitis. J Surg Res 59: 179–184
Singh V (1999) Disposable bioreactor for cell culture using wave-induced agitation. Cytotechnol 30: 149–158
Sinskey AJ, Fleishaker RJ, Tyo MA, Giard DJ, Wang DIC (1981) Production of cell-derived products: virus and interferon. Ann NY Acad Sci 369: 47–59
Smith CG, Greenfield PF, Randerson DH (1987) A technique for determining the shear sensitivity of mammalian cells in suspension culture. Biotechnol Lett 1: 39–44
Spraque EA, Steinbach BL, Nerem RM, Schwartz CJ (1987) Influence of a laminar steady-state fluid-imposed wall shear stress on binding, internalization, and degradation of low-density lipoproteins by cultured arterial endothelium. Circulation 76: 648–656
Stathopoulos NA, Hellums JD (1985) Shear stress effects on human embyonic kidney cells in vitro. Biotechnol Bioeng 27: 1021–1026
Stevens J (1994) Entwicklung eines neuen Verfahrens zur kontinuierlichen Fermentation von Tierzellen. Dissertation Universität Dortmund
Storhas W (1994) Bioreaktoren und periphere Einrichtungen. Vieweg
Strathmann H (1979) Trennung von molekularen Mischungen mit Hilfe synthetischer Membranen. Dr. Dietrich Steinkopf Verlag, Darmstadt
Tan WS, Dai GC, Chen YL (1994) Quantitative investigation of cell-bubble interactions using foam fractionation technique. Cytotechnol 15: 321–328
Taylor GI (1934) The formation of emulsions in definable fields of flow. Proc Roy Soc 146:501–525
Thiele EW (1939) Relation between catalytic activity and size of particle. Ind Eng Chem 31: 916–920
Tramper J, de Gooijer CD, Vlak JM (1993) Scale-up considerations and bioreactor development for animal cell cultivation. In: Goosen MFA, Daugulis AJ, Falkner P (eds): Insect Cell Culture Engineering, pp 139–177. Marcel Dekker Inc., New York
Tramper J, Smit D, Straatman J, Vlak JM (1987) Bubble column design for growth of fragile insect cell. Bioprocess Eng 2: 37–41
Tramper J, Vlak JM (1988) Bioreactor design for growth of shear-sensitive mammalian and insect cells. Adv Biotechnol Processes 7: 199–228.
Tramper J, Williams JB, Joustra D, Vlak JM (1986) Shear sensitivity of insect cells in suspension. Enz Microb Technol 8: 33–36
Truesdale GA, Downing AL, Lowden GF (1955) The solubility of oxygen in pure water and sea water. J Appl Chem 5: 53–62
van der Velden-de Groot CAM (1995) Microcarrier technology, present status and perspective. Cytotechnol 18: 51–56
van Lier FL, van Duijnhoven GC, de Vaan MM, Vlak JM, Tramper J (1994) Continuous beta-galactosidase production in insect cells with a p10 gene based baculovirus vector in a two-stage bioreactor system. Biotechnol Prog 10: 60–64
van Wezel AL (1967) Growth of cell strains and primary cells on microcarriers in homogenous culture. Nature 216: 64–65
Varley J, Birch J (1999) Reactor design for large scale suspension animal cell culture. Cytotechnol 29: 177–205

Voisard D, Meuwly F, Ruffieux PA, Baer G, Kadouri A (2003) Potential of cell retention techniques for large-scale high-density perfusion culture of suspended mammalian cells. Biotechnol Bioeng 82: 751–765
Werner RG, Walz F, Noé W, Konrad A (1992) Safety and economic aspects of continuous mammalian cell culture. J Biotechnol 22: 51–68
Wlashin KF, Hu WS (2006) Fedbatch Culture and Dynamic Nutrient Feeding. Adv. Biochem. Engin/Biotechnol 101:43–74
Wittmann C, Kim HM, John G, Heinzle E (2003) Characterization and application of an optical sensor for quantification of dissolved O2 in shake flasks. Biotechnol Lett 25: 377–380
Wolfbeis OS (2000) Fiber optic chemical sensors and biosensors. Anal Chem 72: 81R–89R
Wolfbeis OS (ed) (1991) Fiber Optic Chemical Sensors and Biosensors, Vol 1&2. CRC, Boca Raton
Wrotnowski C (2000) Cell culture now a drug discovery bottleneck. Gen Eng N 20: 15
Wu J (1995) Mechanisms of animal cell damage associated with gas bubbles and cell protection by medium additives. J Biotechnol 43: 81–94
Wu J, Goosen, Mattheus FA (1995) Evaluation of the killing volume of gas bubbles in sparged animal cell culture bioreactors. Enzyme Microb Technol 17: 1036–1042
Yoshida H, Mizutani S, Ikenaga H (1993) Production of monoclonal antibodies with a radial-flow bioreactor. In: Kaminogawa S et al. (eds) Animal Cell Technology: Basic and Applied Aspects, pp 347–353. Kluwer, The Netherlands
Zhang S, Handa-Corrigan A, Spier RE (1992a) Foaming and media surfactant effects on the cultivation of animal cells in stirred and sparged bioreators. Biotechnol 25: 289–306
Zhang Z, Al-Rubeai M, Thomas CR (1992b) Mechanical properties of hybridoma cells in batch culture. Biotechnol Lett 14, 11–16
Zhang S, Handa-Corrigan A, Spier RE (1993) A comparison of oxygenation methods for high density perfusion cultures of animal cells. Biotechnol Bioeng 41: 685–692
Zhou W, Hu WS (1994) On-line characterization of a hybridoma cell culture process. Biotechnol Bioeng 44: 170–177
Zhou W, Rehm J, Hu WS (1995) High viable cell concentration fed-batch cultures of hybridoma cells through on-line nutrient feeding. Biotechnol Bioeng 46: 579–587

Complementary Reading

Butler M (2004) Animal Cell Culture and Technology – The Basics. Oxford University Press, New York
Chisti Y (2000) Animal-cell damage in sparged bioreactors. Trends Biotechnol 18: 420–432
Chisti Y (2001) Hydrodynamic damage to animal cells. Crit Rev Biotechnol 21: 67–110
Chmiel H (ed) (2006) Bioprozesstechnik, Elsevier – Spektrum Akademischer Verlag
Doran P (2006) Bioprocess Engineering Principles. Academic Press, London
Doyle A, Griffith JB (1998) Cell and Tissue Culture: Laboratory Procedures in Biotechnology, p 192. Wiley, Chichester
Griffith B (2000) Scaling up of animal cell cultures. In: Masters JRW (ed) Animal Cell Culture. 3rd ed, p 19–66. Oxford University Press, New York
Henzler HJ, Kauling OJ (1993) Oxygenation of cell cultures. Bioproc Eng 9: 61–75
Krahe M (2003) Biochemical Engineering. Reprint from Ullmann's Encyclopedia of Industrial Chemistry; Vol 6. VCH Publishers, Weinheim, Germany
Lundgren B, Blüml G (1998) Microcarriers in cell culture production. In: G. Subramanian: Bioseparation and Bioprocessing – A Handbook. Wiley-VCH, New York
Marks DM (2003) Equipment design considerations for large scale cell culture. Cytotechnol 42: 21–33
Ozturk SS, Hu WS (eds) (2006) Cell Culture Technology For Pharmaceutical and Cell-Based Therapies. Taylor & Francis Group, New York

Pörtner R (1998) Reaktionstechnik der Kultur tierischer Zellen, Shaker, Aachen
Pörtner R (ed) (2007) Animal Cell Biotechnol – Methods and Protocols. Humana Press, Clifton, UK
Pörtner R, Schäfer Th (1996) Modelling hybridoma cell growth and metabolism – A comparision of selected models and data. J Biotechnol 49: 119–135
Shuler ML, Kargi F (2002) Bioprocess Engineering – Basic Concepts. Prentice Hall PTR, Englewood Cliffs, NJ
van der Velden-de Groot CAM (1995) Microcarrier technology, present status and perspective. Cytotechnol 18: 51–56
Varley J, Birch J (1999) Reactor design for large scale suspension animal cell culture. Cytotechnol 29: 177–205